INFORMATION TO USERS

This material was produced from a microfilm copy of the original document. While the most advanced technological means to photograph and reproduce this document have been used, the quality is heavily dependent upon the quality of the original submitted.

The following explanation of techniques is provided to help you understand markings or patterns which may appear on this reproduction.

1. The sign or "target" for pages apparently lacking from the document photographed is "Missing Page(s)". If it was possible to obtain the missing page(s) or section, they are spliced into the film along with adjacent pages. This may have necessitated cutting thru an image and duplicating adjacent pages to insure you complete continuity.

2. When an image on the film is obliterated with a large round black mark, it is an indication that the photographer suspected that the copy may have moved during exposure and thus cause a blurred image. You will find a good image of the page in the adjacent frame.

3. When a map, drawing or chart, etc., was part of the material being photographed the photographer followed a definite method in "sectioning" the material. It is customary to begin photoing at the upper left hand corner of a large sheet and to continue photoing from left to right in equal sections with a small overlap. If necessary, sectioning is continued again — beginning below the first row and continuing on until complete.

4. The majority of users indicate that the textual content is of greatest value, however, a somewhat higher quality reproduction could be made from "photographs" if essential to the understanding of the dissertation. Silver prints of "photographs" may be ordered at additional charge by writing the Order Department, giving the catalog number, title, author and specific pages you wish reproduced.

5. PLEASE NOTE: Some pages may have indistinct print. Filmed as received.

University Microfilms International
300 North Zeeb Road
Ann Arbor, Michigan 48106 USA
St. John's Road, Tyler's Green
High Wycombe, Bucks, England HP10 8HR

Reproduced with permission of the copyright owner. Further reproduction prohibited without permission.

77-9260

SANTA CRUZ, Thomas David, 1948-
ENERGY TRANSFER AND KINETIC STUDIES OF ELECTROCHEMILUMINESCENCE OF AROMATIC HYDROCARBONS.

University of South Florida, Ph.D., 1976
Chemistry, analytical

**Xerox University Microfilms,** Ann Arbor, Michigan 48106

Reproduced with permission of the copyright owner. Further reproduction prohibited without permission.

# ENERGY TRANSFER AND KINETIC STUDIES OF ELECTROCHEMILUMINESCENCE OF AROMATIC HYDROCARBONS

by

Thomas David Santa Cruz

A dissertation submitted in partial fulfillment of the
requirements for the degree of Doctor of Philosophy
in
The University of South Florida

December, 1976

Major Professor: Associate Professor Daniel L. Akins

Reproduced with permission of the copyright owner. Further reproduction prohibited without permission.

GRADUATE COUNCIL
UNIVERSITY OF SOUTH FLORIDA
TAMPA, FLORIDA

CERTIFICATE OF APPROVAL

PH.D. DISSERTATION

This is to certify that the Ph.D. Dissertation of

Thomas D. Santa Cruz

with a major in Chemistry has been approved by the Examining Committee on October 15, 1976 as satisfactory for the dissertation requirement for the Ph.D. degree.

Examining Committee:

Major Professor: Dr. Daniel L. Akins

Member: Dr. Robert S. Braman

Member: Dr. Jefferson C. Davis, Jr.

Member: Dr. George R. Jurch, Jr.

Member: Dr. Brian O. Stevens

Chairperson,
Examining Committee: Dr. Chris P. Tsokos

Reproduced with permission of the copyright owner. Further reproduction prohibited without permission.

This dissertation is dedicated to

my parents, Roque and Alma



Reproduced with permission of the copyright owner. Further reproduction prohibited without permission.

ACKNOWLEDGMENT

The author wishes to express his appreciation to Dr. Daniel L. Akins for the valuable criticism and guidance given in the direction of this research and the preparation of this manuscript. The author, also, extends his appreciation to Dr. Brian Stevens for the loan of equipment and chemicals, Dr. Arthur Snider for his assistance with the mathematical derivation, Mr. Ralph Parks of Nuclear Data for the loan of equipment, Mr. James Kendall for the help in converting paper tape information, the staff of the Central Florida Regional Data Center for their assistance and use of an IBM 360/65 computer, the Department of Chemistry for the teaching assistantship, Mrs. Ferrell for the typing of this manuscript, and the unnamed colleagues and friends for their encouragement, assistance, and patience. Many thanks.



Reproduced with permission of the copyright owner. Further reproduction prohibited without permission.

TABLE OF CONTENTS


| CHAPTER | | PAGE |
|---|---|---|
| I. | INTRODUCTION | |
| | I.1. General Electrochemiluminescence | 1 |
| | I.2. The Electrochemistry of Aromatic Hydrocarbons | 3 |
| | I.3. Energetic Considerations in *ECL* | 4 |
| | I.4. Mechanisms for *ECL* | 8 |
| | I.5. Relevant BPO Chemistry | 12 |
| | I.6. Objectives and Nature of This Study | 13 |
| II. | *ECL* OBSERVED UPON THE REDUCTION OF AROMATIC HYDROCARBONS IN PRESENCE OF BPO | |
| | II.1. Introduction | 15 |
| | II.2. Experimental | |
| | II.2.1. Chemicals, Solvents, and Gases | 16 |
| | II.2.2. Equipment | 17 |
| | II.3. Results and Discussion | 20 |
| III. | MIXED SYSTEMS AND ENERGY TRANSFER | |
| | III.1. Introduction | 29 |
| | III.2. Experimental | 31 |
| | III.3. Results and Discussion | |
| | III.3.1. Mixtures Involving Rubrene | 34 |
| | III.3.2. Mixtures of Fluoranthene with Anthracene, Coronene, and 9,10-DPA | 38 |




Reproduced with permission of the copyright owner. Further reproduction prohibited without permission.

| CHAPTER | | PAGE |
|---|---|---|
| III (con't) | III.3.3. Mixtures of 9,10-DPA with Anthracene and Coronene | 38 |
| | III.3.4. Mixtures of Coronene and Anthracene | 39 |
| | III.4. Summary | 39 |
| IV. TIME DEPENDENCE OF *ECL* EMISSION | | |
| | IV.1. Introduction | 41 |
| | IV.2. Mechanism for Energy Sufficient Systems | 41 |
| | IV.3. Formulation of the Boundary Value Problem | 46 |
| | IV.4. Solution to the Boundary Value Problem | 49 |
| | IV.5. Experimental | |
| | IV.5.1. Chemicals, Solvents, and Gases | 54 |
| | IV.5.2. Equipment | 55 |
| | IV.6. Data Reduction | 59 |
| | IV.7. Results | 79 |
| | IV.8. Discussion of Results | |
| | IV.8.1. Variable Rate Constants | 83 |
| | IV.8.2. Discussion of Excimers | 93 |
| V. CONCLUSION | | 94 |
| REFERENCES | | 95 |
| APPENDIX | | 100 |




Reproduced with permission of the copyright owner. Further reproduction prohibited without permission.

LIST OF TABLES


| TABLE | | PAGE |
|---|---|---|
| 1 | Observations of *ECL* Emission for Selected Aromatic Hydrocarbons | 23 |
| 2 | Spectroscopic and Electrochemical Data for Aromatic Compounds ($^1E^*$ and $^3E^*$ in eV and $E_a$ and $E_c$ in V. *vs.* SCE) | 24 |
| 3 | Values of $-\Delta H$ for the Anion-Cation Annihilation Reaction (in volts), $E_{o,s}$, $E_{o,t}$, and $E_{o,c}$ (in V. *vs.* SCE) | 27 |
| 4 | Luminescing Component of the Binary Mixture | 35 |
| 5 | Proposed Radical Ions Formed Which Annihilate and Their Redox Couples (in V. *vs.* SCE) | 36 |
| 6 | Proposed Excited States which are Formed by the Radical Ion Annihilation, with $-\Delta H$ (in volts) | 37 |
| 7 | Rate Constants at Various Concentrations of Fluoranthene where Total Emission was Detected | 80 |
| 8 | Rate Constants at Various Concentrations of Fluoranthene for the Emission Wavelength of 470 nm | 81 |
| 9 | Rate Constants at Various Concentrations of 9,10-Diphenylanthracene for the Emission Wavelength of 435 nm | 82 |




Reproduced with permission of the copyright owner. Further reproduction prohibited without permission.

LIST OF FIGURES


| FIGURE | | PAGE |
|---|---|---|
| 1 | Molecular Orbital Diagrams Representation of Electron Transfer Luminescence | 5 |
| 2 | The Electrochemical Cell for *ECL* | 18 |
| 3 | Schematic for *ECL* Spectrum Collection System | 21 |
| 4 | *ECL* Spectra of Aromatic Hydrocarbons Recorded in nm vs Relative Intensity: (a) anthracene; (b) fluoranthene; (c) 9,10-DPA; (d) rubrene; and (e) coronene | 32 |
| 5 | An Example of an Intensity versus Time Plot | 42 |
| 6 | Schematic for *ECL* Intensity-Time Collection System | 56 |
| 7 | An Example of a Record of the Raw Data from a Magnetic Tape | 60 |
| 8 | A Listing of the Computer Program which Changes the Raw Data into a Formatted Form | 63 |
| 9 | An Example of the Formatted Data Submitted to the Analysis Program | 68 |
| 10 | The User Supplied Subprogram | 71 |
| 11 | An Example of the Results from the Analysis Program | 76 |
| 12 | Log-Log Plot of Fluoranthene Concentration and the Rate Constant for Triplet Formation (Standard Error = $9.0 \times 10^{-2}$) | 84 |
| 13 | Log-Log Plot of Fluoranthene Concentration and the Rate Constant for Cation Formation (Standard Error = $3.5 \times 10^{-1}$) | 86 |
| 14 | Log-Log Plot of DPA Concentration and the Rate Constant for Triplet Formation (Standard Error = $3.8 \times 10^{-2}$) | 88 |




Reproduced with permission of the copyright owner. Further reproduction prohibited without permission.

FIGURE PAGE

15 Log-Log Plot of DPA Concentration and the Rate Constant for Cation Formation (Standard Error = $3.9 \times 10^{-2}$) 90

16 The Intensity-Time Plots of $1.10 \times 10^{-5}$ M Fluoranthene Collected Using the Total Emission Band for (a) Raw Data, (b) "Fixed" Smoothed Data, and (c) Composite of "Fixed" Smoothed Data and Fitted Data (open squares) 101

17 The Intensity-Time Plots of $2.76 \times 10^{-5}$ M Fluoranthene Collected Using the Total Emission Band for (a) Raw Data, (b) "Fixed" Smoothed Data, and (c) Composite of "Fixed" Smoothed Data and Fitted Data (open squares) 105

18 The Intensity-Time Plots of $6.91 \times 10^{-5}$ M Fluoranthene Collected Using the Total Emission Band for (a) Raw Data, (b) "Fixed" Smoothed Data, and (c) Composite of "Fixed" Smoothed Data and Fitted Data (open squares) 109

19 The Intensity-Time Plots of $1.74 \times 10^{-4}$ M Fluoranthene Collected Using the Total Emission Band for (a) Raw Data, (b) "Fixed" Smoothed Data, and (c) Composite of "Fixed" Smoothed Data and Fitted Data (open squares) 113

20 The Intensity-Time Plots of $4.32 \times 10^{-4}$ M Fluoranthene Collected Using the Total Emission Band for (a) Raw Data, (b) "Fixed" Smoothed Data, and (c) Composite of "Fixed" Smoothed Data and Fitted Data (open squares) 117

21 The Intensity-Time Plots of $1.08 \times 10^{-3}$ M Fluoranthene Collected Using the Total Emission Band for (a) Raw Data, (b) "Fixed" Smoothed Data, and (c) Composite of "Fixed" Smoothed Data and Fitted Data (open squares) 121



Reproduced with permission of the copyright owner. Further reproduction prohibited without permission.

FIGURE PAGE

22 The Intensity-Time Plots of $2.70 \times 10^{-3}$ M Fluoranthene Collected Using the Total Emission Band for (a) Raw Data, (b) "Fixed" Smoothed Data, and (c) Composite of "Fixed" Smoothed Data and Fitted Data (open squares) 125

23 The Intensity-Time Plots of $1.10 \times 10^{-5}$ M Fluoranthene Collected at the Wavelength of 470 nm for (a) Raw Data, (b) "Fixed" Smoothed Data, and (c) Composite of "Fixed" Smoothed Data and Fitted Data (open squares) 129

24 The Intensity-Time Plots of $1.08 \times 10^{-3}$ M Fluoranthene Collected at the Wavelength of 470 nm for (a) Raw Data, (b) "Fixed" Smoothed Data, and (c) Composite of "Fixed" Smoothed Data and Fitted Data (open squares) 133

25 The Intensity-Time Plots of $2.70 \times 10^{-3}$ M Fluoranthene Collected at the Wavelength of 470 nm for (a) Raw Data, (b) "Fixed" Smoothed Data, and (c) Composite of "Fixed" Smoothed Data and Fitted Data (open squares) 136

26 The Intensity-Time Plots of $7.46 \times 10^{-6}$ M DPA Collected at the Wavelength of 435 nm for (a) Raw Data, (b) "Fixed" Smoothed Data, and (c) Composite of "Fixed" Smoothed Data and Fitted Data (open squares) 141

27 The Intensity-Time Plots of $3.73 \times 10^{-5}$ M DPA Collected at the Wavelength of 435 nm for (a) Raw Data, (b) "Fixed" Smoothed Data, and (c) Composite of "Fixed" Smoothed Data and Fitted Data (open squares) 145



Reproduced with permission of the copyright owner. Further reproduction prohibited without permission.

FIGURE PAGE

28 The Intensity-Time Plots of $1.86 \times 10^{-4}$ M DPA Collected at the Wavelength of 435 nm for (a) Raw Data, (b) "Fixed" Smoothed Data, and (c) Composite of "Fixed" Smoothed Data and Fitted Data (open squares) 149

29 The Intensity-Time Plots of $9.32 \times 10^{-4}$ M DPA Collected at the Wavelength of 435 nm for (a) Raw Data, (b) "Fixed" Smoothed Data, and (c) Composite of "Fixed" Smoothed Data and Fitted Data (open squares) 153

30 The Intensity-Time Plots of $4.66 \times 10^{-3}$ M DPA Collected at the Wavelength of 435 nm for (a) Raw Data, (b) "Fixed" Smoothed Data, and (c) Composite of "Fixed" Smoothed Data and Fitted Data (open squares) 157



Reproduced with permission of the copyright owner. Further reproduction prohibited without permission.

# ENERGY TRANSFER AND KINETIC STUDIES OF ELECTROCHEMILUMINESCENCE OF AROMATIC HYDROCARBONS

by

Thomas David Santa Cruz

An Abstract

Of a dissertation submitted in partial fulfillment of the requirements for the degree of Doctor of Philosophy in the Department of Chemistry in the University of South Florida

December, 1976

Major Professor: Associate Professor Daniel L. Akins



Reproduced with permission of the copyright owner. Further reproduction prohibited without permission.

ABSTRACT

A proposed reaction mechanism is examined for the generation of electrochemiluminescence as a consequence of the electroreduction of an aromatic hydrocarbon in the presence of a bulk oxidant precursor, benzoyl peroxide (BPO). The reduced aromatic hydrocarbon, a radical anion, induces the decomposition of the bulk oxidant precursor into a reactive radical oxidant, the benzoyloxy radical. When the benzoyloxy radical oxidizes a radical anion to the neutral species, there exists an excess of energy in the reaction which is sufficient to cause the neutral aromatic hydrocarbon to be electronically excited to the triplet energy state. The triplet state molecule then reacts with BPO forming the cation radical of the aromatic hydrocarbon. The cation radical undergoes an annihilation reaction with an anion radical producing two neutral molecules of the aromatic hydrocarbon. However, there exists sufficient excess energy in this reaction to excite one of the molecules to an electronically excited state. If the amount of this excess energy is large enough, then the lowest excited singlet state is produced and luminescence is detected from its radiant decay; otherwise a triplet state is formed, again. As the population of triplet molecules increases triplet-triplet annihilation occurs producing an excited singlet state and a ground state molecule, the former luminescing.



Reproduced with permission of the copyright owner. Further reproduction prohibited without permission.

A mechanism is postulated as the result of several logical premises; this is followed by experimental evidence testing these premises. Electrochemiluminescence is observed for a variety of aromatic hydrocarbons and binary mixtures of aromatic hydrocarbons. Finally, a mathematical derivation of the time dependency of the emission intensity is presented based on the mechanism. Experimental intensity-time data are fitted by means of a nonlinear least squares analysis to the derived intensity-time function.The analysis of the results indicates: the triplet species undergoes a quenching reaction which does not lead to luminescence, and the induced decomposition of BPO and the anion-cation annihilation reaction are diffusion controlled.

Abstract approved: Daniel L. Akins

Major Professor
Daniel L. Akins
Associate Professor
Department of Chemistry

Oct. 19, 1976

Date of Aproval



Reproduced with permission of the copyright owner. Further reproduction prohibited without permission.

# I. INTRODUCTION

## I.1. General Electrochemiluminescence

Many atoms and molecules exhibit luminescence (radiative decay from excited electronic states) and the means by which the excitation is achieved has been used to classify the various types of luminescence. A comprehensive discussion of luminescence is presented by Harvey [1]; his listing includes candoluminescence, pyroluminescence, thermoluminescence, phosphorescence, and many more.

Quite often studies of luminescence provide information about the composition of the emitting system and information about the processes that take place prior to and after the excitation. In recent years considerable interest has been centered on reactions that convert chemical energy into light (chemiluminescence), of these considerable interest has been given to the reactions leading to a particular type of chemiluminescence of aromatic hydrocarbons in polar aprotic solvents, where the emitting species is the product of a homogeneous electron transfer reaction between electrochemically generated radical anions and a bulk oxident. Such luminescence is termed electrogenerated chemiluminescence (*ecl*). A considerable amount of attention has focused on *ecl* since its recent detection [2-4] and has led to a series of outstanding review articles [5-10]. Studies of *ecl* have traditionally utilized two electrolytic techniques: an alternating current electrolysis [2,4] or a

Reproduced with permission of the copyright owner. Further reproduction prohibited without permission.

direct current electrolysis [3]. In both of these techniques, the radical anion and radical cation are generated and subsequently undergo electron transfer annihilation to produce an excited molecule and a ground state molecule. The alternating current technique is one in which the potential at a single working electrode is repetitively stepped positive and negative, creating first one radical ion and then its complement. The direct current technique involves two electrodes in very close proximity; at one electrode the radical anion is produced and at the other electrode radical cation is produced. The ions mix by diffusion or some other form of mass transfer. The alternating current technique produces an emission which is periodic, while the direct current technique produces a steady-state emission.

Recently, Chandross and Sonntag [11,12] generated chemiluminescene from radical anions by chemical means. The procedure was to produce a solution of radical anions by the stoichiometric (1:1) addition of potassium metal to a solution containing the aromatic hydrocarbon, and then to add to this solution an oxidizing agent. Upon the addition of the oxidizing agent, luminescence was observed. Chandross and Sonntag reported several oxidizing agents: 9,10-dichloro-9,10-diphenylanthracene ($DPACl_2$), benzoyl peroxide (BPO), p-toluenesulfonyl chloride, p-toluenesulfonic acid anhydride, oxalyl chloride, mercuric chloride, aluminium chloride, and chlorine. Shortly thereafter, Weller and Zachariasse [13] reported similar results using the perchlorate salt of the cation radical of tetramethyl-p-phenylene diamine (Wurster's Blue Perchlorate) as the oxidizing agent. Subsequently, Livingston and Leonhardt [14] reported similar results with stannic chloride, antimony pentachloride, tetracyanoethylene, and peroxydisulfate as oxidizing agents. In all of these

Reproduced with permission of the copyright owner. Further reproduction prohibited without permission.

cases the solvents used had low dielectric constants which made electrochemical application almost impossible.

More recently, Siegel and Mark [15,16] observed *ecl* in the electrochemical reduction of 9,10-diphenylanthracene (DPA) and other aromatic hydrocarbons in the presence of $DPACl_2$ or 1,2-dibromo-1,2-diphenylethane ($DPEBr_2$). From their observations they proposed a mechanism for *ecl* which incorporates the direct formation of the excited singlet state of the emitting species. To satisfy the energetics for the systems used, they had to postulate the homogeneous generation of a very strong oxidant.

A short time later Akins and Birke [17] using BPO instead of $DPACl_2$ as the bulk oxidant precursor, reported observations similar to those of Siegel and Mark. They observed emission from several different aromatic hydrocarbons, and their binary mixtures. However, Akins and Birke suggested major modifications in the mechanism for *ecl* put forth by Siegel and Mark; they proposed the formation of excited triplets and the generation of radical cations through triplet quenching by a homogeneous oxidant.

## 1.2. The Electrochemistry of Aromatic Hydrocarbons

There are several good sources [18-21] of information on the electrochemistry of aromatic hydrocarbons in aprotic solvents. An important and unique feature of their electrochemistry is that the electron is not transferred between particular atoms or functional groups, but is transferred directly to or from the π-electron system of the entire molecule. Moreover, the reduction of aromatic hydrocarbons generally occurs in two steps: the reduction of the parent hydrocarbon to a radical anion; followed by reduction to the dianion. The reduction potential of the

Reproduced with permission of the copyright owner. Further reproduction prohibited without permission.

first step generally lies between -1.2 and -2.2 volts *versus* the saturated calomel electrode (v *vs.* SCE) and that for the second step is about 0.5 volts more negative.

The oxidation of aromatic hydrocarbons is much more complicated than the reduction. The oxidation also occurs in two steps but is not as well defined due to chemical reactions which are coupled to the rate of generation of the radical cations and dications [24,25].

Homogeneous electron transfer rate constants between the parent hydrocarbon and the radical ions have been measured [24-26]. They lie between $10^8$-$10^{10}$ $\underline{M}^{-1}$ $sec^{-1}$ and suggest that the heterogeneous electrochemical rate constants [27] lie between $10^2$ and $10^4$ cm $sec^{-1}$ (which makes the corresponding reactions essentially diffusion controlled). This fast transfer of electrons also occurs between species in systems of mixed aromatic hydrocarbons and is important since it leads to an equilibrium state in which the radical anion having the most positive polarographic couple and the radical cation with the least positive polarographic couple are the predominate species present.

Other interesting points referred to by the literature [18-20] are that in certain aprotic solvents radical ions are more stable (i.e., less reactive towards the solvents), electron transfer is enhanced, and aromatic hydrocarbons are more soluble than in aqueous solvents.

## 1.3. Energetic Considerations in *ECL*

Some of the fundamental energy requirements in *ecl* are discussed here.

A simple molecular orbital-reaction diagram to aid in this purpose is shown in Figure 1, it is intended to show changes in the electron

Reproduced with permission of the copyright owner. Further reproduction prohibited without permission.

Figure 1. Molecular Orbital Reaction Diagram Representation of Electron Transfer Luminescence.

Reproduced with permission of the copyright owner. Further reproduction prohibited without permission.

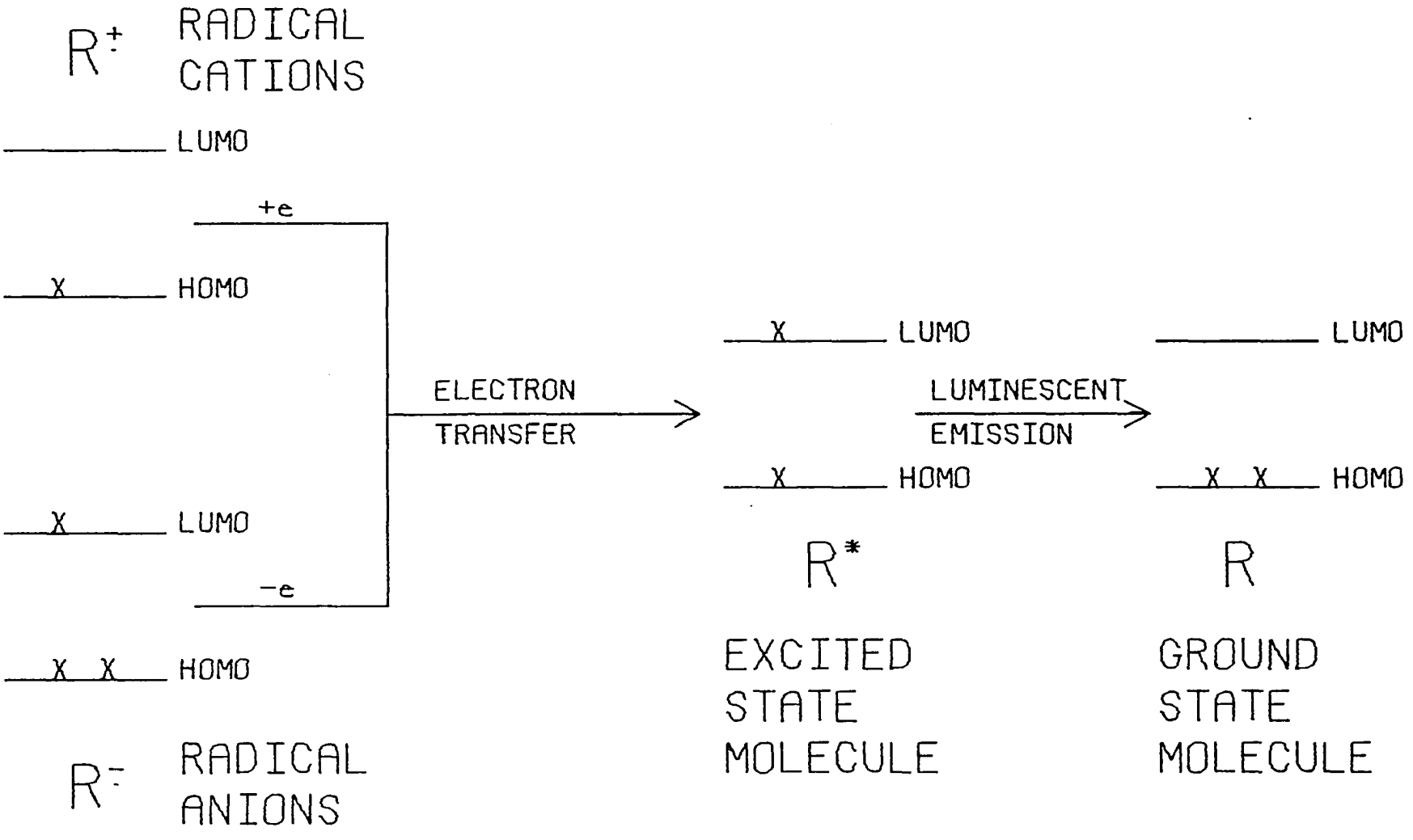


Reproduced with permission of the copyright owner. Further reproduction prohibited without permission.

state of the species and not an overall state diagram. The radical anion ($R^{\cdot -}$ in the lower left of the figure) loses an electron in an oxidation step. If there is sufficient excess energy in the enthalpy change, $-\Delta H$, then the electron can be removed from the highest occupied molecular orbital (HOMO) of the radical anion. Thus an excited state neutral molecule ($R^{*}$ in the center) is formed. In a similar way, the radical cation ($R^{\cdot +}$ in the upper left) can be reduced. Again, if there is sufficient excess energy in the enthalpy change, the electron can be placed in the lowest unoccupied molecular orbital (LUMO). And an excited state neutral molecule is formed.

The enthalpy change, $-\Delta H$, for the annihilation of radical ions can be calculated [28,29] by the following equation

$$-\Delta H = nF\ (E_c - E_a) - T\Delta S \qquad (1.3.1)$$

where $E_c$ and $E_a$ are the standard potentials for the cathodic and anodic reaction of the aromatic hydrocarbon, respectively, and $\Delta S$ is the enthropy change, and can be calculated from the expression,

$$\Delta S = \frac{nF\ \Delta(E_c - E_a)}{\Delta T} \qquad (1.3.2)$$

with an approximate value of $6.7 \times 10^{-4}$ eV/°K. The symbol n, F, and T have their standard meanings of the number of moles of electrons exchanged, Faraday constant, and temperature (°K), respectively.

In order for the annihilation of $R^{\cdot -}$ and $R^{\cdot +}$ to cause *ecl*, $-\Delta H$ must be greater than the energy of some excited state. When the $-\Delta H$ is greater than the energy required for the formation of the lowest excited singlet state, the process is termed energy sufficient. When the $-\Delta H$ is less than the energy required to form the lowest excited singlet state, yet greater than that required for the formation of the triplet state, the

Reproduced with permission of the copyright owner. Further reproduction prohibited without permission.

process is then termed energy deficient. In the case of energy deficient systems the mechanism to explain the observed *ecl* postulates that the triplet molecules ($^3R^*$) undergo triplet-triplet annihilation [5-8,68a]

$$^3R^* + {}^3R^* \rightarrow {}^1R^* + R \qquad (1.3.3)$$

to form an excited singlet molecule ($^1R^*$).

With this foundation, we proceed to a discussion of *ecl* mechanisms.

## 1.4. Mechanisms for *ECL*

There are several mechanisms postulated for *ecl* in systems containing a bulk oxidant and some emitting species [12,15-17,30].

In order to better discuss these mechanisms we shall specify here certain useful symbols and representations:

| | |
|---|---|
| R | the neutral ground state aromatic hydrocarbon; |
| $R^*$ | the excited state; |
| $^1R^*$ | the excited singlet state; |
| $^3R^*$ | the excited triplet state; |
| $R^{\cdot-}$ | the radical anion; |
| $R^{\cdot+}$ | the radical cation; |
| Ox | the bulk oxidant |
| $Ox^{\cdot-}$ | the intermediate reduction product of Ox; |
| $A^-$ | the anion decomposition product of $Ox^{\cdot-}$; |
| $B^{\cdot}$ | the radical decomposition product of $Ox^{\cdot-}$; |
| $B^-$ | reduced $B^{\cdot}$. |

Fundamental to all proposed mechanisms for *ecl* are the electrode reactions

$$R + e \rightarrow R^{\cdot-} \qquad (1.4.1)$$

and

Reproduced with permission of the copyright owner. Further reproduction prohibited without permission.

$$Ox + ne \rightarrow Products \qquad (1.4.2)$$

An apparent simple route leading to *ecl* is the direct formation of $R^*$ through electron transfer between Ox and $R^{\cdot-}$,

$$R^{\cdot-} + Ox \rightarrow R^* + Ox^{\cdot-} \qquad (1.4.3)$$

However, this reaction in order to produce an excited state (singlet or triplet) would require that the electrochemical couple for the oxidant-intermediate, $E(Ox/Ox^{\cdot-})$, be much more positive than what is known for most oxidants.

The induced homogenous generation of another stronger oxidant (e.g., from decomposition of the oxidant) is a more viable postulate. A strong radical oxidant can be generated by the two reactions,

$$R^{\cdot-} + Ox \rightarrow R + Ox^{\cdot-} \qquad (1.4.4)$$

$$Ox^{\cdot-} \rightarrow A^- + B^{\cdot} \; . \qquad (1.4.5)$$

An electron transfer reaction between the radical anion and the stronger oxidant might be expected to generate an excited state

$$R^{\cdot-} + B^{\cdot} \rightarrow R^* + B^- . \qquad (1.4.6)$$

A consideration of energetics suggests what would be the excited state. For the reaction where the excited singlet is produced,

$$R^{\cdot-} + B^{\cdot} \rightarrow {}^1R^* + B^- , \qquad (1.4.7)$$

the electrochemical couple for the radical oxidant-ion, $E(B^{\cdot}/B^-)$, must actually be of greater magnitude than the couple for the radical cation-parent, $E(R^{\cdot+}/R)$, in most cases. In this case, the reaction between the

Reproduced with permission of the copyright owner. Further reproduction prohibited without permission.

radical oxidant and the neutral aromatic hydrocarbon forming the radical cation,

$$R + B^{\cdot} \rightarrow R^{\cdot +} + B^{-}, \qquad (1.4.8)$$

would be thermodynamically favored over reaction 1.4.7 and due to the high concentrations of R and $B^{\cdot}$ would be kinetically favored as well. However, reactions 1.4.7 and 1.4.8 necessitate that the electrochemical couple $E(B^{\cdot}/B)$ be unusually large. Alternatively, the reaction where the excited triplet is produced,

$$R^{\cdot -} + B^{\cdot} \rightarrow {}^{3}R^{*} + B^{-}, \qquad (1.4.9)$$

does not impose the need for as large an electrochemical couple and is feasible on both thermodynamic and kinetic grounds. The excited state triplet molecules can undergo a triplet-triplet annihilation reaction [68b],

$${}^{3}R^{*} + {}^{3}R^{*} \rightarrow {}^{1}R^{*} + R \qquad (1.4.10)$$

followed by an emission reaction,

$${}^{1}R^{*} \rightarrow R + h\nu \qquad (1.4.11)$$

The triplet-triplet annihilation reaction is possible due to the long life of the triplet state. However, the long life can also lead to another possible reaction,

$${}^{3}R^{*} + B^{\cdot} \rightarrow R^{\cdot +} + B^{-} \qquad (1.4.12)$$

Where quenching of the triplets by the radical oxidant produces a radical cation. This reaction is thermodynamically feasible. In fact, the quenching of the triplet molecules by the bulk oxidant,

Reproduced with permission of the copyright owner. Further reproduction prohibited without permission.

$$^3R^* + Ox \rightarrow R^{\cdot +} + Ox^{\cdot -} \qquad (1.4.13)$$

is also thermodynamically feasible and more likely due to the high concentration of bulk oxidant.

With the generation of radical cations, the radical anion-cation annihilation reaction can occur,

$$R^{\cdot -} + R^{\cdot +} \rightarrow R^* + R \qquad (1.4.14)$$

For aromatic hydrocarbon systems in which radical anion-cation annihilation is energy deficient, reaction 1.4.14 is an extremely inefficient step; it is analogous to delayed fluorescence in photoluminescence.

The discussion, thus far, has dealt with the presence of only one aromatic hydrocarbon (unmixed systems). In Chapter III, the discussion widens to include the cases where more than one aromatic hydrocarbon is present (mixed systems). Presented below is a postulated mechanism for unmixed systems initially proposed by Akins and Birke [17]:

Electrode Reactions

$$R + e \rightarrow R^{\cdot -} \qquad (1.4.1)$$

$$Ox + ne \rightarrow \text{Products} \qquad (1.4.2)$$

Radical Oxidant Generations

$$R^{\cdot -} + Ox \rightarrow R + Ox^{\cdot -} \qquad (1.4.4)$$

$$Ox^{\cdot -} \rightarrow A^- + B^{\cdot} \qquad (1.4.5)$$

Triplet Generation

$$R^{\cdot -} + B^{\cdot} \rightarrow {}^3R^* + B^- \qquad (1.4.9)$$

Reproduced with permission of the copyright owner. Further reproduction prohibited without permission.

Triplet Quenching

$$^3R^* + Ox \rightarrow R^{\cdot +} + Ox^{\cdot -} \qquad (1.4.12)$$

Radical Anion-Cation Annihilation

$$R^{\cdot -} + R^{\cdot +} \rightarrow {}^{1,3}R^* + R \qquad (1.4.14)$$

Triplet-Triplet Annihilation

$$^3R^* + {}^3R^* \rightarrow {}^1R^* + R \qquad (1.4.10)$$

Luminescence Emission

$$^1R^* \rightarrow R + h\nu \qquad (1.4.11)$$

This scheme is reasonable for both energy sufficient and energy deficient systems, with triplet-triplet annihilation being unimportant in the energy sufficient case.

## 1.5. Relevant BPO Chemistry

Since BPO plays an essential role in this investigation specific mention is given here of its relevant chemistry.

The electrochemical reduction of BPO is known [31-34] to cause a homolytic cleavage of the oxygen-oxygen bond (O/O) in a two electron step producing benzoate ions. This reduction is clearly irreversible. The half wave potential for the reduction is a function of the protogenic character of the solvent. In aqueous systems, a value of +0.10 V *vs.* SCE is reported [32-34]; in 95% ethanol, a value of -0.04 V *vs.* SCE is reported [31]; in dimethylformamide (DMF) an aprotic solvent, a value of -0.04 V *vs.* SCE is reported [31].

As early as 1934, Haber and Weiss [35] had proposed a general

Reproduced with permission of the copyright owner. Further reproduction prohibited without permission.

mechanism for induced decomposition of peroxides. The Haber-Weiss mechanism postulates the induced decomposition of a peroxide by ions, molecules, or radicals which transfer one electron to the peroxide. The peroxide containing the additional electron is then postulated to heterolytically break down to form a radical plus an anion. Horner and Schwenk reported [36] the decomposition of BPO by amines in a one electron transfer step to form the benzoyloxy radical, benzoate ion, and amine product. Wieland, Ploetz, and Indest [37] reported the production of triphenylmethyl benzoate, tetraphenylmethane, and benzoic acid upon the addition of the triphenylmethyl radical to a benzene solution of BPO at room temperature. Later, Hammond, Rudesill, and Modic [38] re-examined this reaction and verified Wieland's proposed mechanism. The mechanism involved the one electron transfer to the BPO from the triphenylmethyl radical to form benzoyloxy radical and benzoate ion. Hammond pointed out that no carbon dioxide was generated.

Garst, Walmsley, and Richards [39] reported that alkali benzophenone ketyl induced a radical-anion decomposition of BPO and is evidence for step (I.4.4) and (I.4.5) in the mechanism proposed by Akins and Birke [17]. In the reaction of the radical-anion with BPO in benzene, only benzoic acid is produced and the solvent plays no part in the reaction scheme. Hartman, Sellers, and Turnbull [40] observed that the decomposition of the benzoyloxy radical is strongly affected by the temperature and the solvent, so precautions must be taken to avoid the formation of $CO_2$.

Thus the mechanism for *ecl* which we presented above involving BPO and benzoyloxy radicals as the bulk oxidant and radical oxidant, respectively, is reasonable.

Reproduced with permission of the copyright owner. Further reproduction prohibited without permission.

## 1.6. Objectives and Nature of this Study

The work presented in this dissertation is concerned with the verification of the mechanism proposed by Akins and Birke [17] for *ecl* produced as a consequence of the electroreduction of an aromatic hydrocarbon in the presence of BPO, a bulk oxidant precursor. The objectives of this study are to show that this type of chemiluminescence is observable from a large number of aromatic hydrocarbons and that the postulated elementary reactions are essential.

Reproduced with permission of the copyright owner. Further reproduction prohibited without permission.

# II. *ECL* OBSERVED UPON THE REDUCTION OF AROMATIC HYDROCARBONS IN THE PRESENCE OF BPO

## II.1. Introduction

In surveying the literature of *ecl* of aromatic hydrocarbons, two general types of *ecl* have been investigated. The more widely studied type is that resulting when the radical anions and cations are electrolytically generated and undergo radical anion-cation annihilation to produce an excited state molecule [3-9]. The second type of *ecl* involves the reduction of the aromatic hydrocarbon in the presence of a bulk oxidant at an electrode without the electrolytic generation of radical cations. This second type of *ecl* has received only minor attention [15-17,30,41,42].

The bulk oxidants which have been used are $DPACl_2$, $DPEBr_2$, 5,12-dibromo-5,12-dihydro-5,6,11,12-tetraphenylnaphthacene ($RBr_2$) and BPO. An intrinsic disadvantage of the halogenated hydrocarbons for the general production of *ecl* is that they produced the radical anion of their parent compound as a product and they produced the *ecl* of their parent compound at the reduction potential of their parent compound, with the exception of $DPEBr_2$ whose parent compound does not emit [16]. The parent compound of BPO would be benzoic acid which has a very negative reduction potential and very high energy excited states and therefore BPO seemed to be a logical choice as a general purpose bulk oxidant to eliminate the problems of the parent compounds reduction.

Reproduced with permission of the copyright owner. Further reproduction prohibited without permission.

## II.2. Experimental

### II.2.1. Chemicals, Solvents, and Gases

The following aromatic hydrocarbons were received from the manufacturer with stated purity greater than or equal to 99%. The aromatic hydrocarbons were used without any further purification.

1. Carbazole, Aldrich Chemical Company.
2. Pyrene, Aldrich Chemical Company.
3. Picene, Aldrich Chemical Company.
4. Anthracene, Eastman Organic Chemicals.
5. Benzophenone, J. T. Baker Chemical Company.
6. Acridine, Eastman Organic Chemicals.
7. 9,10-Dimethylanthracene (DMA), Aldrich Chemical Company.
8. Fluoranthene, Aldrich Chemical Company.
9. 9,10-Diphenylanthracene (DPA), Aldrich Chemical Company.
10. Coronene, Aldrich Chemical Company.
11. Thianthrene, Aldrich Chemical Company.
12. Perylene, Aldrich Chemical Company.
13. Decacyclene, Professor Brian Stevens, University of South Florida.
14. Rubrene, Aldrich Chemical Company.
15. Azulene, Aldrich Chemical Company.
16. Acenaphthylene, Aldrich Chemical Company.
17. Phenylcarbazole, Aldrich Chemical Company.
18. Thioxanthene, Aldrich Chemical Company.
19. 9-Fluorenone, Aldrich Chemical Company.
20. Fluorescein, J. T. Baker Chemical Company.
21. 2,2'-Bipyridine, Eastman Organic Chemicals.
22. 9,10-Dichloranthracene (DCA), Aldrich Chemical Company.

Reproduced with permission of the copyright owner. Further reproduction prohibited without permission.

The BPO was used as received from the J. T. Baker Chemical Company. The tetraethylammonium perchlorate (TEAP) was used as received from Eastman Chemicals as the supporting electrolyte. Spectroquality N,N'-dimethylformamide (DMF) was used as received from Matheson, Coleman, and Bell. The purified dry nitrogen gas was supplied by Airco.

Lengthy and arduous purification procedures were omitted for much of these experiments because the position and relative intensities of the emission features conform to those found by others when *ecl* was observed from similar systems under strenuous purification.

Solutions of the aromatic hydrocarbon and BPO were prepared at approximately 1 mM aromatic hydrocarbon and 20 mM BPO in DMF with a supporting electrolyte concentration of 0.10 M TEAP.

II.2.2. Equipment and Procedure

The electrolysis was done in a commercial electrochemical cell (Brinkman Instruments, Model EA 880), see Figure 2. The potential was controlled by a Wenking, Model 68 FR 0.5, potentiostat which was operated in the conventional three electrode configuration. The working electrode was a rectangular platinum sheet electrode with a surface area of $\sim$1 $cm^2$. The counter electrode was a coiled platinum wire which was in an isolated compartment connected by a fine sintered glass frit. The reference electrode was a saturated calomel electrode (SCE) which was also isolated from the reaction by a salt bridge with a fine sintered glass frit at the end near the electrode.

The electrolysis cell was mounted on an optical bench where lenses were used to focus the observed emission into the entrance slits of a scanning monochromator (SPEX 1704). The intensity was detected by an photomultiplier (EMI 9558 QB) tube (PM tube) cooled to -20°C, which was

Reproduced with permission of the copyright owner. Further reproduction prohibited without permission.

Figure 2. The Electrochemical Cell for *ECL*.

Reproduced with permission of the copyright owner. Further reproduction prohibited without permission.

Reproduced with permission of the copyright owner. Further reproduction prohibited without permission.

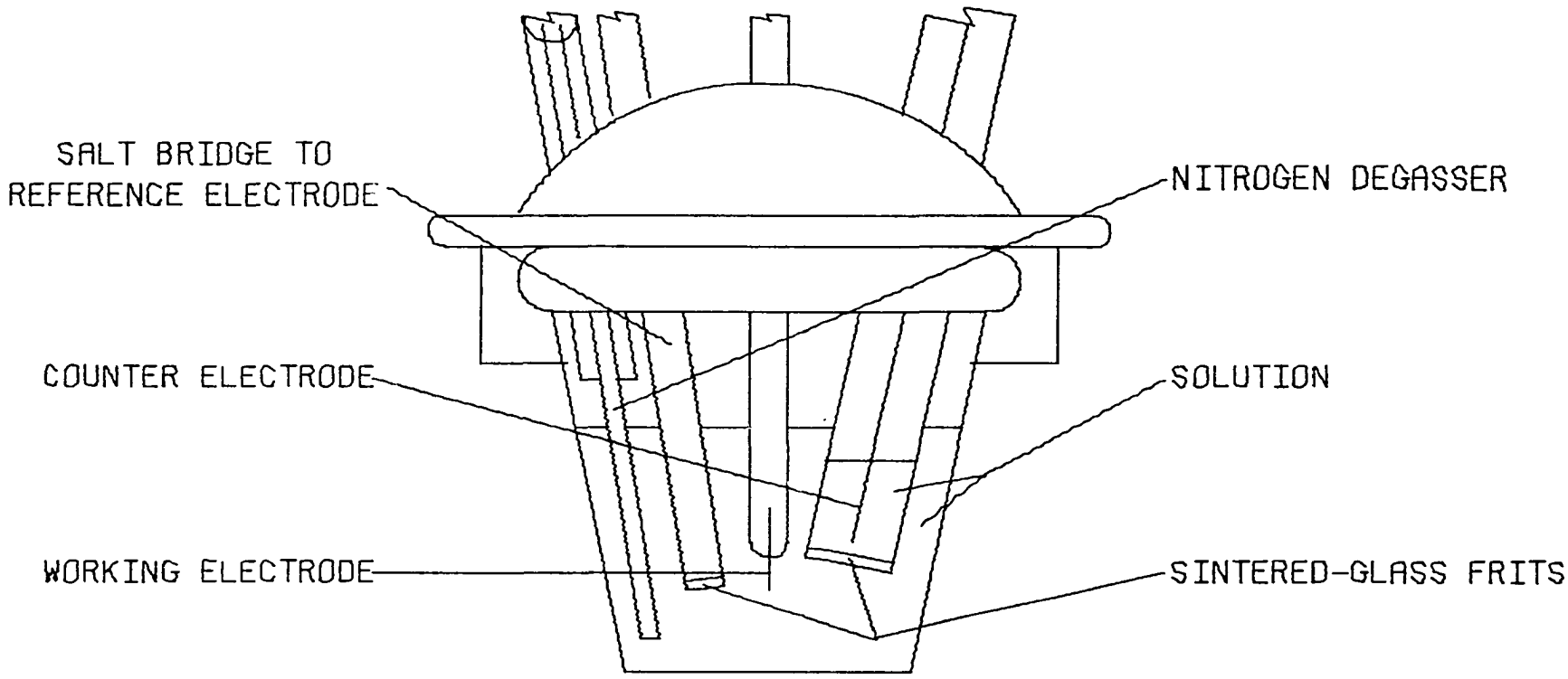

housed at the exit slit of the monochromator.

The solutions were thoroughly degassed with a stream of dry nitrogen gas before the beginning of electrolysis. During electrolysis while *ecl* was observed, a stream of dry nitrogen gas was continually and vigorously passed through the solution. This, although imprecise, convective hydrodynamic control is thought to have limited the concentration gradients to a thin Nerstian layer at the surface of the electrode.

The *ecl* spectra were recorded when the applied potential was 0.15 to 0.20 volts more negative than the reduction potential of the aromatic hydrocarbon. The slit apertures of the monochromator were set at 1.000 nm and the scan rate was 25 nm/min. The photocurrent of the detector was converted to a voltage output by either an electrometer or an integrated spike to pulse converter. The R-C time constant in both cases was approximately 7.5 seconds. A schematic of the system for recording spectra is seen in Figure 3. A record of the emission spectrum of *ecl* was recorded on a Hewlett Packard Model 7100 B strip chart recorder.

## II.3. Results and Discussion

The results of the reduction of several aromatic hydrocarbons in the presence of BPO as a test for *ecl* are shown in Table 1. In this table, the peak wavelength of the *ecl* emission is given in nanometers, otherwise if the emission was weak and unstructured or absent it is duly noted.

These results demonstrate that *ecl* is generally observed upon the electroreduction of aromatic hydrocarbons in the presence of BPO.

Spectroscopic and electrochemical data are presented for thirteen of these aromatic hydrocarbons in Table 2. The energy level of the lowest excited state of the singlet and the triplet are given in the second and

Reproduced with permission of the copyright owner. Further reproduction prohibited without permission.

Figure 3. Schematic for *ECL* Spectrum Collection System.

Reproduced with permission of the copyright owner. Further reproduction prohibited without permission.

Reproduced with permission of the copyright owner. Further reproduction prohibited without permission.

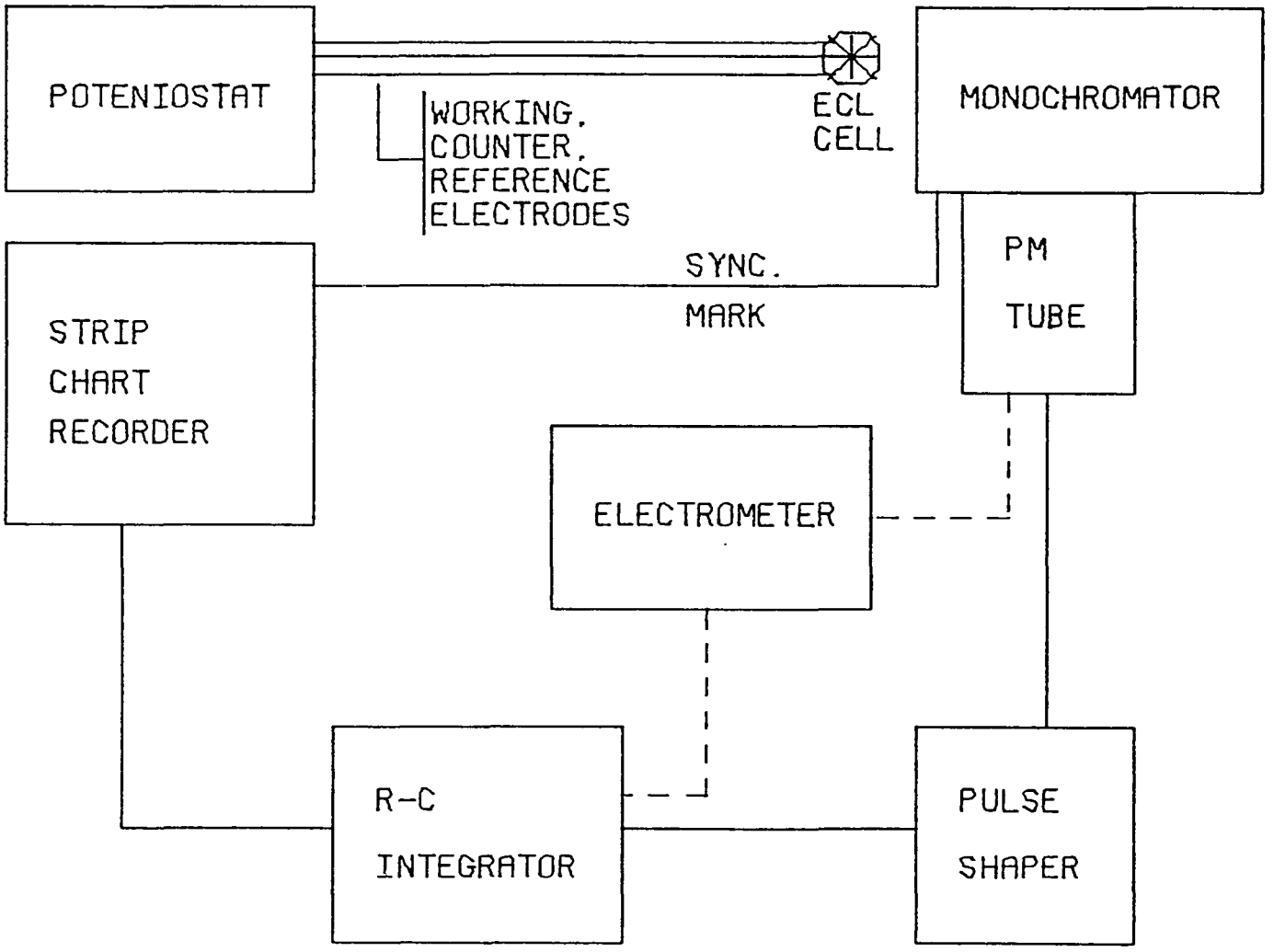

TABLE 1

Observations of *ECL* Emission for Selected Aromatic Hydrocarbons

| Chemical | Observed Emission Peak or Explanation |
|---|---|
| Carbazole | very weak emission, no distinct structure |
| Pyrene | very weak emission, no distinct structure |
| Picene | 410 nm |
| Anthracene | 450 nm |
| Benzophenone | large intersystem crossing rate [44,45] |
| Acridine | 405 nm |
| 9,10-DMA[a] | very weak emission, no distinct structure |
| Fluoranthrene | 480 nm |
| 9,10-DPA[b] | 437 nm |
| Coronene | 472 nm |
| Thianthrene | radical anion is very unstable [46] |
| Perylene | 473 nm |
| Decacyclene | 514 nm |
| Rubrene | 575 nm |
| Azulene | non-radiative decay occurs [44] |
| Acenaphthylene | the excited states are known to dimerize [47] |
| Phenylcarbazole | 370 nm |
| Thioxanthene | radical anion is very unstable [48] |
| 9-Fluorenone | large intersystem crossing rate [45] |
| Fluorescein | very weak emission, no distinct structure |
| 2,2'-Bipyridine | very weak emission, no distinct structure |
| 9,10-DCA[c] | 432 nm |

[a]DCA = dichloroanthracene

[b]DMA = dimethylanthracene

[c]DPA = diphenylanthracene

Reproduced with permission of the copyright owner. Further reproduction prohibited without permission.

TABLE 2

Spectroscopic and Electrochemical Data for Aromatic Compounds

($^1E^*$ and $^3E^*$ in eV and $E_a$ and $E_c$ in V. *vs.* SCE)

| Chemical | $^1E^*$ | $^3E^*$ | $E_a$ | $E_c$ |
|---|---|---|---|---|
| Carbazole | 4.04 [49] | 3.04 [50] | 1.16 [51] | 2.68 [6] |
| Pyrene | 3.33 | 2.08 | 1.12 | 2.09 |
| Picene | 3.30 | 2.49 | 1.33 [52] | 2.28 [13] |
| Anthracene | 3.28 | 1.82 | 1.29 | 1.92 |
| Benzophenone | 3.27 | 3.01 | - | 1.72 |
| Acridine | 3.19 | 1.96 [53] | 1.58 | 1.54 [54] |
| 9,10-DMA[a] | 3.10 | 1.80 | 0.91 [52] | 1.96 [8] |
| Fluoranthrene | 3.0 [16] | 2.29 | 1.44 | 1.74 |
| 9,10-DPA[b] | 3.0 [16] | 1.81 | 1.19 [55] | 1.84 [55] |
| Coronene | 2.95 | 2.37 | 1.23 | 2.04 |
| Thianthrene | 2.86 [56] | 2.60 [56] | 1.22 [46] | 2.54 [46] |
| Perylene | 2.85 | 1.56 | 1.01 | 1.67 |
| Rubrene | 2.36 | 1.73 [58] | 0.82 | 1.41 |

[a] DMA = dimethylanthracene

[b] DPA = diphenylanthracene

Reproduced with permission of the copyright owner. Further reproduction prohibited without permission.

third columns, respectively. The majority of this information is taken from the thesis of K. Zachariasse [28] except where noted otherwise. The electrochemical data of the polarographic oxidant and reduction potentials are given in the fourth and fifth columns, respectively. The majority of this information is taken from the Mann and Barnes [19] unless otherwise noted. An examination of the postulated mechanism can be made using the data of Table 2 and the observed results in Table 1.

Reactions of particular interest in the proposed mechanism are the annihilation reaction,

$$R^{\cdot -} + R^{\cdot +} \rightarrow R^{*} + R, \qquad (II.3.1)$$

the reaction in which the excited state is produced by the homogeneous oxidation of the radical anion by the radical oxidant,

$$R^{\cdot -} + B^{\cdot} \rightarrow R^{*} + B^{-}, \qquad (II.3.2)$$

and the reaction in which the excited triplet is quenched by an oxidant to form the radical cation,

$$^{3}R^{*} + Ox \rightarrow R^{\cdot +} + Ox^{\cdot -}. \qquad (II.3.3)$$

Thermodynamic suppositions on the feasibility of these reactions can be made based on the tabulated data and experimental observations.

A statement of whether the energetics of the reaction II.3.1, the radical ion annihilation, are energy sufficient or energy deficient can be made once the enthalpy change, $-\Delta H$, is calculated

$$-\Delta H = E_a - E_c - 0.1. \qquad (II.3.4)$$

Reproduced with permission of the copyright owner. Further reproduction prohibited without permission.

Calculated values of $-\Delta H$ for reaction II.3.1 are presented in the second column of Table 3. When the enthalpy change is greater than the energy level of the lowest excited singlet state,

$$-\Delta H > {}^1E^*, \tag{II.3.5}$$

the reaction is said to be energy sufficient. Otherwise the reaction is said to be energy deficient (i.e., so long as, $-\Delta H > {}^3E^*$). Therefore, it can be said, based on the second column, that carbazole, anthracene, acridine, 9,10-DMA, perylene, and rubrene are energy deficient and that picene, fluoranthene, coronene, and thianthrene are energy sufficient. However, there is an uncertainty of about 0.1 volts in this calculation, which is contributed by the spectroscopic and electrochemical data and the assumption that the entropy correction is 0.1 eV. This certainty clouds the issue of the energy sufficiency for pyrene and 9,10-DPA. Although other workers have assigned pyrene as being energy deficient [58] and 9,10-DPA as being energy sufficient [59].

The energetics of the reaction, the production of the excited state, II.3.2, can also be examined. In this case the enthalpy change cannot be calculated but a minium value of $\Delta H$ can be assigned from the spectroscopic data. The entropy, here, is assumed to be zero. The equations

$${}^1E^* \leq -\Delta H = E_{o,s} - E_c \tag{II.3.6}$$

and

$${}^3E^* \leq -\Delta H = E_{o,t} - E_c \tag{II.3.7}$$

are used to find $E_{o,s}$ and $E_{o,t}$ which are the minimum electrochemical potentials of the couple of the radical oxidant-ion, $E(B^{\cdot}/B^{-})$, respectively, for the formation singlet or triplet states. The evaluation of $E_{o,s}$ and $E_{o,t}$ is presented in the third and fourth columns of Table 3.

Reproduced with permission of the copyright owner. Further reproduction prohibited without permission.

TABLE 3

Values of $-\Delta H$ for the Anion-Cation Annihilation Reaction (in volts), $E_{o,s}$, $E_{o,t}$, and $E_{o,c}$ (in V. *vs.* SCE)

| Chemical | $-\Delta H$ | $E_{o,s}$ | $E_{o,t}$ | $E_{o,c}$ |
|---|---|---|---|---|
| Carbazole | 3.74 | 1.36 | 0.36 | -1.88 |
| Pyrene | 3.24 | 1.34 | -0.01 | -0.83 |
| Picene | 3.51 | 1.02 | 0.21 | -1.16 |
| Anthracene | 3.11 | 1.36 | -0.10 | -0.53 |
| Benzophenone | - | 1.55 | 1.29 | - |
| Acridine | 3.02 | 1.65 | 0.42 | -0.42 |
| 9,10-DMA[a] | 2.78 | 1.13 | -0.17 | -0.89 |
| Fluoranthrene | 3.08 | 1.40 | 0.55 | -0.85 |
| 9,10-DPA[b] | 2.93 | 1.35 | -0.03 | -0.62 |
| Coronene | 3.17 | 0.91 | 0.33 | -1.14 |
| Thianthrene | 3.66 | 1.04 | 0.78 | -1.38 |
| Perylene | 2.58 | 1.18 | -0.11 | -0.55 |
| Rubrene | 2.13 | 0.95 | 0.33 | -0.92 |

[a] DMA = dimethylanthracene

[b] DPA = diphenylanthracene

Reproduced with permission of the copyright owner. Further reproduction prohibited without permission.

There are two points here which conflict with the direct production of singlets. For every compound examined except picene, fluoranthene, coronene, and thianthrene the calculated value $E_{o,s}$ is greater than the oxidation potential of the aromatic hydrocarbons. This would imply the formation of radical cations from the neutral ground state species of the parent compound instead of reaction II.3.2. Also, from cyclic voltammetry [12,17] of benzoate an irreversible oxidation wave from +0.8 to 1.8 V *vs*. SCE is observed. This suggests that the electrochemical couple between the benzoyloxy radical ($B^{\cdot}$) and benzoate ($B^{-}$) is about +0.8 V *vs*. SCE. This potential is less than the minima $E_{o,s}$ calculated. The calculated $E_{o,t}$ values are in harmony with experimental observations except for benzophenone which, however, does not exhibit *ecl*.

A similar type of evaluation can be made for reaction II.3.3, the radical cation formation. The negative of the enthalpy change must be greater than the energy level of the lowest triplet state (i.e.,

$$^{3}E^{*} < -\Delta H = E_{a} - E_{o,c} \qquad (II.3.8)$$

where $E_{o,c}$ represents the most negative reduction potential for the bulk oxidant possible for producing the radical cation from the excited triplet). The evaluation of $E_{o,c}$ is more negative than the reduction potential of BPO (-0.4 *vs*. SCE) for all the cases examined; this evidence lends credence to the formation of the radical cation.

In summary, *ecl* produced by the electroreduction of aromatic hydrocarbons in the presence of BPO is observed in a large number of cases, the *ecl* observed in these cases is consistent with our postulated mechanism. It is also shown that the direct production of the singlet state, as proposed in other mechanisms, is not feasible since the potential required for the redox couple of the radical oxidant would have to be very large.

Reproduced with permission of the copyright owner. Further reproduction prohibited without permission.

# III. MIXED SYSTEMS AND ENERGY TRANSFER

## III.1. Introduction

*Ecl* [17,61-74] and chemiluminescence [13,28,65-67] have been observed for mixed systems (i.e., systems having two or more aromatic hydrocarbons present). A considerable amount of information about the mechanism can be revealed by the use of mixed systems, and various types of energy transfer are involved.

The electron exchange rates of aromatic hydrocarbons are diffusion controlled as discussed in section I.2. The reactions

$$R_1^{\cdot -} + R_2 \rightleftarrows R_1 + R_2^{\cdot -} , \qquad (III.1.1)$$

and

$$R_1^{\cdot +} + R_2 \rightleftarrows R_1 + R_2^{\cdot +} , \qquad (III.1.2)$$

are equilibrium reactions where $R_1$ and $R_2$ represent different aromatic hydrocarbons. The Nernst equations can be written for reactions III.1.1 and III.1.2 above,

$$[R_2^{\cdot -}] = \frac{[R_1^{\cdot -}][R_2]}{[R_1]} \exp\left\{\frac{nF}{rT}\left[E(R_1/R_1^{\cdot -}) - E(R_2/R_2^{\cdot -})\right]\right\} \qquad (III.1.3)$$

$$[R_2^{\cdot +}] = \frac{[R_1^{\cdot +}][R_2]}{[R_1]} \exp\left\{\frac{nF}{rT}\left[E(R_2^{\cdot +}/R_2) - E(R_1^{\cdot +}/R_1)\right]\right\} \qquad (III.1.4)$$

where the representation E(o/r) stands for the redox couple of the reduction reaction,

$$o + e^- \rightarrow r .$$

Reproduced with permission of the copyright owner. Further reproduction prohibited without permission.

This is a reassertion of the fact that there should be only one species of radical anion, in a mixed system, that being the one with the least negative redox reduction couple and there will be only one species of radical cation present that being the one with the least positive redox oxidation couple.

Apart from the redox type of energy transfer, there can be energy transfer by the electronically excited states. The basic energy transfer reactions which must be examined are

$$^1R_1^* + R_2 \rightarrow R_1 + {}^1R_2^* \qquad \text{(III.1.5)}$$

and

$$^3R_1^* + R_2 \rightarrow R_1 + {}^3R_2^* \; . \qquad \text{(III.1.6)}$$

These reactions can occur by means of either of two processes: collisional transfer or radiative transfer.

Since the excited singlet states have a very short lifetime before radiative decay, collisional transfer of energy is negligible. Radiative transfer of energy between singlet states is possible, but the critical concentrations required [68b] for such a process to be observed are significantly greater than the concentrations used in these studies. The excited triplet state is much longer lived than the excited singlet state, and collisional transfer processes are important. In all the collisional encounters between excited triplets and other aromatic hydrocarbons, the triplet energy can be transferred to the aromatic hydrocarbon having the lower triplet energy level. The radiative transfer of the excited triplet state is normally negligible because of the low absorption intensity of acceptors for singlet to triplet transitions.

In these mixed systems, another type of energy transfer can occur

Reproduced with permission of the copyright owner. Further reproduction prohibited without permission.

which is the mixed annihilation of radical ions. This is represented by the reaction shown below,

$$\left.\begin{array}{c} R_1^{\cdot +} + R_2^{\cdot +} \\ \text{or} \\ R_1^{\cdot +} + R_2^{\cdot -} \end{array}\right\} \rightarrow (R_1R_2)^{*} \rightarrow \left\{\begin{array}{c} R_1^{*} + R_2 \\ \text{or} \\ R_1 + R_2^{*} \end{array}\right. \qquad \text{(III.1.7)}$$

In this reaction, an exciplex $(R_1R_2)^{*}$ is formed, which is short lived. Upon the dissociation of the exciplex the aromatic hydrocarbon with the lower excited singlet level (in the case of energy sufficiency) is excited, or the aromatic hydrocarbon with the lower excited triplet (in the case of energy deficiency) remains in the excited state. The lifetimes of the exciplex species in these studies is assumed to be short lived, since no exciplex emission is observed. Other workers [13,28, 55,64-67] have observed and characterized exciplexes, but they used solvents which have lower dielectric constants and thereby prolong the exciplex lifetimes.

## III.2. Experimental

This experimental is essentially the same as in section II.2. The solvent used was DMF with 0.10 M TEAP used as the supporting electrolyte and 0.020 M BPO used as the bulk oxidant. The aromatic hydrocarbons used were all *ca.* 1 mM in concentration.

The applied potentials were 0.15 to 0.20 volts more negative than the potential requires to reduce both aromatic hydrocarbons present.

All the binary combinations of anthracene, coronene, 9,10-DPA, fluoranthracene, and rubrene were observed for *ecl* with BPO present.

Identification of the emitting species was made by spectral feature comparison. Figure 4 shows the *ecl* spectrum of each of the aromatic

Reproduced with permission of the copyright owner. Further reproduction prohibited without permission.

Figure 4. *ECL* Spectra of Aromatic Hydrocarbons Recorded in nm vs Relative Intensity: (a) anthracene; (b) fluoranthene; (c) 9,10-DPA; (d) rubrene; and (e) coronene.

Reproduced with permission of the copyright owner. Further reproduction prohibited without permission.

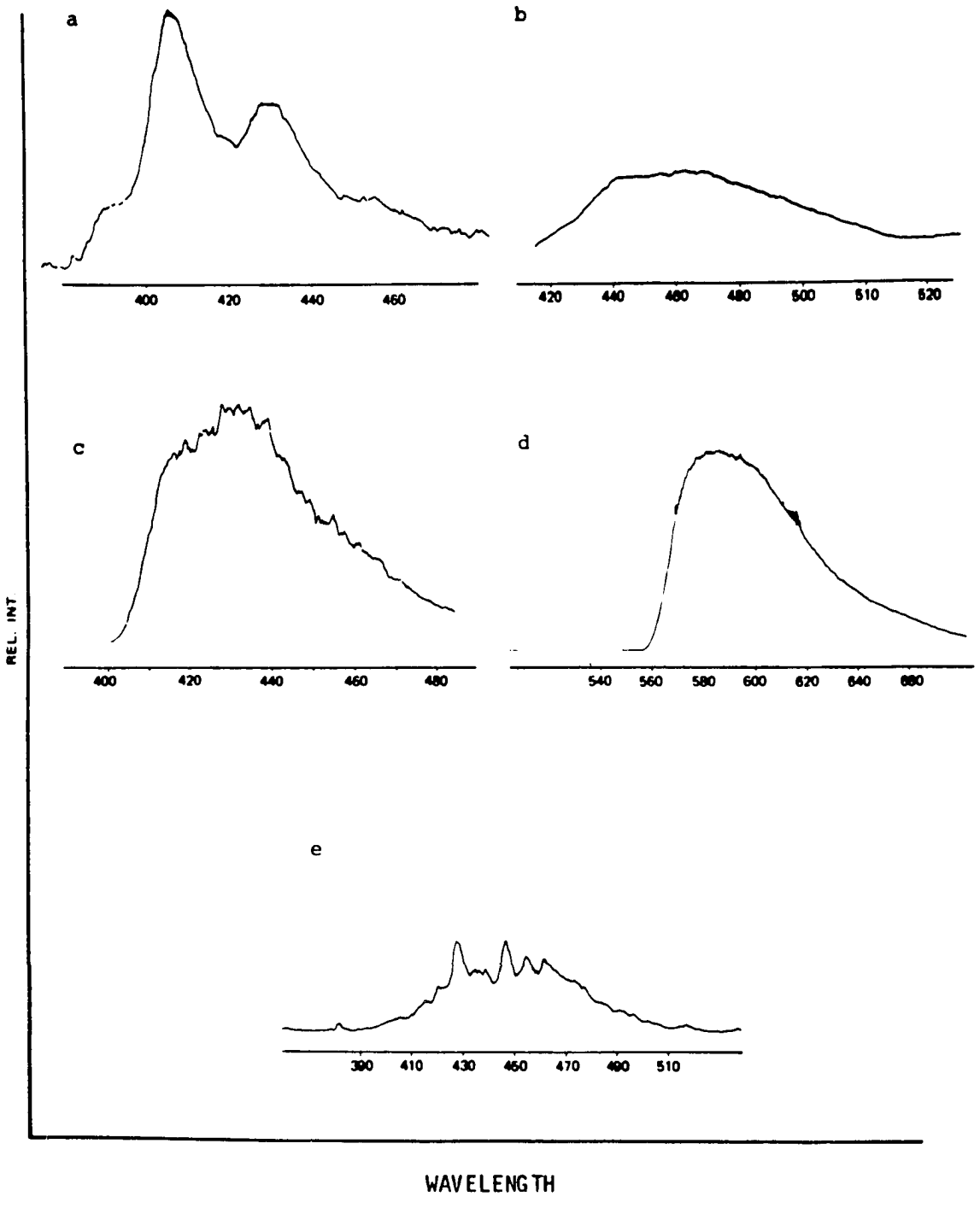


Reproduced with permission of the copyright owner. Further reproduction prohibited without permission.

hydrocarbons. It is obvious that each spectrum is reasonably characteristic. In all cases, *ecl* was observed from only one of the components of the mixtures

III.3. Results and Discussion

The resulting emissions of the binary mixtures were presented in Table 4, where the emitting species observed are indicated. These results are consistent with predictions which are made using our postulated mechanism. In Table 5, the predicted radical ion species which are predicted to be formed are shown; beneath each pair are their related polarographic potentials of reduction or oxidation in volts versus the saturated calomel electrode. Using these potentials the negative enthalpy change for the radical ion annihilation reaction was calculated; the excited state species can then be predicted. In Table 6, the predicted excited state species is shown; beneath each is given the negative enthalpy change in volts or electron volts.

III.3.1. Mixtures Involving Rubrene

In all the mixtures involving rubrene, its uniquely low oxidation and reduction potentials favor only the generation of rubrene radical ions. Their annihilation reaction is energy deficient producing the excited triplet state. No collisional transfer of triplet energy is possible due to the uniquely low triplet energy level of rubrene, and the triplets must then undergo a triplet-triplet annihilation reaction in order to produce the observed emission.

Reproduced with permission of the copyright owner. Further reproduction prohibited without permission.

Reproduced with permission of the copyright owner. Further reproduction prohibited without permission.

TABLE 4

Luminescing Component of the Binary Mixture

| | R | F | D | C |
|---|---|---|---|---|
| A | R | F | D | C |
| C | R | C | D | |
| D | R | D | | |
| F | R | | | |

A = anthracene, C = coronene, D = 9,10-DPA, F = fluoranthene, R = rubrene

Reproduced with permission of the copyright owner. Further reproduction prohibited without permission.

TABLE 5

Proposed Radical Ions Formed which Annihilate, and Their Redox Couples (in V. *vs*. SCE)

| | R | F | D | C |
|---|---|---|---|---|
| A | $R^{+\cdot}/R^{-\cdot}$ (0.82/-1.41) | $A^{+\cdot}/F^{-\cdot}$ (1.29/-1.74) | $D^{+\cdot}/D^{-\cdot}$ (1.19/-1.84) | $C^{+\cdot}/A^{-\cdot}$ (1.23/-1.92) |
| C | $R^{+\cdot}/R^{-\cdot}$ (0.82/-1.41) | $C^{+\cdot}/F^{-\cdot}$ (1.23/-1.74) | $D^{+\cdot}/D^{-\cdot}$ (1.19/-1.84) | |
| D | $R^{+\cdot}/R^{-\cdot}$ (0.82/-1.41) | $D^{+\cdot}/F^{-\cdot}$ (1.19/-1.74) | | |
| F | $R^{+\cdot}/R^{-\cdot}$ (0.82/-1.41) | | | |

A = anthracene, C = coronene, D = 9,10-DPA, F = fluoranthene, R = rubrene

Reproduced with permission of the copyright owner. Further reproduction prohibited without permission.

TABLE 6

Proposed Excited States which are formed by the Radical Ion Annihilation, with $-\Delta H$ (in volts)

| | R | F | D | C |
|---|---|---|---|---|
| A | $^3R^*$ (2.13) | $^1F^*$ (2.93) | $^1D^*$ (2.93) | $^1C^*$ (3.05) |
| C | $^3R^*$ (2.13) | $^1C^*$ (2.87) | $^1D^*$ (2.93) | |
| D | $^3R^*$ (2.13) | $^3D^*$ (2.83) | | |
| F | $^3R^*$ (2.13) | | | |

A = anthracene, C = coronene, D = 9,10-DPA, F = fluoranthene, R = rubrene

### III.3.2. Mixtures of Fluoranthene with Anthracene, Coronene, and 9,10-DPA

In the case of the mixture of fluoranthene with anthracene, the radical cation of anthracene and the radical anion of fluoranthene are formed. Their annihilation reaction is energy sufficient for the generation of the excited singlet state of fluoranthene which is observed to emit.

In the case of the mixtures of fluoranthene with coronene, the radical cations of coronene and the radical anions of fluoranthene are formed. Their annihilation reaction is energy sufficient for the generation of the excited singlet state of coronene which is observed to emit.

In the case of the mixture of fluoranthene with 9,10-DPA, the radical cations of 9,10-DPA and radical anions of fluoranthene are formed. Their annihilation reaction is energy deficient for either 9,10-DPA or fluoranthene. Therefore the excited triplet state of 9,10-DPA is generated since it has the lower triplet energy level. The triplets must undergo a triplet-triplet annihilation reaction in order to produce the excited singlet state of 9,10-DPA which is observed to emit.

### III.3.3. Mixtures of 9,10-DPA with Anthracene and Coronene

In the cases of the mixtures of 9,10-DPA with anthracene and 9,10-DPA with coronene, the radical ions of 9,10-DPA are the only ones formed. Their annihilation reaction is energy sufficient for the generation of the excited singlet state of 9,10-DPA which is observed to emit in both cases. It should be noted that coronene has a lower excited singlet energy level than 9,10-DPA, but is not involved in the annihilation ion reaction and collisional transfer does not occur.

Reproduced with permission of the copyright owner. Further reproduction prohibited without permission.

III.3.4. Mixtures of Coronene with Anthracene

In the case of the mixture of coronene with anthracene, the radical cations of coronene and the radical anions of anthracene are formed. Their annihilation reaction is energy sufficient for the generation of the excited singlet state of coronene which is observed to emit.

III.4. Summary

In summary, the results are in total agreement with the predictions using our postulated mechanism. Significant are the mixtures of 9,10-DPA with coronene and 9,10-DPA with fluoranthene. In the case of the 9,10-DPA-coronene mixture, emission is observed from 9,10-DPA which has the higher excited singlet energy level, our mechanism predicts this, others do not. In the case of 9,10-DPA-fluoranthene, compounds in which normally (unmixed systems) follow a singlet route, must in these mixtures follow an energy deficient triplet route. Neither of these mixtures had been reported in the literature.

Having extended the discussion of our postulated mechanism to mixed systems, the scheme of section I.4 should also be expanded. Below such a scheme is given subscripts i and j are used to differentiate between multiple aromatic hydrocarbons.

Electrode Reactions

$$R_i + e \rightarrow R_i^{\cdot -} \qquad \text{(III.4.1)}$$

$$R_j + e \rightarrow R_j^{\cdot -} \qquad \text{(III.4.2)}$$

$$Ox + ne \rightarrow \text{Products} \qquad \text{(III.4.3)}$$

Anion Exchange

$$R_i^{\cdot -} + R_j \rightarrow R_i + R_j^{\cdot -} \qquad \text{(III.4.4)}$$

Reproduced with permission of the copyright owner. Further reproduction prohibited without permission.

Cation Exchange

$$R_i^{+\cdot} + R_j \rightarrow R_i + R_j^{+\cdot} \qquad \text{(III.4.5)}$$

Radical Oxidant Generation

$$R_i^{-\cdot} + Ox \rightarrow R_i + Ox^{-\cdot} \qquad \text{(III.4.6)}$$

$$Ox^{-\cdot} \rightarrow A^- + B \qquad \text{(III.4.7)}$$

Triplet Generation

$$R_i^{-\cdot} + B^{\cdot} \rightarrow {}^3R_i^* + B^- \qquad \text{(III.4.8)}$$

Triplet Exchange

$${}^3R_i^* + R_j \rightarrow R_i + {}^3R_j^* \qquad \text{(III.4.9)}$$

Triplet Quenching (to form the cation)

$${}^3R_i^* + Ox \rightarrow R_i^{+\cdot} + Ox^{-\cdot} \qquad \text{(III.4.10)}$$

Radical Anion-Cation Annihilation

$$R_{i,j}^{-\cdot} + R_{i,j}^{+\cdot} \rightarrow {}^{1,3}R_{i,j}^* + R_{i,j} \qquad \text{(III.4.11)}$$

Triplet-Triplet Annihilation

$${}^3R_i^* + {}^3R_i^* \rightarrow {}^1R_i^* + R_i \qquad \text{(III.4.12)}$$

Luminescence Emission

$${}^3R_i^* \rightarrow R_i + h\nu \qquad \text{(III.4.13)}$$

This scheme explains both energy sufficient and energy deficient cases. It is also general enough to describe mixed and unmixed systems of aromatic hydrocarbons.

Reproduced with permission of the copyright owner. Further reproduction prohibited without permission.

# IV. TIME DEPENDENCE OF *ECL* EMISSION

## IV. 1. Introduction

The temporal dependency of the *ecl* emission intensity is clearly an important check of any proposed mechanism for *ecl*. The intensity can be measured as a function of time, and is illustrated in Figure 5. Characteristic to the observation is the slow rise of the intensity to a peak and then even slower decay of the intensity to a constant level, for the systems we have dealt with. The detailed shape can be modified by changes in the emitter species. Prior attempts have been made [30, 58,69-77] to match experimental observation with proposed mechanisms; in all of the previous cases, the digital simulation technique of Feldberg [78] was used. This technique has the limitation of being a simulation of a phenomenon, physically controlled by a number of intermediate reaction processes which cannot be properly accounted for. In this chapter, the postulated mechanism for *ecl*, which was based on Akins and Birke's mechanism [17], is used to formulate an intensity-time function which is fitted to the experimental data and returns rate constants for the specific elementary steps in the mechanism.

## IV.2. The Mechanism for Energy Sufficient Systems

The *ecl* mechanism postulated to specify the important heterogeneous and homogeneous chemical reactions in an energy sufficient system in which radical ions are generated in the presence of BPO are shown below:

Reproduced with permission of the copyright owner. Further reproduction prohibited without permission.

Figure 5. An Example of an Intensity versus Time Plot

Reproduced with permission of the copyright owner. Further reproduction prohibited without permission.

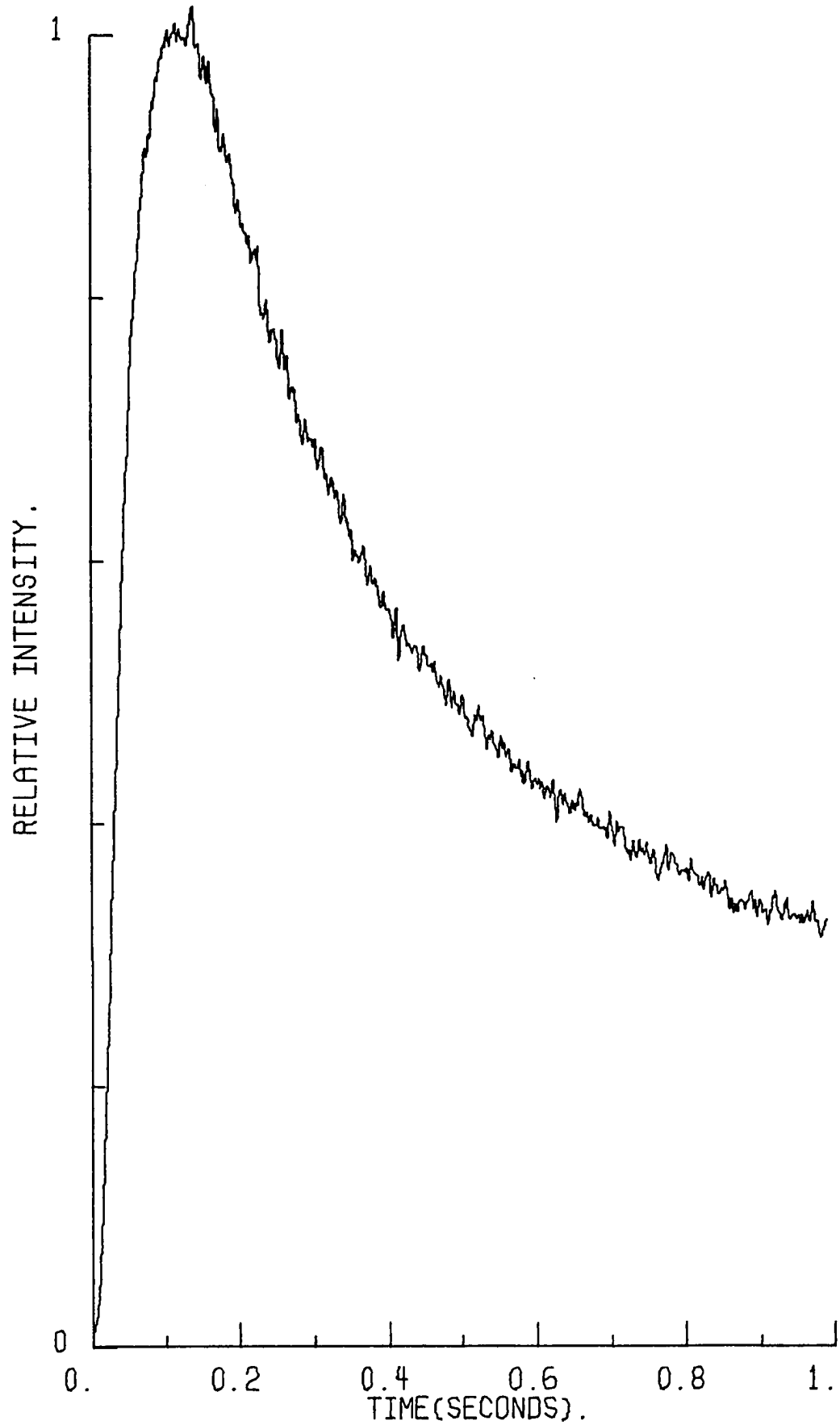


Reproduced with permission of the copyright owner. Further reproduction prohibited without permission.

$$R + e^- \xrightarrow{k_1} R^{\cdot-} \qquad (IV.2.1)$$

$$BPO + 2e^- \xrightarrow{k_2} 2B^- \qquad (IV.2.2)$$

$$R^{\cdot-} + BPO \xrightarrow{k_3} R + BPO^{\cdot-} \qquad (IV.2.3)$$

$$BPO^{\cdot-} \xrightarrow{k_4} B^- + B^{\cdot} \qquad (IV.2.4)$$

$$R^{\cdot-} + B^{\cdot} \xrightarrow{k_5} {}^3R^* + B^- \qquad (IV.2.5)$$

$${}^3R^* + BPO \xrightarrow{k_6} R^{\cdot+} + BPO^{\cdot-} \qquad (IV.2.6)$$

$$R^{\cdot+} + R^{\cdot-} \xrightarrow{k_7} {}^1R^* + R \qquad (IV.2.7)$$

$${}^1R^* \xrightarrow{k_8} R + h\nu \qquad (IV.2.8)$$

where R, $R^{\cdot+}$, $R^{\cdot-}$, $^1R^*$, $^3R^*$, and $BPO^{\cdot-}$ have their previous meaning and $B^-$ and $B^{\cdot}$ are, respectively, the benzoate ion and the benzoyloxy radical of the BPO radical intermediate decomposition.

It is known that several of the above elementary reactions have very large rate constants, and hence, for reasonable concentration levels, occur quite rapidly. By coupling the reactions with faster reaction rates to those with slower reaction rates, the number of reactions and reactant species are reduced. The reaction process described by coupling two reactions has the reaction rate of the rate determining step (i.e., the slower process). The disproportionation of the BPO intermediate and the

Reproduced with permission of the copyright owner. Further reproduction prohibited without permission.

luminescence emission, reactions IV.2.4 and IV.2.8, respectively, are the reactions which are known to have fast reaction rates. Thereby, the combining of reactions IV.2.3 and IV.2.4, respectively, the formation of the radical intermediate and its disproportionation by the radical anion, gives

$$R^{\cdot -} + BPO \xrightarrow{k_3} R + B^- + B^{\cdot} \ , \qquad (IV.2.9)$$

while combining reactions IV.2.4 and IV.2.6, this time the formation and disproportionation of the B radical intermediate by the triplet, gives

$$^3R^* + BPO \xrightarrow{k_6} R^{\cdot +} + B^- + B^{\cdot} \ , \qquad (IV.2.10)$$

and combining reactions IV.2.7 and IV.2.8, respectively, the excited singlets formation and its luminescent emission, give

$$R^{\cdot +} + R^{\cdot -} \xrightarrow{k_7} 2R + h\nu \ . \qquad (IV.2.11)$$

In this description of the processes leading to *ecl* the quenching of reactive species has been totally ignored. This is done with the intent of eliminating complications, the inclusion of possible quenching reactions would be collossal. Besides the physical and chemical quenching of the electronically excited states, there can also be quenching of the free radicals by impurities to consider. The specific impurities and their concentrations are not known. The omission of these reactions definitely introduces a source of error. It also introduces a clear hierarchy of cumulative reaction efficiencies due to the order of reaction processes. A visualization of the *ecl* process by a verbal discussion should make this concept clearer. Initially, at the time before the electrode is stepped from an electroinactive to an electroactive potential, the solution contains the bulk concentrations

Reproduced with permission of the copyright owner. Further reproduction prohibited without permission.

of the aromatic hydrocarbon and the BPO. After the electrode potential is stepped to an electroactive potential, in which both the aromatic hydrocarbon and the BPO are reduced at the electrode surface. The rates of the reduction reactions are controlled by the diffusion of the aromatic hydrocarbon and the BPO up to the electrode surface and their respective reduction products away from the electrode surface. Of the reduction products only the radical anion of the aromatic hydrocarbon is significant, it forms a gradient of concentration from the electrode out into the solution bulk. In specific volume elements there the radical anion is oxidized by the BPO yielding the principle products of the radical oxidant and the neutral ground state aromatic hydrocarbon. This reaction is the major source of the highly reactive radical oxidant which oxidizes another radical anion. This time the neutral species is excited to a triplet energy state. The triplet state can be further oxidized to the radical cation by the abundant BPO present, also generated is radical oxidant. The radical cation and a radical anion then undergo annihilation producing the neutral species and a photon.

Important to realize in the above description is that $R^{\cdot -}$ concentration is in a spacial gradient which diminishes as one moves away from the electrode surface. The BPO concentration is seen to be constant over the volume elements of chemical activity. The species $^{3}R^{*}$, $R^{\cdot +}$, and $B^{\cdot}$ are generated in a localized volume element and are consumed in that element.

## IV.3. Formulation of the Boundary Value Problem

The expression for the *ecl* intensity as a function of time is also a function of the kinetic rate constants and concentrations of the

Reproduced with permission of the copyright owner. Further reproduction prohibited without permission.

initial species. The solution of the full time and spatial dependent boundary-value problem provides such an expression. The mass transfer-reaction rate expression for the heterogeneous processes and the reaction rate expressions for the homogeneous processes which were described earlier in this chapter are given below.

$$\frac{\partial C_R}{\partial t} = D_R \frac{\partial^2 C_R}{\partial x^2} + k_3 C_R\text{-} C_{BPO} + k_7 C_R\text{-} C_R+ \qquad \text{(IV.3.1)}$$

$$\frac{\partial C_{BPO}}{\partial t} = D_{BPO} \frac{\partial^2 C_{BPO}}{\partial x^2} - k_3 C_R\text{-} C_{BPO} - k_6 C_R C_{BPO} \qquad \text{(IV.3.2)}$$

$$\frac{\partial C_R\text{-}}{\partial t} = D_R\text{-} \frac{\partial^2 C_R\text{-}}{\partial x^2} - k_3 C_R\text{-} C_{BPO} - k_5 C_R\text{-} C_B - k_7 C_R\text{-} C_R+ \qquad \text{(IV.3.3)}$$

$$\frac{\partial C_B}{\partial t} = k_3 C_R\text{-} C_{BPO} + k_6 C_{3_R} C_{BPO} - k_5 C_R\text{-} C_B \qquad \text{(IV.3.4)}$$

$$\frac{\partial C_{3_R}}{\partial t} = k_5 C_R\text{-} C_B - k_6 C_{3_R} C_{BPO} \qquad \text{(IV.3.5)}$$

and

$$\frac{\partial C_R+}{\partial t} = k_6 C_{3_R} C_{BPO} - k_7 C_R\text{-} C_R+ \qquad \text{(IV.3.6)}$$

where $C_R$, $C_{BPO}$, $C_R\text{-}$, $C_B$, $C_{3_R}$, and $C_R+$ represent the concentrations of R, BPO, $R^{\cdot}$, $B^{\cdot}$, $^3R^*$, and $R^+$ and $D_R$, $D_{BPO}$, and $D_R\text{-}$ represent the diffusion coefficients of R, BPO, and $R^{\cdot}$, respectively.

The initial and boundary conditions for the above equations are: $C_R(x,o) = C_R^\circ$, $C_R(o,t>o) = o$; $C_{BPO}(x,o) = C_{BPO}^\circ$, $C_{BPO}(o,t>o) = o$; $C_R\text{-}(x,o) = o$, $C_{R\text{-}}(o,t>o) = C_R^\circ$; as well as, $C_B(x,o) = C_{3_R}(x,o) = C_R+(x,o) = o$; where

Reproduced with permission of the copyright owner. Further reproduction prohibited without permission.

$C_R^\circ$ and $C_{BPO}^\circ$ are the respective bulk concentrations of R and BPO.

The observed intensity of the *ecl* emission, $I_{obs}$, is directly proportional to the spacial integral of the product of the radical ions' concentrations, as shown

$$I_{obs}(t) \propto \int_0^\infty C_R^-(x,t) C_R^+(x,t)\, dx \qquad (IV.3.7)$$

Several simplifying assumptions to this rigorous description are necessary in order that the formulation of the intensity-time equation can be made. A critical assumption is that the BPO concentration is constant and equal to the initial bulk concentration of BPO. The bulk concentration is so large that its depletion by higher order reactions is negligible and its depletion at the electrode surface exists over a very small distance. Another good assumption is that all the diffusion coefficients are equal, D; this assumption is standard to problems involving mass transport. Two other necessary assumptions are that

$$k_3 C_R^- C_{BPO}^\circ >> k_5 C_R^- C_B^+ + k_7 C_R^- C_R^+ , \qquad (IV.3.8)$$

and that

$$k_3 C_R^- C_{BPO}^\circ >> k_6 C_{3R} C_{BPO} \qquad (IV.3.9)$$

since the process (reaction IV.2.3) represented on the left of the inequalities is proposed to be more efficient than the other processes represented, the concentrations of $R^\cdot$ and BPO are also in greater concentrations than the other species, and that reaction IV.3.3 is suggested to have a fast reaction rate.

With these stated assumptions, the mass transfer and reaction rate equations can be rewritten as follows;

Reproduced with permission of the copyright owner. Further reproduction prohibited without permission.

$$\frac{\partial C_R}{\partial t} = D \frac{\partial^2 C_R}{\partial x^2} + k_3 C_R - C^\circ_{BPO} \,, \tag{IV.3.10}$$

$$C_{BPO} = C^\circ_{BPO} \tag{IV.3.11}$$

$$\frac{\partial C_R^-}{\partial t} = D \frac{\partial^2 C_R^-}{\partial x^2} - k_3 C_R - C^\circ_{BPO} \tag{IV.3.12}$$

$$\frac{\partial C_B}{\partial t} = k_3 C_R - C^\circ_{BPO} + k_5 C_R - C_B \,, \tag{IV.3.13}$$

$$\frac{\partial C_{3_R}}{\partial t} = k_5 C_R - C_B - k_6 C_{3_R} C^\circ_{BPO} \,, \tag{IV.3.14}$$

and

$$\frac{\partial C_R^+}{\partial t} = k_6 C_{3_R} C^\circ_{BPO} - k_7 C_R - C_R^+ \tag{IV.3.15}$$

## IV.4. Solution to the Boundary Value Problem

The concentration of $R^-$ can be found by applying Laplace transformation techniques to equation IV.3.12. The transformation equation has a solution:

$$\bar{C}_R = c_1 \exp\left[x \left(\frac{s + k_3 C^\circ_{BPO}}{D}\right)^{\frac{1}{2}}\right] + c_2 \exp\left[-x \left(\frac{s + k_3 C^\circ_{BPO}}{D}\right)^{\frac{1}{2}}\right] \tag{IV.4.1}$$

which upon the application of the initial and boundary conditions becomes

$$\bar{C}_R^- = \frac{C^\circ_R}{s} \exp\left[-x \left(\frac{s + k_3 C^\circ_{BPO}}{D}\right)^{\frac{1}{2}}\right] . \tag{IV.4.2}$$

Reproduced with permission of the copyright owner. Further reproduction prohibited without permission.

The inverse transformation [79] of equation IV.4.2 is

$$C_R^- = \frac{C_R^\circ}{2} \exp\left[-\left(\frac{k_3 C^\circ_{BPO}}{D}\right)^{\frac{1}{2}}\right] \operatorname{erfc}\left[\frac{x}{2(Dt)^{\frac{1}{2}}} - (k_3 C^\circ_{BPO} t)^{\frac{1}{2}}\right]$$

$$\exp\left[\frac{k_3 C^\circ_{BPO})}{D}^{\frac{1}{2}}\right] \operatorname{erfc}\left[\frac{x}{2(Dt)^{\frac{1}{2}}} + (k_3 C^\circ_{BPO} t)^{\frac{1}{2}}\right] \qquad \text{(IV.4.3)}$$

where erfc is the complementary error function (i.e.,

$$\operatorname{erfc}(x) = 1 - \frac{2}{\pi^{\frac{1}{2}}} \int_0^x \exp[-t^2]dt \ .)$$

It is evident at this point that an approximation for $C_R^-$ must be made in order to continue the derivation. The assumption that a "steady state" concentration-distance profile is established

$$\lim_{t \to \infty} C_R^-(x,t) = C_R^\circ \exp\left[-x\left(\frac{k_3 C^\circ_{BPO}}{D}\right)^{\frac{1}{2}}\right] \qquad \text{(IV.4.4)}$$

at diffusion limited times or greater (i.e., $t \geq x^2/D$) and at times less than those of the diffusion limit $C_R^- = D$. Therefore, the following discontinuous function can be written for $C_R^-$:

$$C_R^-(x,t) = \begin{cases} 0 & \text{for } (t < x^2/D) \\ C_R^\circ \exp\left[-x\left(\frac{k_3 C^\circ_{BPO}}{D}\right)^{\frac{1}{2}}\right] & \text{for } (t \geq x^2/D) \end{cases} \qquad \text{(IV.4.5)}$$

The rate expressions for $B^\cdot$, $^3R^*$, and $R^{+\cdot}$ concentrations are of a general class of differential equations [80],

$$y' = f(x) + g(x)\, y \qquad \text{(IV.4.6)}$$

Reproduced with permission of the copyright owner. Further reproduction prohibited without permission.

The general solution for this class of differential equation is

$$y = c_1 \exp\left[\int_o^x g(t)dt\right] +$$

$$\exp\left[\int_o^x g(t)dt\right]\int_o^x f(t)\exp\left[-\int_o^t g(z)dz\right]dt \qquad (IV.4.7)$$

Since the initial condition for each of the species is zero then the solution is simplified to:

$$y = \exp\left[\int_o^x g(t)dt\right]\int_o^x f(t)\exp\left[-\int_o^t g(z)dz\right]dt \qquad (IV.4.8)$$

Therefore the solutions for $C_B$, $C_{3_R}$, and $C_R{}^+$ can be found:

$$C_\phi(x,t) = k_3 C^\circ_{BPO}\exp\left[-k_5\int_o^t C_R{}^-(x,\tau)d\tau\right]\int_o^t C_R{}^-(x,\tau)$$

$$\exp\left[k_5\int_o^\tau C_R{}^-(x,t')dt'\right]d\tau \,, \qquad (IV.4.9)$$

$$C_{3_R}(x,t) = k_5 \exp\left[-k_6 C^\circ_{BPO}t\right]\int_o^t C_R{}^-(x,\tau)C_B(x,\tau)\exp\left[k_6 C^\circ_{BPO}\tau\right]d\tau \,, \qquad (IV.4.10)$$

and

$$C_R{}^+(x,t) = k_6 C^\circ_{BPO}\exp\left[-k_7\int_o^t C_R{}^-(x,\tau)d\tau\right]\int_o^t C_{3_R}(x,\tau)$$

$$\exp\left[k_7\int_o^\tau C_R{}^-(x,t')dt'\right]d\tau \,. \qquad (IV.4.11)$$

Reproduced with permission of the copyright owner. Further reproduction prohibited without permission.

It is apparent here that a further approximation of $C_R^-$ is necessary for the evaluation of the above equations. By taking the first order term of a series expansion, one obtains:

$$C_R^-(x,t) = \begin{cases} o \quad \text{for } (t < x^2/D) \\ C_R^\circ \text{ for } (t > x^2/D) \end{cases} \tag{IV.4.12}$$

The evaluation of $C_B$ is possible with this $C_R^-$ approximation, and one obtains:

$$C_B(x,t) = \begin{cases} o & \text{for } (t < x^2/D) \\ \dfrac{k_3 C^\circ_{BPO}}{k_5}\left[1 - \exp\left[k_4 C_R^\circ\left(\dfrac{x^2}{D} - t\right)\right]\right] & \text{for } (t \geq x^2/D) \end{cases} \tag{IV.4.13}$$

Now knowing $C_B$, $C_{3_R}$ can be evaluated,

$$C_{3_R}(x,t) = \begin{cases} o & \text{for } (t < x^2/D) \\ \dfrac{k_3 C_R^\circ}{k_6} - \dfrac{k_3 C^\circ_{BPO} C_R^\circ}{(k_6 C^\circ_{BPO} - k_5 C_R^\circ)} \exp\left[k_5 C_R^\circ\left(\dfrac{x^2}{D} - t\right)\right] + & \\ \dfrac{k_3 k_5 C_R^{\circ 2}}{k_6 (k_6 C^\circ_{BPO} - k_5 C_R^\circ)} \exp\left[k_6 C^\circ_{BPO}\left(\dfrac{x^2}{D} - t\right)\right] & \text{for } (t \geq x^2/D) \end{cases} \tag{IV.4.14}$$

Finally, knowing $C_{3_R}$, $C_R^+$ can be evaluated,

$$C_R^+(x,t) = \begin{cases} o & \text{for } (t < x^2/D) \\ a_1 + a_2 \exp\left[k_5 C_R^\circ\left(\dfrac{x^2}{D} - t\right)\right] + & \\ a_3 \exp\left[k_6 C^\circ_{BPO}\left(\dfrac{x^2}{D} - t\right)\right] + & \\ a_4 \exp\left[k_7 C_R^\circ\left(\dfrac{x^2}{D} - t\right)\right] . & \text{for } (t \geq x^2/D) \end{cases} \tag{IV.4.15}$$

Reproduced with permission of the copyright owner. Further reproduction prohibited without permission.

where

$$a_1 = k_3 C^\circ_{BPO}/k_7$$

$$a_2 = \frac{k_3 k_6 C^{\circ\,2}_{BPO}}{(k_7 - k_5)(k_6 C^\circ_{BPO} - k_4 C^\circ_R)}$$

$$a_3 = \frac{k_3 k_5 C^{\circ 2}_R C^\circ_{BPO}}{(k_6 C^\circ_{BPO} - k_5 C^\circ_R)(k_7 C^\circ_R - k_6 C^\circ_{BPO})}$$

and

$$a_4 = -(a_1 + a_2 + a_2).$$

Since functional forms of $C_R^+$ and $C_R^-$ have been found, the observed intensity proportionality can be evaluated,

$$I_{obs}(t) \propto \begin{cases} 0 & \text{for } (t < x^2/D) \\ \dfrac{1 - \exp[-(k_3 C^\circ_{BPO} t)^{\frac{1}{2}}]}{k_7 (k_3 C^\circ_{BPO})^{\frac{1}{2}}} + & \\ \dfrac{b_1\ \mathrm{Daw}[(k_5 C^\circ_R t)^{\frac{1}{2}}]}{(k_5 C^\circ_R)^{\frac{1}{2}}} + & \text{for } (t \geq x^2/D) \\ \dfrac{b_2\ \mathrm{Daw}[(k_6 C^\circ_{BPO} t)^{\frac{1}{2}}]}{(k_6 C^\circ_{BPO})^{\frac{1}{2}}} + & \\ \dfrac{b_3\ \mathrm{Daw}\ [(k_7 C^\circ_R t)^{\frac{1}{2}}]}{(k_7 C^\circ_R)^{\frac{1}{2}}} & \end{cases} \qquad \text{(IV.4.16)}$$

where:

$$b_1 = \frac{-k_6 C^\circ_{BPO}}{(k_7 - k_5)(k_6 C^\circ_{BPO} - k_5 C^\circ_R)}$$

Reproduced with permission of the copyright owner. Further reproduction prohibited without permission.

$$b_2 = \frac{k_5 C_R^{\circ 2}}{(k_6 C_{BPO}^{\circ} - k_5 C_R^{\circ})(k_7 C_R^{\circ} - k_6 C_{BPO}^{\circ})}$$

$$b_3 = -(1/k_7 + b_1 + b_2)$$

and Daw is the Dawson function (i.e.,

$$\text{Daw}(t) = \exp[-x^2] \int_0^x \exp[t^2]dt \quad .)$$

Equation IV.4.16 is a proportionality in order to change it into an equality it must be divided onto itself at a particular time, tp,

$$I(t) = \frac{I_{obs}(t)}{I_{obs}(tp)} \quad . \qquad \text{(IV.4.17)}$$

A convenient choice of tp is the time at which there is a peak maximum in intensity. The experimental data is then normalized and tp is easily found.

## IV. 5. Experimental

### IV.5.1. Chemicals, Solvents, and Gases

Fluoranthene (Flu) and 9,10-diphenylanthracene (DPA) were the aromatic hydrocarbons used. Both were received from the Aldrich Chemical Company and used without any further purification. Their stated purities were 99% for Flu and 99.9% + for DPA. The BPO was also received from the Aldrich Chemical Company and used at stated purity of 98% without further purification. The TEAP was received from Eastman Organic Chemicals Company as the perchlorate salt or as the chloride or bromide salt and converted to the perchlorate salt [81]. The TEAP was in all cases recrystallized a minimum of twice in ethanol (100%) and dried at 50°C under vacuum in excess of five days (mp 351-352°C).

Reproduced with permission of the copyright owner. Further reproduction prohibited without permission.

Benzonitrile was the solvent used. It was received from the Aldrich Chemical Company and was distilled with only the boiling fraction between 191-192°C being retained. The benzonitrile was then stored in an air tight brown bottle over a slurry of molecular sieve and activated alumina. and the bottle remained sealed until used in order to insure dryness.

Dry nitrogen gas was used to degas the solutions free of oxygen prior to the start of an experiment and it was also used to maintain a blanket of inert gas over the solutions surface during an experiment. The nitrogen gas was used as received from Airco Products.

The solutions prepared contained varying concentrations of aromatic hydrocarbons but all the solutions contained 20.0 mM BPO and 0.100 M TEAP.

IV.5.2. Equipment

A schematic of the equipment used is shown in Figure 6.

The electrochemical cell is the same as described in section II.2.2. Also, the same counter and reference electrodes were used, however, the working electrode was changed to a platinum wire electrode of length 0.63 cm and diameter 0.075 cm, thereby having a surface area of 0.15 $cm^2$. The potential of the working electrode was controlled by a Wenking, model 68FR 0.5, potentiostat operated in the conventional three electrode configuration. The applied potential was programmed by a Hewlett Packard, model 3300A function generator. The function used was a square wave, appropriately adjusted to step from +0.15 V *vs*. SCE to 0.10 to 0.20 volts more negative than the reduction potential of the aromatic hydrocarbon.

Reproduced with permission of the copyright owner. Further reproduction prohibited without permission.

Figure 6. Schematic for *ECL* Intensity-Time Collection System.

Reproduced with permission of the copyright owner. Further reproduction prohibited without permission.

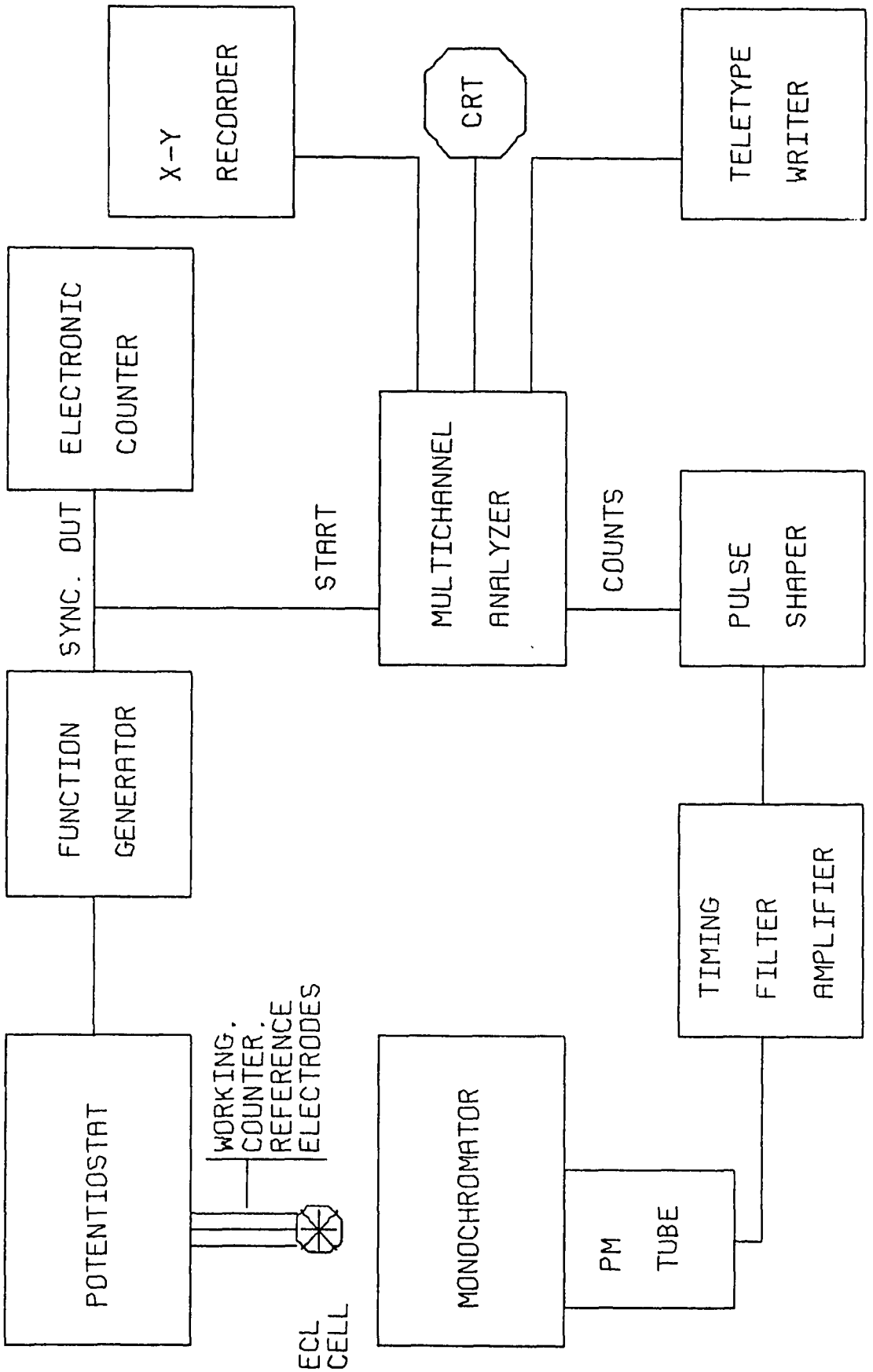


Reproduced with permission of the copyright owner. Further reproduction prohibited without permission.

The electrolysis cell was mounted on an optical bench where lenses were used to focus the emission into the entrance slits of a SPEX 1704 scanning monochromator. The slit apertures of the monochromator were set at 1.000 mm. An EMI9558QB photomultiplier tube (PM-tube), which was housed at the exit slit of the monochromator, detected the emission intensity. The PM-tube was cooled to -20°C for the purpose of minimizing thermal noise. The PM-tube transduced light photons into current spikes. They were sent to an Ortec 454 timing filter amplifier across a 50 Ω load resistor. The voltage output was then sent through a pulse-shaping and discriminating circuit [43] which discrimates against shot noise and shapes the spikes into pulses of 3 μsec duration and +3 to 10 volt amplitude. Good disparity between an average single photon pulse and an average dark or shot noise pulse was noted. The pulses were then counted by a multichannel analyzer (Nuclear Data Series 100 or Series 1100) in a multichannel scaling model. The individual channels of the multichannel analyzer's memory were used as a sequence of counters with each channel counting pulses for a predetermined dwell time. At the completion of each dwell time, the counting operation is shifted to the next channel in the memory. The result is a time histogram of the count rate data where each channel represents a sequential time interval. Since the voltage function of the applied potential is repetitive, it was possible to signal average the data over a number of cycles. The beginning of each cycle was signaled by the syncronous output of the function generator which triggered the multichannel analyzer and registered a count on an electronic counter.

The frequency of cycling was 0.10 Hz, which allowed collection every

Reproduced with permission of the copyright owner. Further reproduction prohibited without permission.

ten seconds for five seconds with a five-second relaxation time.

Upon the completion of an experiment, the multichannel analyzers offered several modes of data output, which included oscilloscope traces, x-y recorder plots, hard copy teletype printouts, and paper tapes.

## IV.6. Data Reduction

The output record of each experiment is released by the multichannel analyzer as counts per channel. The physical form of the records obtained is paper tape. Before the analysis could begin, various transformations on the data record were necessary.

The paper tape record was converted into a magnetic tape record which facilitated the handling. The record written on magnetic tape is formatted as card images; an example of this data stored on the magnetic tape is shown in Figure 7. The first card (or line) is the label which is needed as a identifier of the record as it is referenced by the computer programs and referenced to in experimental notes. The second card contains information on the instrumental parameters of a particular experiment (here e.g., 465 voltage cycles were recorded, 950 channels of the multichannel analyzer were used, the information in channel one is to be ignored, and the dwell time used was 0.8 milliseconds). The remainder of cards after the information card contained the counts for each channel. This is a serial listing from left to right, listing ten channels per card, card by card.

The next stage in preparing the data record for analysis is rewrite in a suitable format for analysis after "fix-up" criteria have been applied. At the beginning of each record, there are several

Reproduced with permission of the copyright owner. Further reproduction prohibited without permission.

Figure 7. An Example of a Record of Raw Data from Magnetic Tape.

Reproduced with permission of the copyright owner. Further reproduction prohibited without permission.

Reproduced with permission of the copyright owner. Further reproduction prohibited without permission.

channels containing counts which were collected prior to the application of the excitation potential. The counts in these channels represent the PM-tube's level of background noise. This count level is subtracted from the record and these channels are eliminated from the record. The use of all channels of counts as data in the analysis is prohibitive, since each record contains several hundred channels, therefore the counts are then smoothed by averaging five adjacent channels and weighting the average arithmetically (the central channel receiving the heaviest weight). The counts are then normalized to the counts in the peak maximum. A computer program for performing the above operations is shown in Figure 8.

The program is written in FORTRAN computer language. The program writes the data, beginning with the channels containing normalized counts of greater than 0.4, queued from every third channel. These counts are written with their corresponding time variable and weighting factor. The weighting factor assigned is the square root of the number of counts until the peak intensity is reached, then the weighting factor is assigned unity. Besides writing the data in proper format, the program inserts the information cards required by the analysis program. An example of the data set produced is shown in Figure 9. The information cards consist of: a problem (PROBLM) card, a maximum (MAXMUM) card, a minimum (MINMUM) card, a parameter (PARAM) card, and a finish (FINISH) card. The problem card transmits to the analysis program: an identifying label (12IB1), the number of variables per observations (3), the index of the dependent variable (2), the number of observations (271), the number of parameters (4), the tolerance for pivoting (0.10000), the criterion of convergence (0.00001), the maximum number of iterations (100), the number of variable format cards (1), and the index of the weighting variable (3). The maximum and minimum cards set respective

Reproduced with permission of the copyright owner. Further reproduction prohibited without permission.

Figure 8. A Listing of the Computer Program which Changes the Raw Data into a Formatted Form.

Reproduced with permission of the copyright owner. Further reproduction prohibited without permission.

```
C                                                                       PRE-BMD
C------PROGRAM FOR PREPARING RAW DATA FOR ANALYSIS----------------------PRE-BMD
C                                                                       PRE-BMD
      DIMENSION NCT(1030),DATA(1030),SATA(1030)                         PRE-BMD
      DO 1003 MC = 1, 5                                                 PRE-BMD
C                                                                       PRE-BMD
C------INFORMATION VALUES ARE INPUTED---------------------------------PRE-BMD
C                                                                       PRE-BMD
C      PT = PREDICTED TIME OF THE PEAK.                                 PRE-BMD
C                                                                       PRE-BMD
C      CRX = CONCENTRATION OF THE AROMATIC HYDROCARBON.                 PRE-BMD
C                                                                       PRE-BMD
C      NCS = NUMBER OF DEAD TIME CHANNELS.                              PRE-BMD
C                                                                       PRE-BMD
C      NP = CHANNEL WHERE DATA TO BE ANALYZED STARTS.                   PRE-BMD
C                                                                       PRE-BMD
C      IP = CHANNEL OF THE PEAK INTENSITY.                              PRE-BMD
C                                                                       PRE-BMD
C-----------------------------------------------------------------------PRE-BMD
C                                                                       PRE-BMD
      READ(14,500,END=14) PT,CRX,NCS,NP,IP                              PRE-BMD
14    END FILE 14                                                       PRE-BMD
      WRITE(6,605) PT, CRX, NCS, NP, IP                                 PRE-BMD
      READ(15,501)                                                      PRE-BMD
C                                                                       PRE-BMD
C------MORE EXPERIMENTAL PARAMETERS ARE INPUTED-----------------------PRE-BMD
C                                                                       PRE-BMD
C      NS = NUMBER OF SWEEPS OF DATA COLLECTION.                        PRE-BMD
C                                                                       PRE-BMD
C      NCH = NUMBER OF CHANNELS.                                        PRE-BMD
C                                                                       PRE-BMD
C      ID = 0, THEN CHANNEL ONE IS SKIPPED, OTHERWISE NOT.              PRE-BMD
C                                                                       PRE-BMD
C      DT = DWELL TIME.                                                 PRE-BMD
C                                                                       PRE-BMD
C-----------------------------------------------------------------------PRE-BMD
C                                                                       PRE-BMD
C------TOTAL NUMBER OF CHANNELS IS CORRECTED---------------------------PRE-BMD
C                                                                       PRE-BMD
      READ(15,501) NS, NCH, ID, DT                                      PRE-BMD
      NON=0                                                             PRE-BMD
```

Reproduced with permission of the copyright owner. Further reproduction prohibited without permission.

Reproduced with permission of the copyright owner. Further reproduction prohibited without permission.

Reproduced with permission of the copyright owner. Further reproduction prohibited without permission.

```
600   FORMAT(2(2X,I4))
      CALL EXIT
      END
C-----SUBROUTINE FOR SMOOTHING THE RAW DATA----------
      SUBROUTINE SMOOTH(IN,OUT,N)
      REAL*4 IN(N),OUT(N)
      OUT(1)=(IN(1)+3.0*IN(2)+IN(3))/5.0
      N1=N-1
      N2=N-2
      OUT(N)=IN(N)
      OUT(N-1)=(IN(N-2)+3.0*IN(N-1)+IN(N))/5.0
      DO 1 I=3,N2
      I1=I-1
      I2=I-2
      J1=I+1
      J2=I+2
1     OUT(I)=(3.0*IN(I1)+IN(I2)+5.0*IN(I)+3.0*IN(J1)+IN(J2))/13.0
      RETURN
      END
C---------------------------------------------------
```

Reproduced with permission of the copyright owner. Further reproduction prohibited without permission.

Figure 9. An Example of Formatted Data Submitted to the Analysis Program.

Reproduced with permission of the copyright owner. Further reproduction prohibited without permission.

Reproduced with permission of the copyright owner. Further reproduction prohibited without permission.

limits on the parameters. The parameter card gives the initial estimate for the parameters. The finish card indicates the end of the information.

The analysis program used was the nonlinear least squares routine (BMD07R) of the BMD Biomedical Computer Programs package [82]. The program returns r parameters, p, from a weighted least squares fit of a user supplied function, f.

$$y = f(x_1, \ldots, x_t; P_1, \ldots, P_r) \qquad (IV.6.1)$$

with t independent variables, x. The exordium is specified by the user in the initial estimates of parameter values, the program then minimizes the mean square error:

$$S^2 = \frac{1}{n - r} \sum_{i=1}^{n} [(y_i - f(x_{i1}, \ldots, x_{it}; P_1, \ldots, P_r))^2 \cdot w_i] \qquad (IV.6.2)$$

by means of stepwise Gauss-Newton iterations [83,84], where in equation IV.6.2, n is the number of observations and $w_i$'s are the weighting variables. A user supplied subprogram (see Figure 10) is required in which the function and the partial derivatives of the function with respect to each parameter are evaluated.

The user supplied subprogram (Figure 10) and the data (Figure 9) are submitted together with the analysis program to the computer. After approximately 300 seconds of computer time (IBM 360/65), the results which are shown in Figure 11 are returned. The results can be divided into four parts: information, iterations, diagnostics, and data. The information is a documented listing of the data from the problem card and a listing of the upper and lower limits allow the parameters. Next is a listing of the iteration steps which starts with the user supplied

Reproduced with permission of the copyright owner. Further reproduction prohibited without permission.

Figure 10. The User Supplied Subprogram.

Reproduced with permission of the copyright owner. Further reproduction prohibited without permission.

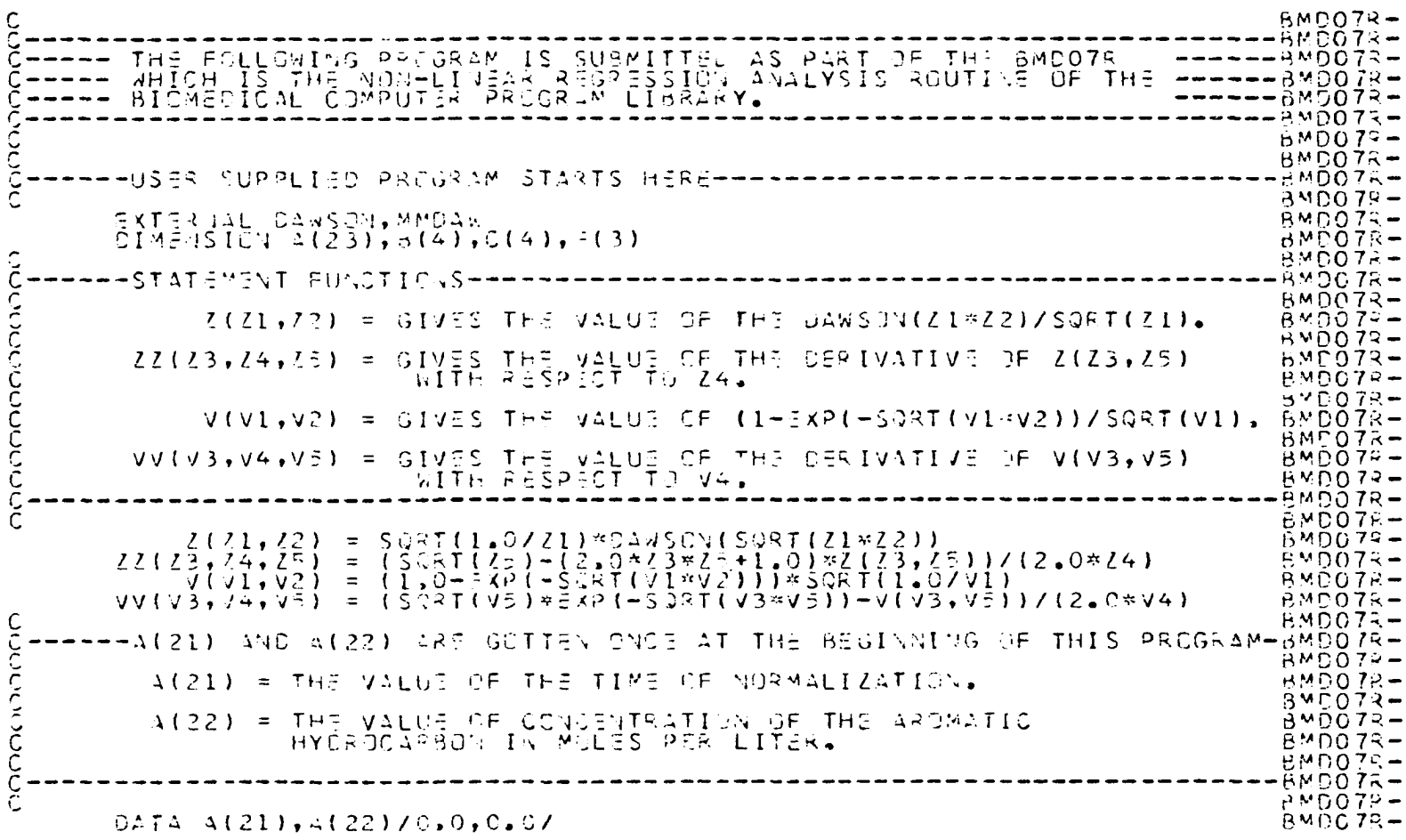

```
C                                                                      BMD07R-
C-----------------------------------------------------------------------BMD07R-
C-----  THE FOLLOWING PROGRAM IS SUBMITTED AS PART OF THE BMD07R  -------BMD07R-
C-----  WHICH IS THE NON-LINEAR REGRESSION ANALYSIS ROUTINE OF THE -------BMD07R-
C-----  BIOMEDICAL COMPUTER PROGRAM LIBRARY.                      -------BMD07R-
C-----------------------------------------------------------------------BMD07R-
C                                                                       BMD07R-
C                                                                       BMD07R-
C------USER SUPPLIED PROGRAM STARTS HERE-------------------------------BMD07R-
C                                                                       BMD07R-
      EXTERNAL DAWSON,MMDAW                                             BMD07R-
      DIMENSION A(23),B(4),C(4),F(3)                                    BMD07R-
C                                                                       BMD07R-
C------STATEMENT FUNCTIONS---------------------------------------------BMD07R-
C                                                                       BMD07R-
C          Z(Z1,Z2) = GIVES THE VALUE OF THE DAWSON(Z1*Z2)/SQRT(Z1).    BMD07R-
C                                                                       BMD07R-
C       ZZ(Z3,Z4,Z5) = GIVES THE VALUE OF THE DERIVATIVE OF Z(Z3,Z5)    BMD07R-
C                      WITH RESPECT TO Z4.                              BMD07R-
C                                                                       BMD07R-
C          V(V1,V2) = GIVES THE VALUE OF (1-EXP(-SQRT(V1*V2))/SQRT(V1). BMD07R-
C                                                                       BMD07R-
C       VV(V3,V4,V5) = GIVES THE VALUE OF THE DERIVATIVE OF V(V3,V5)    BMD07R-
C                      WITH RESPECT TO V4.                              BMD07R-
C-----------------------------------------------------------------------BMD07R-
C                                                                       BMD07R-
C          Z(Z1,Z2) = SQRT(1.0/Z1)*DAWSON(SQRT(Z1*Z2))                  BMD07R-
C       ZZ(Z3,Z4,Z5) = (SQRT(Z5)-(2.0*Z3*Z5+1.0)*Z(Z3,Z5))/(2.0*Z4)     BMD07R-
C          V(V1,V2) = (1.0-EXP(-SQRT(V1*V2)))*SQRT(1.0/V1)              BMD07R-
C       VV(V3,V4,V5) = (SQRT(V5)*EXP(-SQRT(V3*V5))-V(V3,V5))/(2.0*V4)   BMD07R-
C                                                                       BMD07R-
C------A(21) AND A(22) ARE GOTTEN ONCE AT THE BEGINNING OF THIS PROGRAM-BMD07R-
C                                                                       BMD07R-
C         A(21) = THE VALUE OF THE TIME OF NORMALIZATION.               BMD07R-
C                                                                       BMD07R-
C         A(22) = THE VALUE OF CONCENTRATION OF THE AROMATIC            BMD07R-
C                 HYDROCARBON IN MOLES PER LITER.                       BMD07R-
C-----------------------------------------------------------------------BMD07R-
C                                                                       BMD07R-
      DATA A(21),A(22)/0.0,0.0/                                         BMD07R-
```

Reproduced with permission of the copyright owner. Further reproduction prohibited without permission.

```
      IF(A(21).NE.0.0) GO TO 10                                          BMD07R-
      READ(1,501) A(21),A(22)                                            BMD07R-
501   FORMAT(2E10.3)                                                     BMD07R-
10     CONTINUE                                                          BMD07R-
C-----PARAMETERS-------------------------------------------------------BMD07R-
C                                                                        BMD07R-
C       P(1) = RATE CONSTANT FOR THE FORMATION OF THE TRIPLET.           BMD07R-
C       P(2) = RATE CONSTANT FOR THE FORMATION OF THE CATION RADICAL.    BMD07R-
C       P(3) = RATE CONSTANT FOR CATION-ANION ANNIHILATION.              BMD07R-
C       P(4) = RATE CONSTANT FOR THE FORMATION OF BENZOYLOXY RADICALS.   BMD07R-
C       X(1) = TIME.                                                     BMD07R-
C-----ALGEBRAIC COEFFICIENTS-------------------------------------------BMD07R-
C          A(1) THRU A(11).                                              BMD07R-
C-----------------------------------------------------------------------BMD07R-
      A(1)   = P(1)*A(22)                                                BMD07R-
      A(2)   = P(2)*0.020                                                BMD07R-
      A(3)   = P(3)*A(22)                                                BMD07R-
      A(4)   = P(4)*0.020                                                BMD07R-
      A(5)   = 1.0/(A(2)-A(1))                                           BMD07R-
      A(6)   =  1.0/(P(3)-P(1))                                          BMD07R-
      A(7)   =  1.0/(A(3)-A(2))                                          BMD07R-
      A(8)   = 1.0/P(3)                                                  BMD07R-
      A(9)   = -A(2)*A(5)*A(6)                                           BMD07R-
      A(10)  = A(1)*A(22)*A(5)*A(7)                                      BMD07R-
      A(11)  = -(A(8)+A(9)+A(10))                                        BMD07R-
C-----EQUATIONS OF I(OBSERVED)-----------------------------------------BMD07R-
C                                                                        BMD07R-
C          E(1) = I(OBSERVED) FOR TIME = X(1).                           BMD07R-
C          E(2) = I(OBSERVED) AT TIME = A(21).                           BMD07R-
C             F = I(NORMALIZED) TO TIME = A(21).                         BMD07R-
```

Reproduced with permission of the copyright owner. Further reproduction prohibited without permission.

```
C                                                                       BMD07R-
C-----------------------------------------------------------------------BMD07R-
C                                                                       BMD07R-
      E(1)  =  A(8)*V(A(4),X(1))+A(9)*Z(A(1),X(1))                      BMD07R-
     *         +A(10)*Z(A(2),X(1))+A(11)*Z(A(3),X(1))                   BMD07R-
      E(2)  =  A(9)*V(A(4),A(21))+A(9)*Z(A(1),A(21))                    BMD07R-
     *         +A(10)*Z(A(2),A(21))+A(11)*Z(A(3),A(21))                 BMD07R-
      E(3)  =  1.0/E(2)**2                                              BMD07R-
      F     =  E(1)/E(2)                                                BMD07R-
C                                                                       BMD07R-
C------DERIVATIVES OF THE COEFFICIENTS----------------------------------BMD07R-
C                                                                       BMD07R-
C          A(12) THRU A(23).                                            BMD07R-
C                                                                       BMD07R-
C-----------------------------------------------------------------------BMD07R-
C                                                                       BMD07R-
      A(12)  =  -(A(8)**2)                                              BMD07R-
      A(13)  =  A(9)*(A(6)+A(5)*A(22))                                  BMD07R-
      A(14)  =  A(9)*(1.0/P(2)-0.020*A(5))                              BMD07R-
      A(15)  =  -A(9)*A(6)                                              BMD07R-
      A(16)  =  A(10)*(1.0/P(1)+A(22)*A(5))                             BMD07R-
      A(17)  =  A(10)*0.020*(A(7)-A(5))                                 BMD07R-
      A(18)  =  -A(10)*A(22)*A(7)                                       BMD07R-
      A(19)  =  -(A(13)+A(16))                                          BMD07R-
      A(20)  =  -(A(14)+A(17))                                          BMD07R-
      A(23)  =  -(A(12)+A(15)+A(18))                                    BMD07R-
C                                                                       BMD07R-
C------DERIVATIVES OF THE I-FUNCTIONS-----------------------------------BMD07R-
C                                                                       BMD07R-
C     B'S = ARE THE DERIVATIVES OF E(1) WITH RESPECT TO THE PARAMETERS. BMD07R-
C                                                                       BMD07R-
C     C'S = ARE THE DERIVATIVES OF E(2) WITH RESPECT TO THE PARAMETERS. BMD07R-
C                                                                       BMD07R-
C     D'S = ARE THE DERIVATIVES OF F WITH RESPECT TO THE PARAMETERS.    BMD07R-
C                                                                       BMD07R-
C-----------------------------------------------------------------------BMD07R-
C                                                                       BMD07R-
      B(1)  =  A(13)*Z(A(1),X(1))+A(16)*Z(A(2),X(1))                    BMD07R-
     *         +A(19)*Z(A(3),X(1))+A(9)*ZZ(A(1),P(1),X(1))              BMD07R-
      B(2)  =  A(14)*Z(A(1),X(1))+A(17)*Z(A(2),X(1))                    BMD07R-
     *         +A(20)*Z(A(3),X(1))+A(10)*ZZ(A(2),P(2),X(1))             BMD07R-
```

Reproduced with permission of the copyright owner. Further reproduction prohibited without permission.

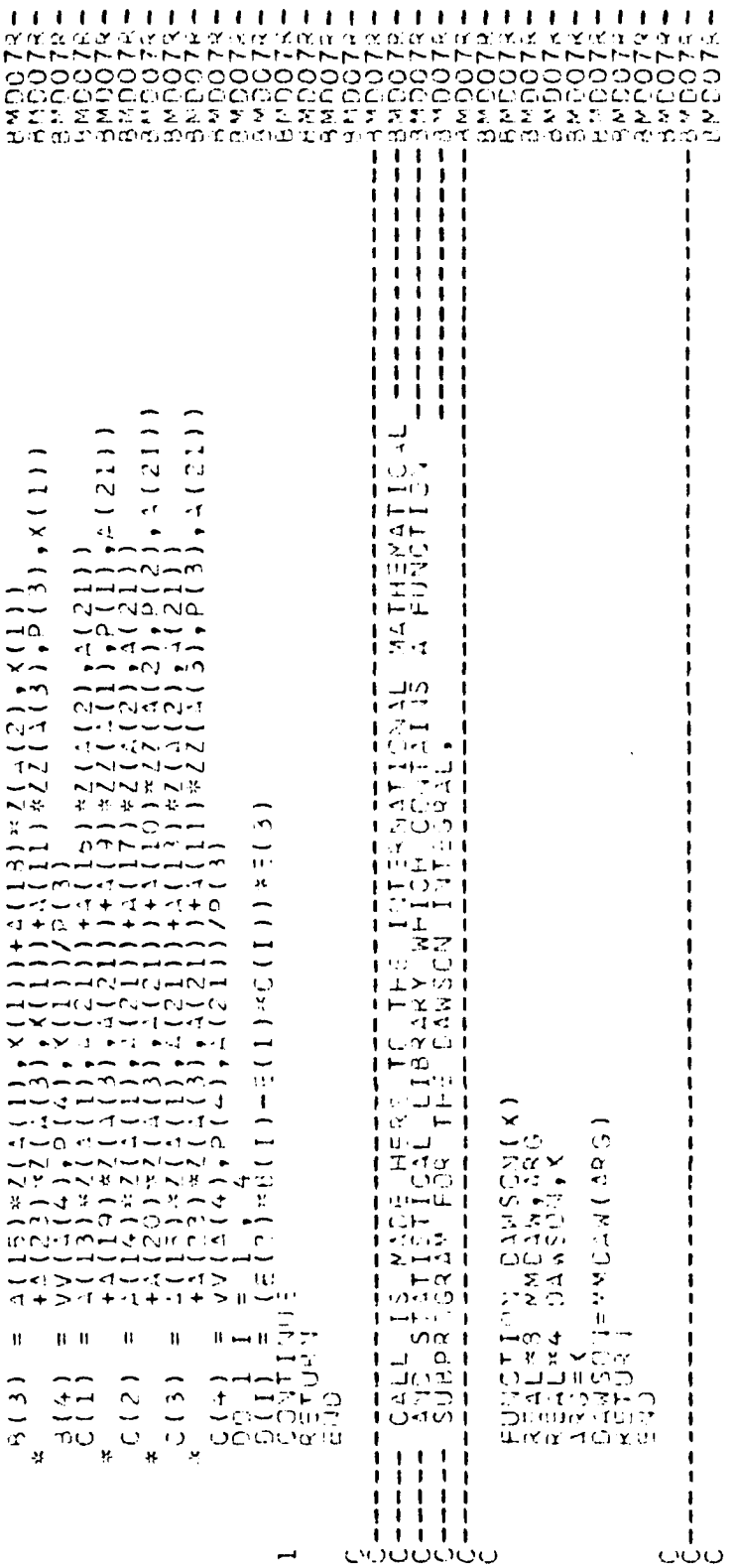

Reproduced with permission of the copyright owner. Further reproduction prohibited without permission.

Figure 11. An Example of the Results from Computer Analysis.

Reproduced with permission of the copyright owner. Further reproduction prohibited without permission.

Reproduced with permission of the copyright owner. Further reproduction prohibited without permission.

Reproduced with permission of the copyright owner. Further reproduction prohibited without permission.

initial estimates and the error mean square, followed by changes in the parameters to minimize the error mean square. The last line of the iterations are best estimates found by the program under the stated conditions. Since the technique of nonlinear least squares is intrinsically dependent upon the initial estimates of the parameters, repeated submissions to the computer with different estimates may be necessary. The diagnostics are meant to help make the judgements on changes in the estimates. The asymptotic standard deviation and correlation matrix indicate the "goodness" of the final parameter values. Finally, the data is listed in addition to that imputed, the values of the function, the residual error and the standard deviation of the predicted value of the function are given.

IV.7. Results

The results from the numerical analysis of fifteen experiments are presented in Tables 7, 8, and 9. The rate constants in these tables, $k_3$, $k_5$, $k_6$, and $k_7$ correspond to the reactions for the formation of the radical oxidant, the formation of the triplet, the formation of the cation, and the annihilation-emission. In all cases, the rate constants, $k_3$ and $k_7$, were found to be insensitive to change for values between $1.0 \times 10^9$ and $1.0 \times 10^{10}$ (i.e., the diffusion limit), except in one case. However, the error mean square was best minimized in this range, in all cases the error mean square was less than $5 \times 10^{-3}$ except for $7.46 \times 10^{-6}$ M DPA which was $9 \times 10^{-2}$.

In Table 7, seven concentrations of fluoranthene are presented; for this table, the emission intensity detected was from the total emission band. In Table 8, three concentrations of fluoranthene are presented; here the emission intensity detected was 470 nm. In Table 9, five

Reproduced with permission of the copyright owner. Further reproduction prohibited without permission.

Reproduced with permission of the copyright owner. Further reproduction prohibited without permission.

TABLE 7

Rate Constants at Various Concentrations of Fluoranthene

where Total Emission was Detected

| [Flu] | $k_3$ | $k_5$ | $k_6$ | $k_7$ | Error Mean Square |
|---|---|---|---|---|---|
| $1.10 \times 10^{-5}$ | $1.0 \times 10^{10}$ | $2.26 \times 10^{5}$ | $1.00 \times 10^{4}$ | $9.0 \times 10^{9}$ | $3.23 \times 10^{-3}$ |
| $2.76 \times 10^{-5}$ | $5.0 \times 10^{9}$ | $1.26 \times 10^{5}$ | $1.54 \times 10^{4}$ | $5.0 \times 10^{9}$ | $6.36 \times 10^{-4}$ |
| $6.91 \times 10^{-5}$ | $1.0 \times 10^{9}$ | $6.27 \times 10^{4}$ | $1.56 \times 10^{4}$ | $1.0 \times 10^{9}$ | $2.80 \times 10^{-3}$ |
| $1.74 \times 10^{-4}$ | $5.0 \times 10^{9}$ | $3.03 \times 10^{4}$ | $9.96 \times 10^{3}$ | $5.0 \times 10^{9}$ | $9.05 \times 10^{-4}$ |
| $4.32 \times 10^{-4}$ | $6.9 \times 10^{9}$ | $2.58 \times 10^{4}$ | $5.39 \times 10^{2}$ | $9.0 \times 10^{9}$ | $1.10 \times 10^{-3}$ |
| $1.08 \times 10^{-3}$ | $5.0 \times 10^{9}$ | $9.84 \times 10^{3}$ | $7.93 \times 10^{2}$ | $5.0 \times 10^{9}$ | $8.68 \times 10^{-4}$ |
| $2.70 \times 10^{-3}$ | $5.0 \times 10^{9}$ | $3.26 \times 10^{3}$ | $1.08 \times 10^{3}$ | $5.0 \times 10^{9}$ | $1.21 \times 10^{-3}$ |

concentrations are in units of moles/liter

rate constants are in units of liters/mole/second

Reproduced with permission of the copyright owner. Further reproduction prohibited without permission.

TABLE 8

Rate Constants at Various Concentrations of Fluoranthene

for the Emission Wavelength of 470 nm

| [DPA] | $k_3$ | $k_5$ | $k_6$ | $k_7$ | Error Mean Square |
|---|---|---|---|---|---|
| $1.10 \times 10^{-5}$ | $9.0 \times 10^{9}$ | $3.04 \times 10^{5}$ | $2.35 \times 10^{4}$ | $9.0 \times 10^{9}$ | $4.49 \times 10^{-3}$ |
| $1.08 \times 10^{-3}$ | $5.0 \times 10^{9}$ | $1.23 \times 10^{4}$ | $4.63 \times 10^{3}$ | $5.0 \times 10^{9}$ | $8.68 \times 10^{-4}$ |
| $2.70 \times 10^{-3}$ | $1.0 \times 10^{10}$ | $2.14 \times 10^{3}$ | $1.13 \times 10^{3}$ | $9.0 \times 10^{9}$ | $1.21 \times 10^{-3}$ |

concentratios are in units of moles/liter

rate constants are in units of liters/mole/second

Reproduced with permission of the copyright owner. Further reproduction prohibited without permission.

TABLE 9

Rate Constants at Various Concentrations of 9,10-Diphenylanthracene for the Emission Wavelength of 435 nm

| [DPA] | $k_3$ | $k_5$ | $k_6$ | $k_7$ | Error Mean Square |
|---|---|---|---|---|---|
| $7.46 \times 10^{-6}$ | $2.6 \times 10^{8}$ | $7.53 \times 10^{5}$ | $2.38 \times 10^{3}$ | $9.0 \times 10^{9}$ | $1.49 \times 10^{-2}$ |
| $3.73 \times 10^{-5}$ | $5.0 \times 10^{9}$ | $2.13 \times 10^{5}$ | $2.16 \times 10^{3}$ | $5.0 \times 10^{9}$ | $3.19 \times 10^{-3}$ |
| $1.86 \times 10^{-4}$ | $5.0 \times 10^{9}$ | $6.21 \times 10^{4}$ | $2.28 \times 10^{3}$ | $5.0 \times 10^{9}$ | $2.79 \times 10^{-3}$ |
| $9.32 \times 10^{-4}$ | $1.0 \times 10^{10}$ | $1.26 \times 10^{4}$ | $1.53 \times 10^{3}$ | $1.0 \times 10^{10}$ | $1.09 \times 10^{-3}$ |
| $4.66 \times 10^{-3}$ | $1.0 \times 10^{10}$ | $4.00 \times 10^{3}$ | $9.57 \times 10^{2}$ | $1.0 \times 10^{10}$ | $1.24 \times 10^{-3}$ |

concentrations are in units of moles/liter

rate constants are in units of liters/mole/second

concentrations of DPA are presented; here the emission intensity detected was at 435 nm.

In addition to the results presented in these tables, all fifteen experiments are graphically displayed in the appendix in sets of three figures. The sets comprised of a figure of the raw data from magnetic tape, a figure of the "fixed" smoothed data, and a composite of the "fixed smoothed" data and the fitted data.

## IV.8. Discussion of Results

### IV.8.1. Variable Rate Constants

It is apparent from an examination of the tables of results (Tables 7, 8, and 9) that the rate constants for the reactions of the formation of triplets and the formation of the cations vary with concentration.

In an effort to understand why this variation occurs, log-log plots of concentraiton versus rate constant are constructed from the results in Tables 7 and 9 for $k_5$ and $k_6$, respectively and are shown in Figures 12, 13, 14, and 15. The slopes of the best fitting straight line for the log-log plot of concentration versus $k_5$ for fluoranthene (Figure 12) and DPA (Figure 14) are -0.73 and -0.83, respectively. This would indicate a near-inverse relationship between the rate constant, $k_5$, and the concentration of the aromatic hydrocarbon. The slopes of the best fit straight line for the log-log plot of concentration versus $k_6$ for fluoranthene (Figure 13) and DPA (Figure 15) are -0.61 and -0.13, respectively, although a straight line fit for Figure 13 is not significant due to the wide scatter of points. This would indicate that $k_6$ is essentially independent of the concentration of aromatic hydrocarbon.

We believe that the variation in the rate constants is due to our neglecting the possibilities of quenching of the triplets by a quencher Q,

$$^3R^* + Q \xrightarrow{k_Q} R + Q' \ . \qquad (IV.8.1)$$

Reproduced with permission of the copyright owner. Further reproduction prohibited without permission.

Figure 12. Log-Log Plot of Fluoranthene Concentration and the Rate Constant for Triplet Formation. (Standard Error = $9.0 \times 10^{-2}$)

Reproduced with permission of the copyright owner. Further reproduction prohibited without permission.

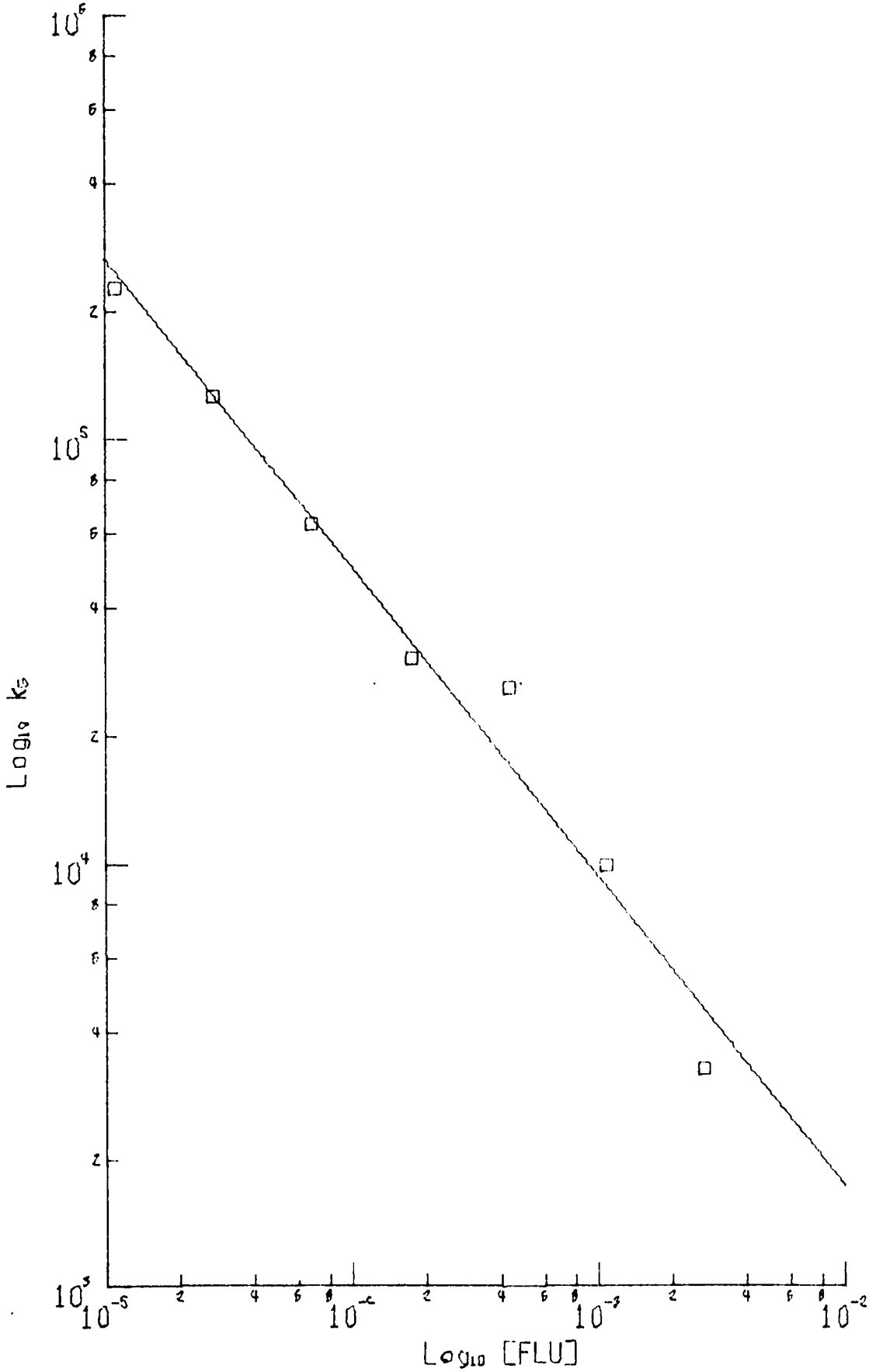


Reproduced with permission of the copyright owner. Further reproduction prohibited without permission.

Figure 13. Log-Log Plot of Fluoranthene Concentration and the Rate Constant for Cation Formation. (Standard Error = $3.5 \times 10^{-1}$)

Reproduced with permission of the copyright owner. Further reproduction prohibited without permission.

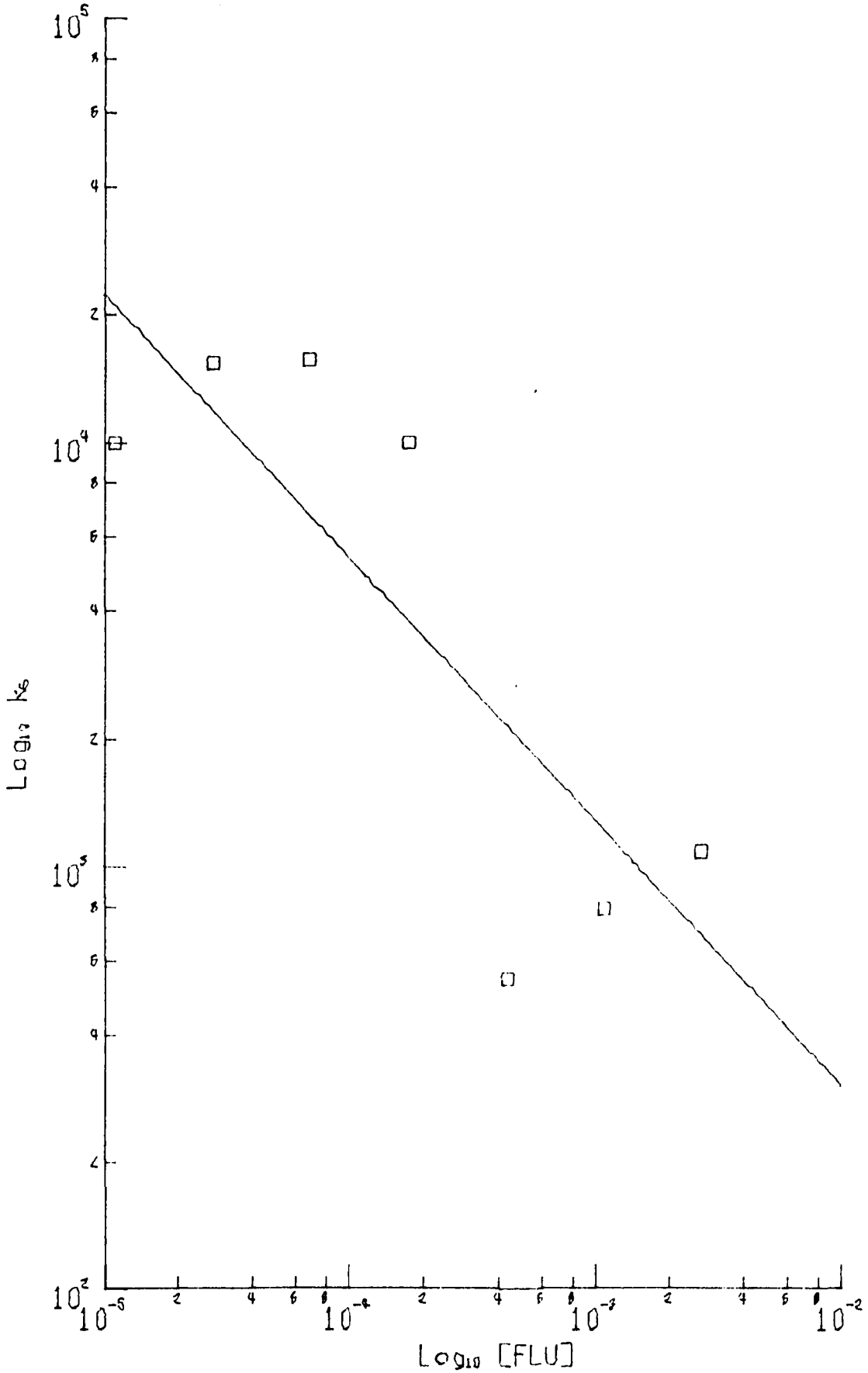


Reproduced with permission of the copyright owner. Further reproduction prohibited without permission.

Figure 14. Log-Log Plot of DPA Concentration and the Rate Constant for Triplet Formation. (Standard Error = $3.8 \times 10^{-2}$)

Reproduced with permission of the copyright owner. Further reproduction prohibited without permission.

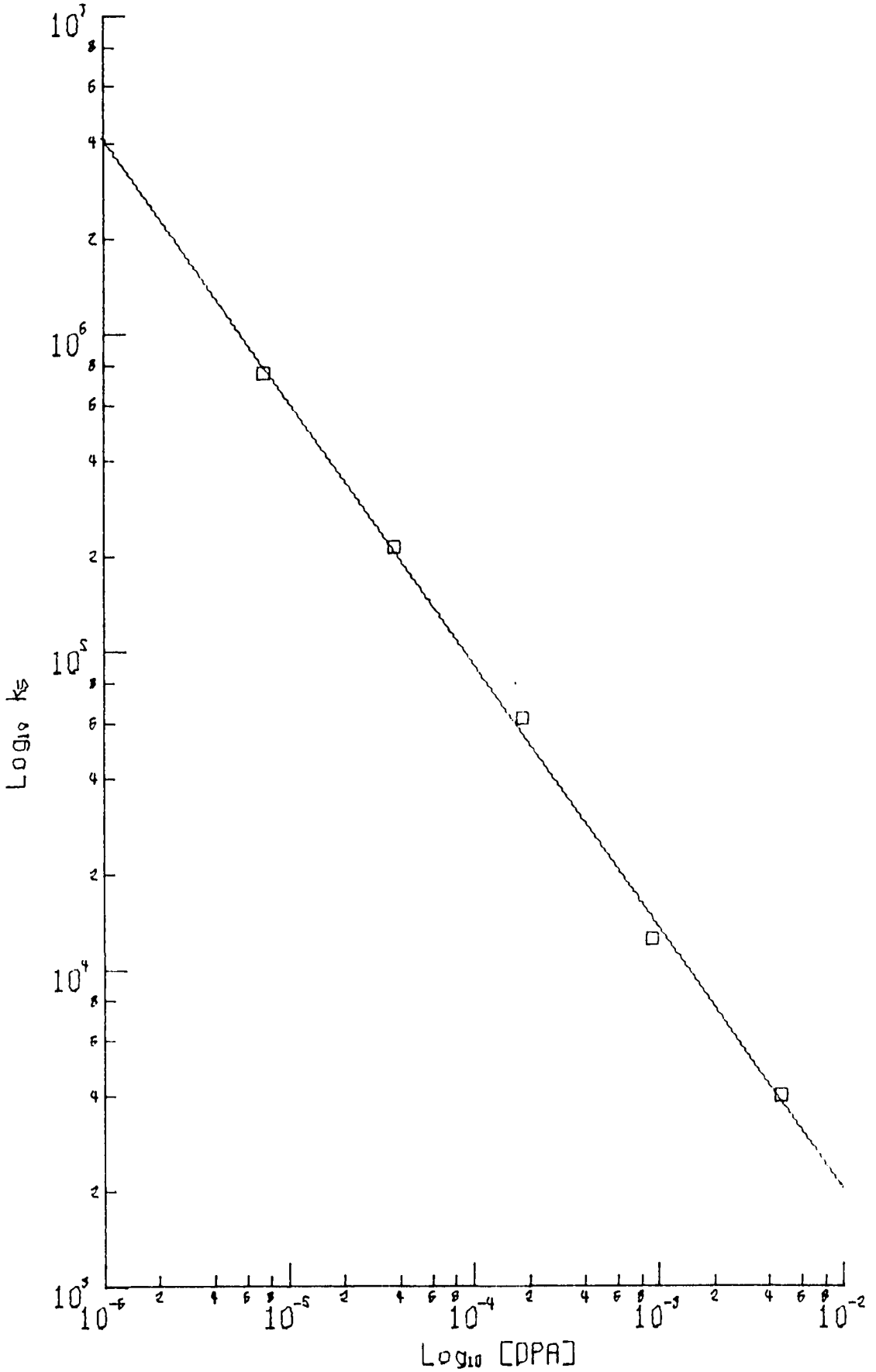


Reproduced with permission of the copyright owner. Further reproduction prohibited without permission.

Figure 15. Log-Log Plot of DPA Concentration and the Rate Constant for Cation Formation. (Standard Error = $3.9 \times 10^{-2}$)

Reproduced with permission of the copyright owner. Further reproduction prohibited without permission.

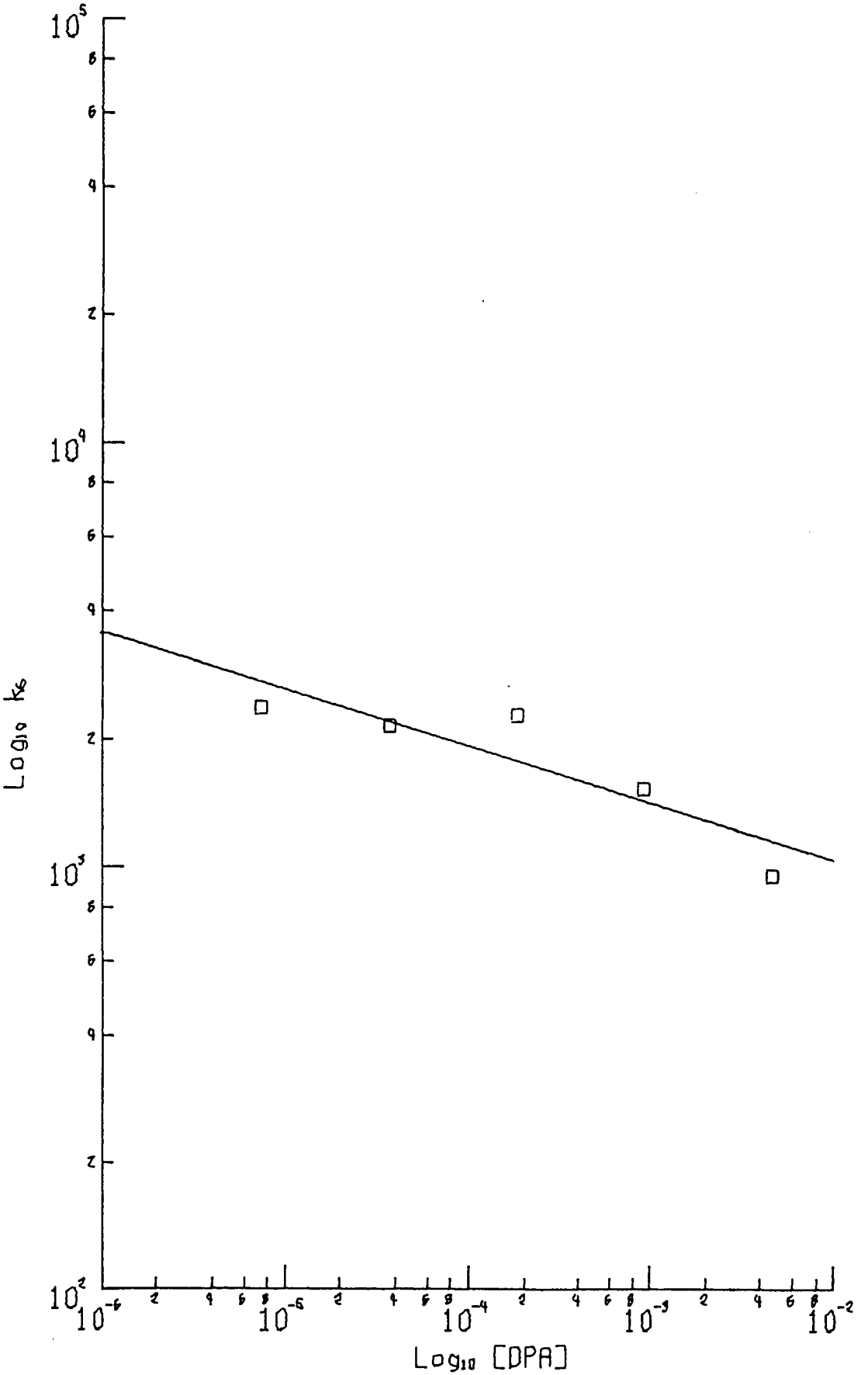


Reproduced with permission of the copyright owner. Further reproduction prohibited without permission.

A justification of this belief is based on the following rationale. The rate expression for $C_{3_R}$ derived from the postulated mechanism is,

$$\frac{dC_{3_R}}{dt} = k_5 C_R\text{-}C_B - k_6 C_{3_R} C^\circ_{BPO} \qquad (IV.8.2)$$

If the mechanism is revised to include reaction IV.8.1 then

$$\frac{dC_{3_R}}{dt} = k_5' C_R\text{-}C_B - k_6' C_{3_R} C^\circ_{BPO} - k_Q C_{3_R} C_Q \qquad (IV.8.3)$$

where $k_5'$ and $k_6'$ are the "revised" rate constants for the respective reactions for triplet formation and cation formation and $C_\phi$ is the concentration of the quenchers. By setting equation IV.7.2. and IV.7.3 to be equal, the meaning of $k_5$ and $k_6$ can be shown,

$$k_5 = k_5' + \frac{(k_6 - k_6')C_{3_R} C^\circ_{BPO} - k_Q C_{3_R} C_Q}{C_R\text{-}C_B} \qquad (IV.8.4)$$

and

$$k_6 = k_6' + \frac{k_Q C_Q}{C^\circ_{BPO}} + \frac{(k_5 - k_5')C_R\text{-}C_B}{C_{3_R} C^\circ_{BPO}} \qquad (IV.8.5)$$

The approximation that

$$C_R\text{-} \simeq C^\circ_R \qquad (IV.8.6)$$

is taken from the solution of the boundary value problem (i.e., equation IV.4.12) to be valid here. If we then assume $k_5'$ is much smaller than $k_5$ then equation IV.8.4 can be interpreted as saying that $k_5$ is inversely proportional to $C^\circ_R$. And, in equation IV.8.5, if $k_5'$ is assumed to be smaller than $k_5$, then $k_5$ cancels the effect of $C_R$- and the expression indicates $C^\circ_R$ is independent of it.

Other workers have reported cases of triplet quenching in *ecl* studies [60-63,69,70,72,74,75,85,86]. These workers suggest two particularly

Reproduced with permission of the copyright owner. Further reproduction prohibited without permission.

common quenchers as being molecular oxygen and radical ions. Oxygen is suspected of being present at concentrations of *ca.* $10^{-6}$ M [85] and is a known quencher of triplets. Radical ions of which the primary reactant $R^{\cdot-}$ is one, can quench triplets since the radical ions are paramagnetic. Besides these quenchers, the possibilities of other impurities are still present.

IV.8.2. Discussion of Excimers

It should be briefly noted in passing that there is no evidence of excimer emission at least in the case of fluoranthene. A comparison of the three results in Table 9 with those of Table 8 shows that there is very little difference in the rate constants derived from emission at a singlet wavelength and that derived from the total emission. This is as expected, since the observations of excimer emissions in *ecl* were found when solvents of much lower dielectric strength were used.

Reproduced with permission of the copyright owner. Further reproduction prohibited without permission.

# V. CONCLUSION

In conclusion, the objectives of this dissertation have been met. A mechanism for explaining the *ecl* process in which emission results as a consequence of electroreduction of an aromatic hydrocarbon in the presence of a bulk oxidant precursor has been developed and tested.

This study has shown that: (i) the process is general to a number of aromatic hydrocarbons, (ii) mixed systems involving energy transfer can be explained, (iii) an attempt to describe the *ecl* process in terms of the emission intensity and time will be possible only with further studies and an understanding of the quenching routes which involve the triplet species produced, (iv) the rates of the reactions for generating the radical oxidant and annihilation-emission are near the diffusion control limit, and (v) excimers do not play an important role in the emission in solvents of medium to high dielectric strength.

Reproduced with permission of the copyright owner. Further reproduction prohibited without permission.

## REFERENCES


1. E. Harvey, *Living Light*, Hafner Publishing Company, New York, 1965.

2. D. M. Hercules, *Science*, *145*, 808 (1964).

3. R. E. Visco and E. A. Chandross, *J. Amer. Chem. Soc.*, *86*, 5350 (1964).

4. K. S. V. Santhanam and A. J. Bard, *J. Amer. Chem. Soc.*, *87*, 139 (1965).

5. T. Kwana, "Photochemistry and Electroluminescence," in *Electroanalytical Chemistry*, A. J. Bard, ed., vol. 1, Marcel Dekker, New York, 1966, chap. 3, p. 197.

6. A. J. Bard, K. S. V. Santhanam, S. A. Cruser, and L. R. Faulkner, "Electrogenerated Chemiluminescence," in *Fluorescence: Theory, Instrumentation and Practice*, G. G. Guilbault, ed., Marcel Dekker, New York, 1967, chap. 14, p. 627.

7. A. Zweig, "Electron Transfer Luminescence in Solution," in *Advances in Photochemistry*, vol. 6, Interscience, New York, 1968, chap. 5, p. 425.

8. D. M. Hercules, "Organic Electroluminescence," in *Physical Methods of Chemistry*, A. Weissberger and B. W. Rossiter, eds., vol. 1, part IIB, Interscience, New Yori, 1971, chap. 13, p. 257.

9. G. G. Guilbault, *Practical Fluorescence*, Marcel Dekker, New York, 1973, chap. 11, p. 447.

10. M. Sato, *Reviews of Polarography (Japan)*, *19*, 29 (1973).

11. E. A. Chandross and F. I. Sonntag, *J. Amer. Chem. Soc.*, *86*, 3179 (1964).

12. E. A. Chandross and F. I. Sonntag, *J. Amer. Chem. Soc.*, *88*, 1089 (1966).

13. A. Weller and K. Zachariasse, *J. Chem. Phys.*, *46*, 4984 (1967).

14. R. Livingston and H. R. Leonhardt, *J. Phys. Chem.*, *72*, 2254 (1968).


Reproduced with permission of the copyright owner. Further reproduction prohibited without permission.

15. T. M. Siegel and H. B. Mark, *J. Amer. Chem. Soc.*, *93*, 6281 (1971).

16. T. M. Siegel and H. B. Mark, *J. Amer. Chem. Soc.*, *94*, 9020 (1972).

17. D. L. Akins and R. L. Birke, *Chem. Phys. Letters*, *29*, 428 (1974).

18. M. E. Peover, "Electrochemistry of Aromatic Hydrocarbons and Related Substances," in *Electroanalytical Chemistry*, A. J. Bard, ed., vol. 2, Marcel Dekker, New York, 1967, chap. 1, p. 1.

19. C. K. Mann and K. K. Barnes, *Electrochemical Reactions in Non-aqueous Systems*, Marcel Dekker, New York, 1970.

20. G. J. Hoijtink, "The Electroreduction of Aromatic Hydrocarbons," in *Advances in Electrochemistry and Electrochemical Engineering*, P. Delahay and C. W. Tobias, eds., vol. 7, Interscience, New York, 1970, chap. 4., p. 221.

21. M. Fujihara and S. Hayano, *Report of the Institute of Industrial Science, The University of Tokyo*, *23*, 85 (1973).

22. J. Jagur-Grodzinski, M. Feld, S. L. Yang, and M. Szwarc, *J. Phys. Chem.*, *69*, 628 (1965).

23. A. G. Evans and B. J. Tabner, *Trans. Faraday Soc.*, *61*, 891 (1965).

24. M. Szwarc, "Chemistry of Radical-Ions," in *Progress in Physical Organic Chemistry*, A Streitwieser and R. W. Taft, eds., vol. 6, Interscience, New York, 1968, chap. 5, p. 323.

25. R. A. Marcus, *J. Phys. Chem.*, *67*, 853 (1963).

26. M. E. Peover and B. S. White, *J. Electroanal. Chem.*, *13*, 93 (1966).

27. A. Zweig, W. G. Hodgson, and W. H. Jans, *J. Amer. Chem. Soc.*, *86*, 4124 (1964).

28. K. A. Zachariasse, Ph.D. Thesis, Vrije Universital te Amsterdam (1972).

29. A. Pigham, *Can. J. Chem.*, *51*, 3467 (1973).

30. K. G. Boto and A. J. Bard, *J. Electroanal. Chem.*, *65*, 945 (1975).

31. M. F. Romantsev and E. S. Levin, *Zhur. Anal. Khim.*, *18*, 1109 (1963).

32. M. Schulz and K. -H. Schwarz, *Abhandl. Deut. Akad. Wiss. Berlin, Kl. Chem. Geol. Biol., 1964*, 119.

33. M. Schulz and K. -H. Schwarz, *Mber. dtsch. Akad. Wiss. Berlin, 6*, 515 (1964).

34. M. Schulz and K. -H. Schwarz, *Z. Chem.*, *7*, 176 (1967).

Reproduced with permission of the copyright owner. Further reproduction prohibited without permission.

35. F. Haber and P. Weiss, *Proc. Roy. Soc., London, A127,* 332 (1934).

36. L. Horner and E. Schwenk, *Angew. Chem., 61,* 411 (1949).

37. H. Wieland, T. Ploetz, and H. Indest, *Ann., 532,* 166 (1937).

38. G. S. Hammond, J. T. Rudesill, and E. J. Modie, *J. Amer. Chem. Soc., 73,* 3929 (1951).

39. J. F. Garst, D. Walmsley, and W. R. Richard, *J. Org. Chem., 27,* 2924 (1962).

40. P. F. Hartman, H. G. Sellers, and D. Turnbull, *J. Amer. Chem. Soc., 69,* 2416 (1947).

41. N. E. Tokel, C. P. Keszthelyi, and A. J. Bard, *J. Amer. Chem. Soc., 94,* 4872 (1972).

42. C. P. Keszthelyi and A. J. Bard, *J. Org. Chem., 39,* 2936 (1974).

43. D. L. Akins, S. E. Schwartz, and C. B. Moore, *Rev. Sci. Instr., 39,* 715 (1968).

44. P. M. Renzepis, *Science, 169,* 239 (1970).

45. E. L. Wehry, "Effects of Molecular Structure and Molecular Environment of Fluorescence," in *Practical Fluorescence,* G. G. Guilbault, ed., Marcel Dekker, New York, 1973, chap. 3, p. 79.

46. C. P. Keszthelyi, *J. Amer. Chem. Soc., 96,* 1243 (1970).

47. E. H. White, J. Wiecko, and C. C. Wei, *J. Amer. Chem. Soc., 92,* 2167 (1970).

48. B. J. Tabner and J. R. Zdysiewicz, *J. Chem. Soc., 1971,* 1659.

49. G. N. Lewis and M. Kasha, *J. Amer. Chem. Soc., 66,* 2100 (1944).

50. I. Berlman, *Handbook of Fluorescence Spectra of Aromatic Molecules,* Academic, New York, 1971.

51. J. F. Ambrose and R. F. Nelson, *J. Electrochem. Soc., 115,* 1159 (1968).

52. E. S. Pysh and N. C. Yang, *J. Amer. Chem. Soc., 85,* 2124 (1963).

53. S. Millefiori, *J. Heterocycl. Chem., 7,* 145 (1970).

54. B. J. Tabner and J. R. Yandle, *J. Chem. Soc., A,* 1968, 381.

55. A. J. Bard, K. S. V. Santhanam, J. T. Maloy, J. Phelps, and L. O. Wheeler, *Disc. Faraday Soc., 45,* 167 (1968).

Reproduced with permission of the copyright owner. Further reproduction prohibited without permission.

56. C. P. Keszthelyi, H. Tachikawa, and A. J. Bard, *J. Amer. Chem. Soc.*, *94*, 1522 (1972).

57. A. Yildiz, P. T. Kissinger, and C. N. Rielly, *J. Chem. Phys.*, *49*, 1403 (1968).

58. J. T. Maloy, K. B. Prater, and A. J. Bard, *J. Phys. Chem.*, *72*, 4348 (1968).

59. L. R. Faulkner, H. Tachikawa, and A J. Bard, *J. Amer. Chem. Soc.*, *94*, 691 (1972).

60. D. J. Freed and L. R. Faulkner, *J. Amer. Chem. Soc.*, *93*, 3565 (1971).

61. J. T. Maloy and A. J. Bard, *J. Amer. Chem. Soc.*, *93*, 5968 (1971).

62. H. Tachikawa and A. J. Bard, *Chem. Phys. Letters*, *19*, 287 (1973).

63. C. P. Keszthelyi, N. E. Tokel-Takvoryan, H. Tachikawa, and A. J. Bard, *Chem. Phys. Letters*, *23*, 219 (1973).

64. C. P. Keszthelyi and A. J. Bard, *Chem. Phys. Letters*, *24*, 300 (1974).

65. A. Weller and K. Zachariasse, *Chem. Phys. Letters*, *10*, 197 (1971).

66. A. Weller and K. Zachariasse, *Chem. Phys. Letters*, *10*, 424 (1971).

67. A. Weller and K. Zachariasse, *Chem. Phys. Letters*, *10*, 590 (1971).

68. (a) C. A. Parker, *Photoluminescence in Solutions* , Elsevier Company, New York, 1968; (b) I. Berlman, *Energy Transfer Parameters of Atomatic Compounds*, Academic, New York, 1973.

69. S. W. Feldberg, *J. Amer. Chem. Soc.*, *88*, 390 (1966).

70. S. W. Feldberg, *J. Phys. Chem.*, *70*, 3928 (1966).

71. S. A. Cruser and A. J. Bard, *J. Amer. Chem. Soc.*, *91*, 267 (1969).

72. R. Bezman and L. R. Faulkner, *J. Amer. Chem. Soc.*, *94*, 3699 (1972).

73. R. Bezman and L. R. Faulkner, *J. Amer. Chem. Soc.*, *94*, 6317 (1972).

74. R. Bezman and L. R. Faulkner, *J. Amer. Chem. Soc.*, *94*, 6324 (1972).

75. R. Bezman and L. R. Faulkner, *J. Amer. Chem. Soc.*, *94*, 6331 (1972).

76. R. Bezman and L. R. Faulkner, *J. Amer. Chem. Soc.*, *95*, 3083 (1973).

77. L. R. Faulkner, *J. Electrochem. Soc.*, *122*, 1190 (1975).

Reproduced with permission of the copyright owner. Further reproduction prohibited without permission.

78. S. W. Feldberg, "Digital Simulation," in *Electroanalytical Chemistry*, A. J. Bard, ed., vol. 3, Marcel Dekker, New York, 1968, chap. 4.

79. P. Delahay and G. L. Stiehl, *J. Amer. Chem. Soc.*, *74*, 3500 (1952).

80. G. M. Murphy, *Ordinary Differential Equations and Their Solutions*, D. Van Postrenid Company, Inc., Princeton, 1960, pp. 13-15.

81. D. T. Sawyer and J. L. Roberts, *Experimental Electrochemistry for the Chemist*, Wiley-Interscience, New York, 1974, p. 212.

82. P. Sampson, "Nonlinear Least Squares," in *BMD Biomedical Computer Programs*, W. J. Dixon, ed., University of California Press, Los Angeles, 1972.

83. H. O. Hartley, *Techometrics*, *3*, 269 (1961).

84. R. !. Jennrich and P. F. Sampson, *Techometrics*, *10*, 63 (1968).

85. J. Chang, D. M. Hercules, and D. K. Roe, *Electrochimica Acta*, *13*, 1197 (1968).

86. L. R. Faulkner and A. J. Bard, *J. Amer. Chem. Soc.*, *91*, 6497 (1969).

Reproduced with permission of the copyright owner. Further reproduction prohibited without permission.

# APPENDIX

Reproduced with permission of the copyright owner. Further reproduction prohibited without permission.

Figure 16. The Intensity-Time Plots of $1.10 \times 10^{-5}$ M Fluoranthene Collected Using the Total Emission Band for (a) Raw Data, (b) "Fixed" Smoothed Data, and (c) Composite of "Fixed" Smoothed Data and Fitted Data (open squares).

Reproduced with permission of the copyright owner. Further reproduction prohibited without permission.

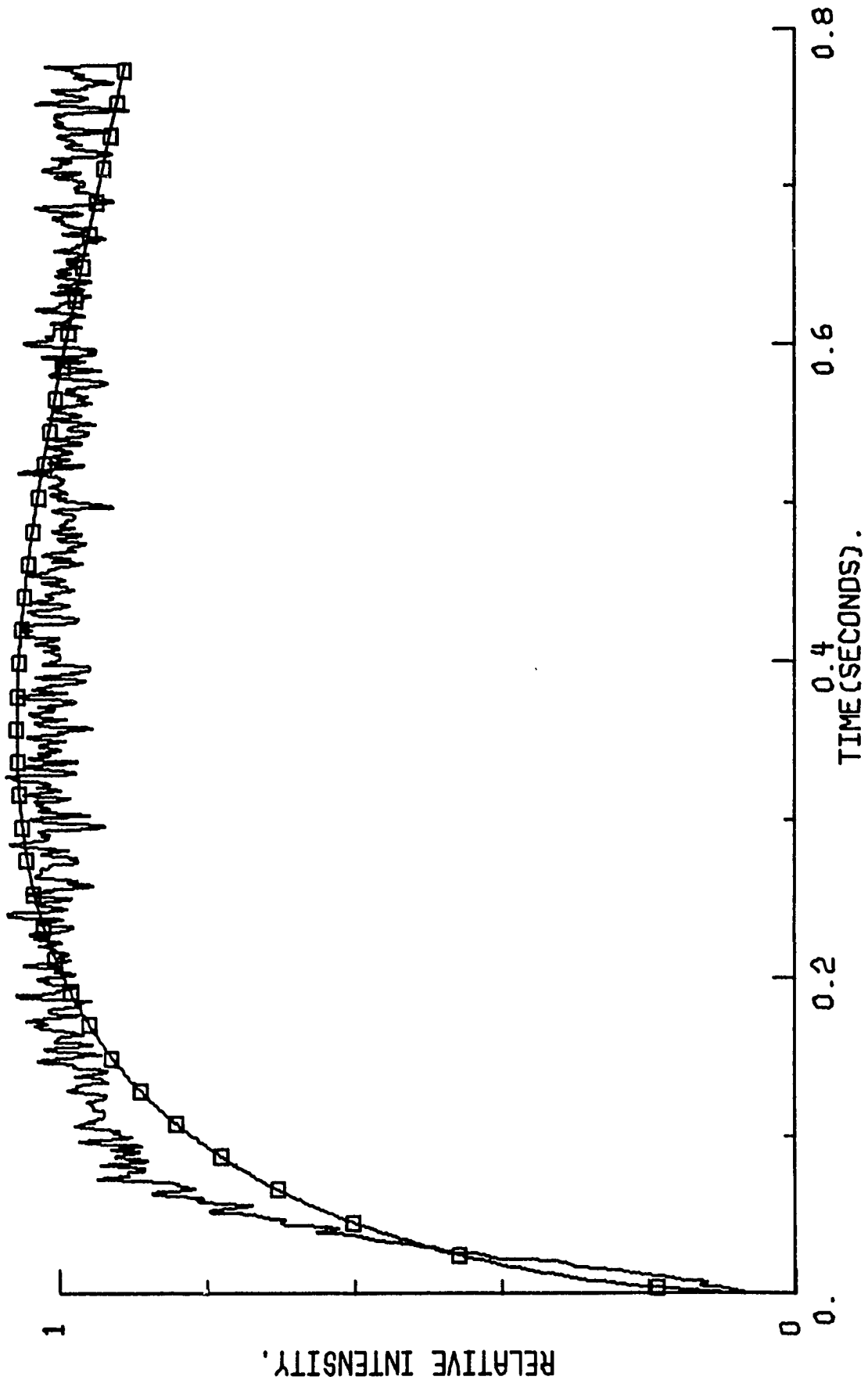


Reproduced with permission of the copyright owner. Further reproduction prohibited without permission.

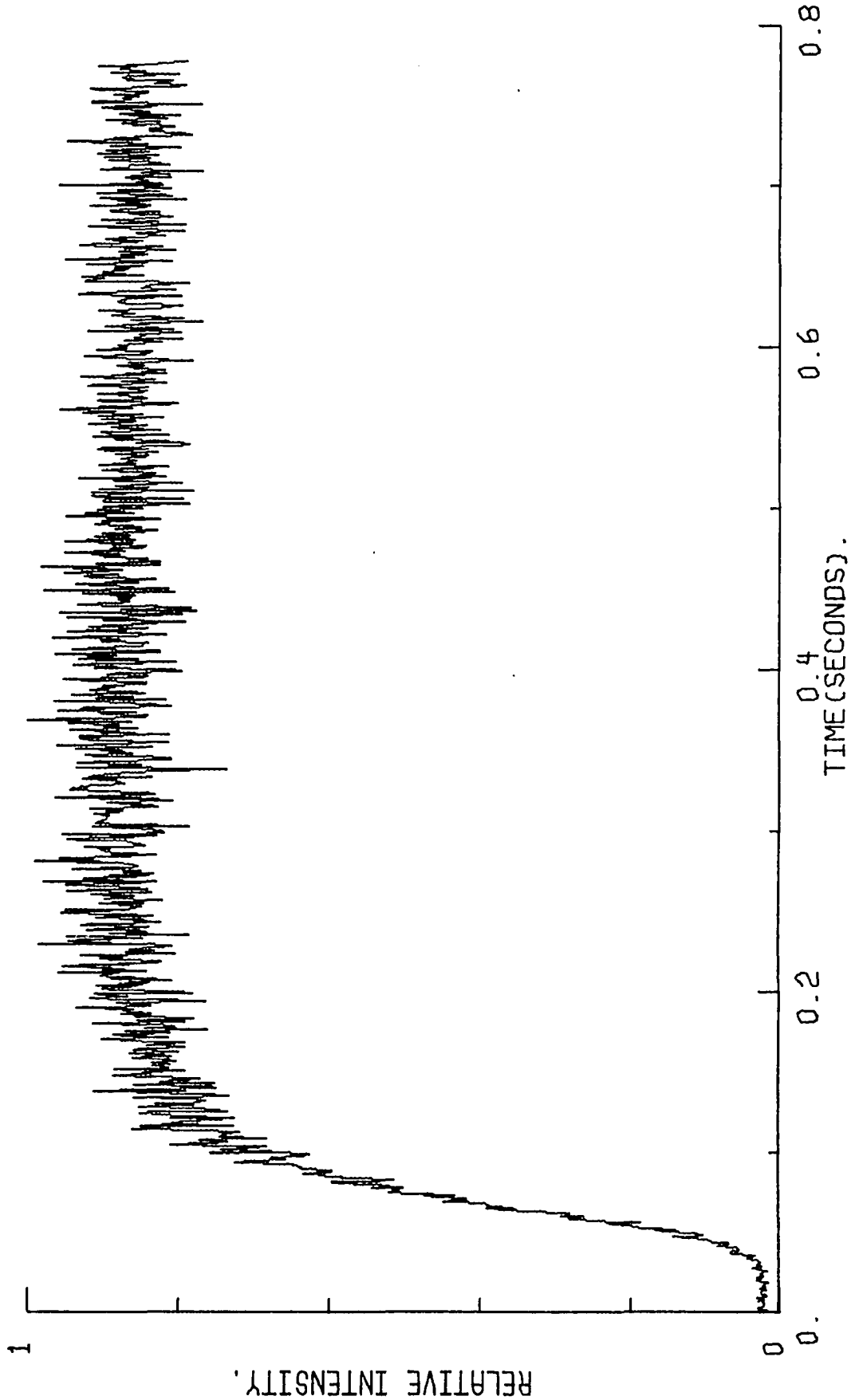


Reproduced with permission of the copyright owner. Further reproduction prohibited without permission.

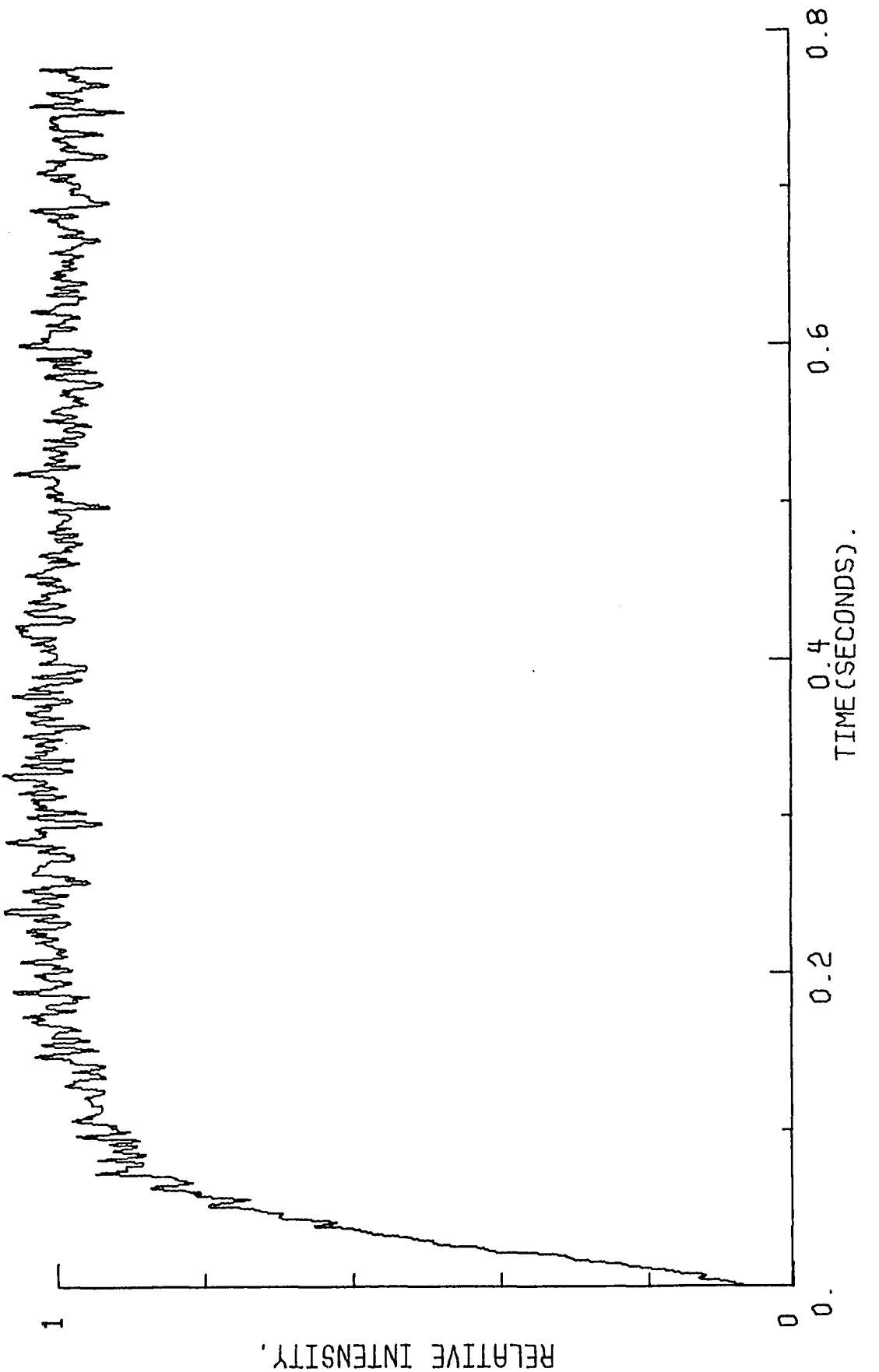


Reproduced with permission of the copyright owner. Further reproduction prohibited without permission.

Figure 17. The Intensity-Time Plots of $2.76 \times 10^{-5}$ M Fluoranthene Collected Using the Total Emission Band for (a) Raw Data, (b) "Fixed" Smoothed Data, and (c) Composite of "Fixed" Smoothed Data and Fitted Data (open squares).

Reproduced with permission of the copyright owner. Further reproduction prohibited without permission.

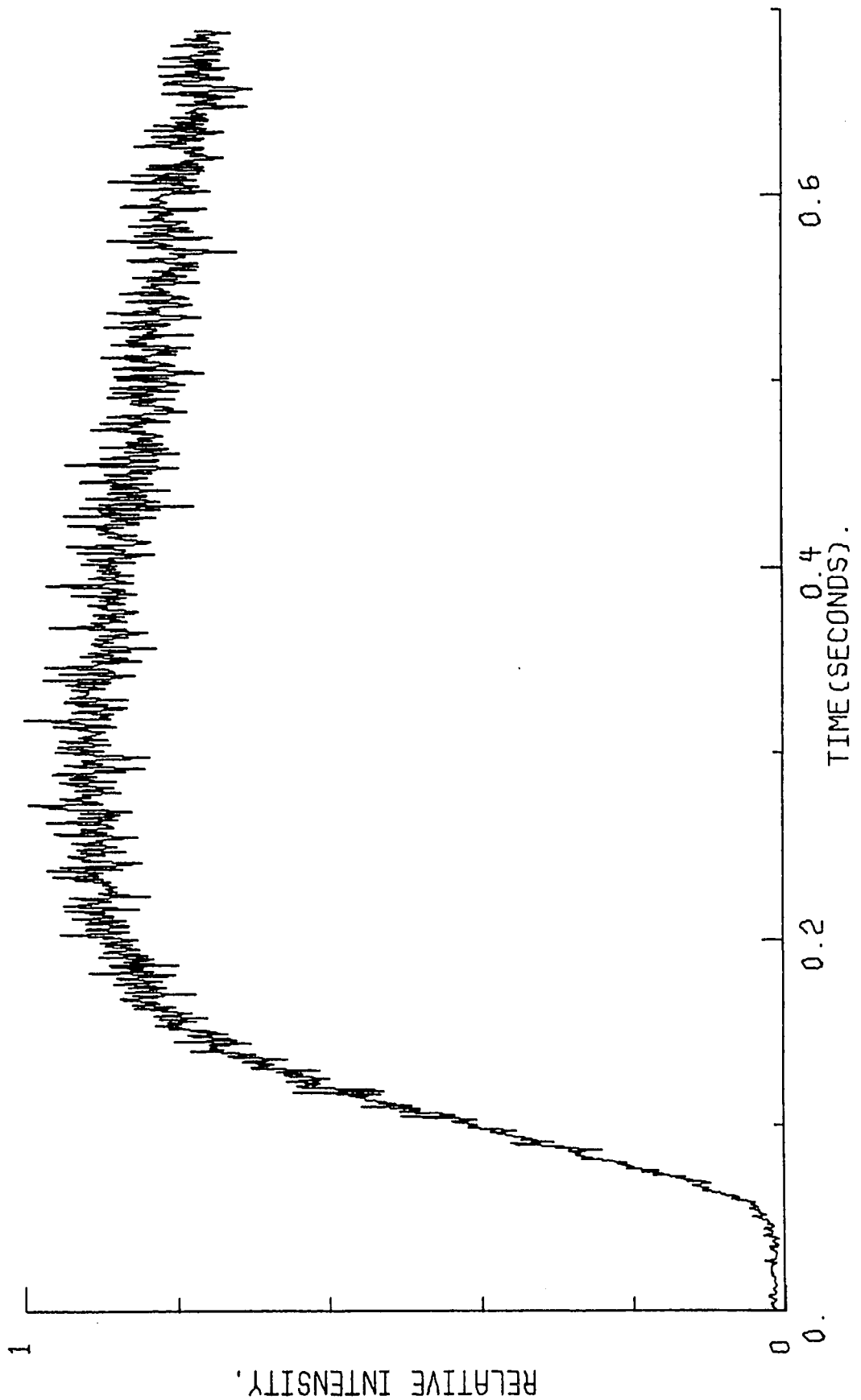


Reproduced with permission of the copyright owner. Further reproduction prohibited without permission.

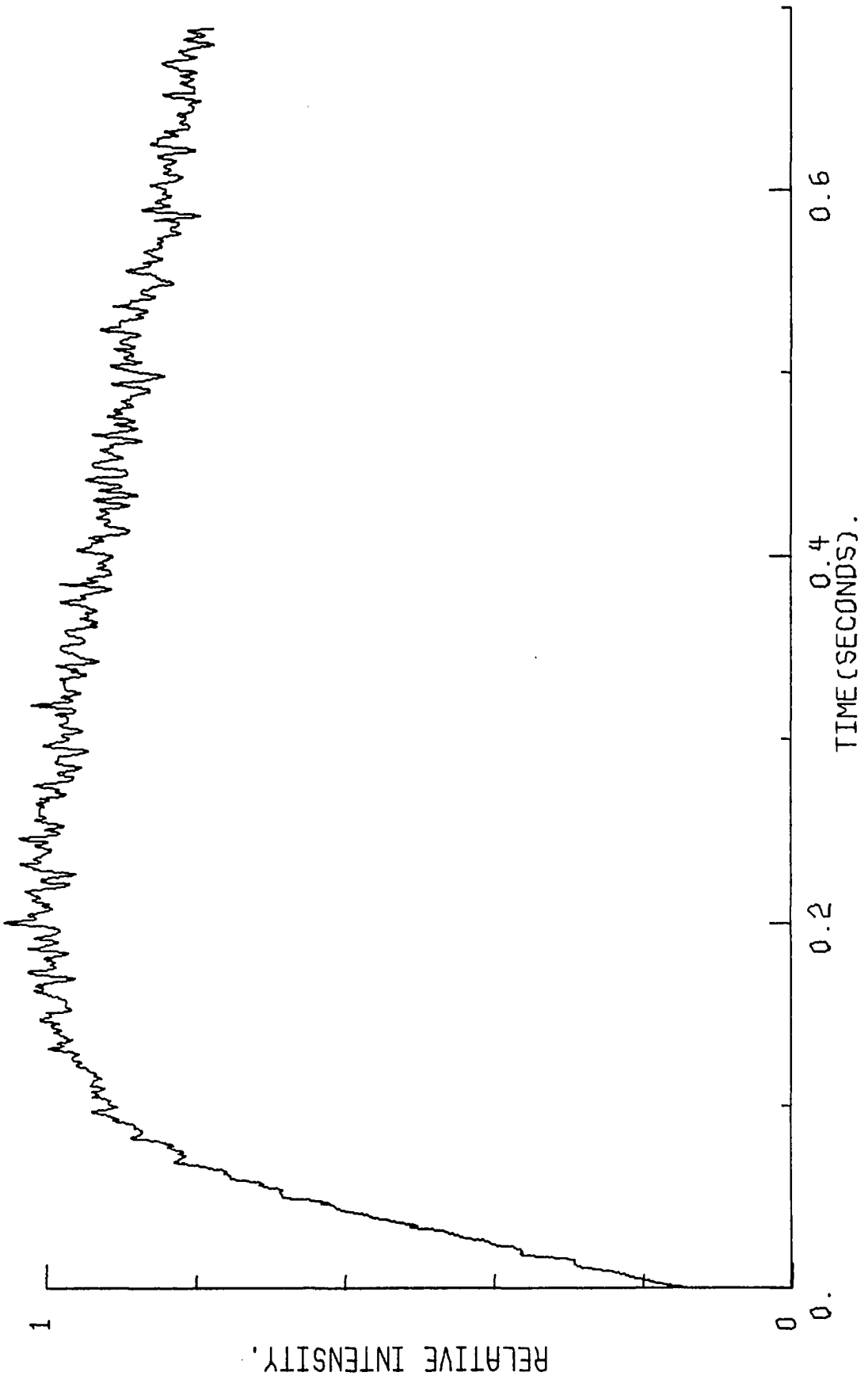


Reproduced with permission of the copyright owner. Further reproduction prohibited without permission.

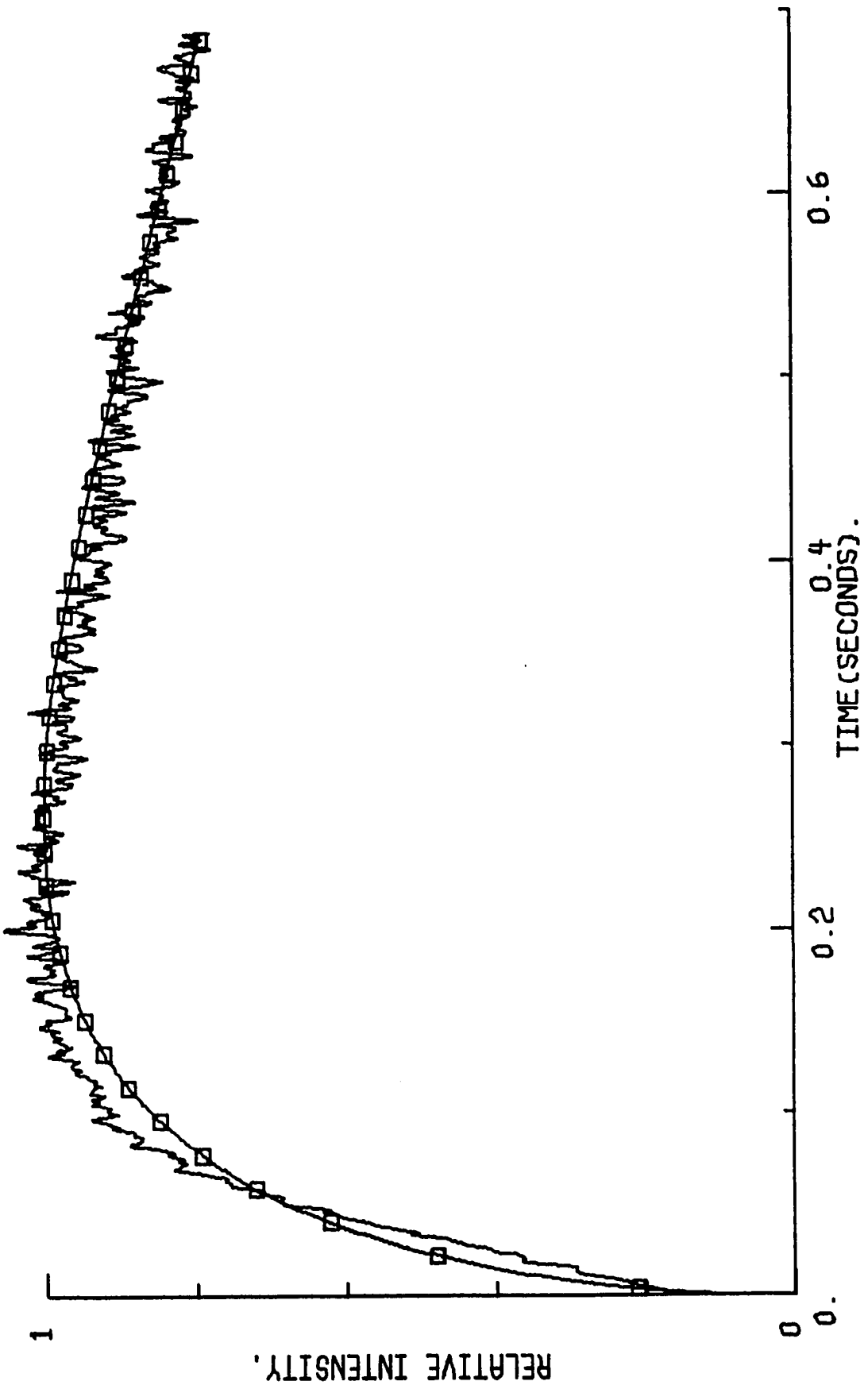


Reproduced with permission of the copyright owner. Further reproduction prohibited without permission.

Figure 18. The Intensity-Time Plots of $6.91 \times 10^{-5}$ M Fluoranthene Collected Using the Total Emission Band for (a) Raw Data, (b) "Fixed" Smoothed Data, and (c) Composite of "Fixed" Smoothed Data and Fitted Data (open squares).

Reproduced with permission of the copyright owner. Further reproduction prohibited without permission.

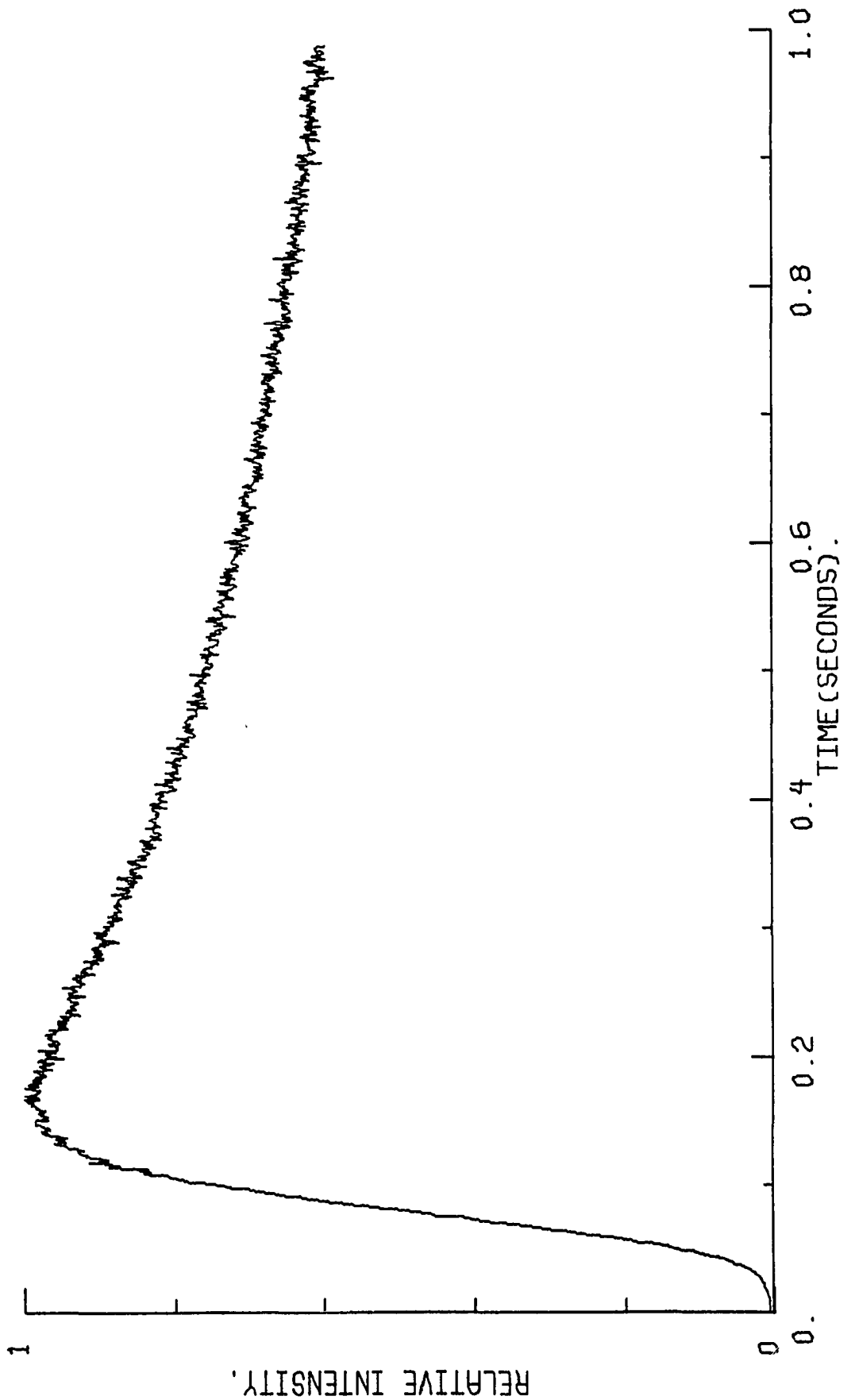


Reproduced with permission of the copyright owner. Further reproduction prohibited without permission.

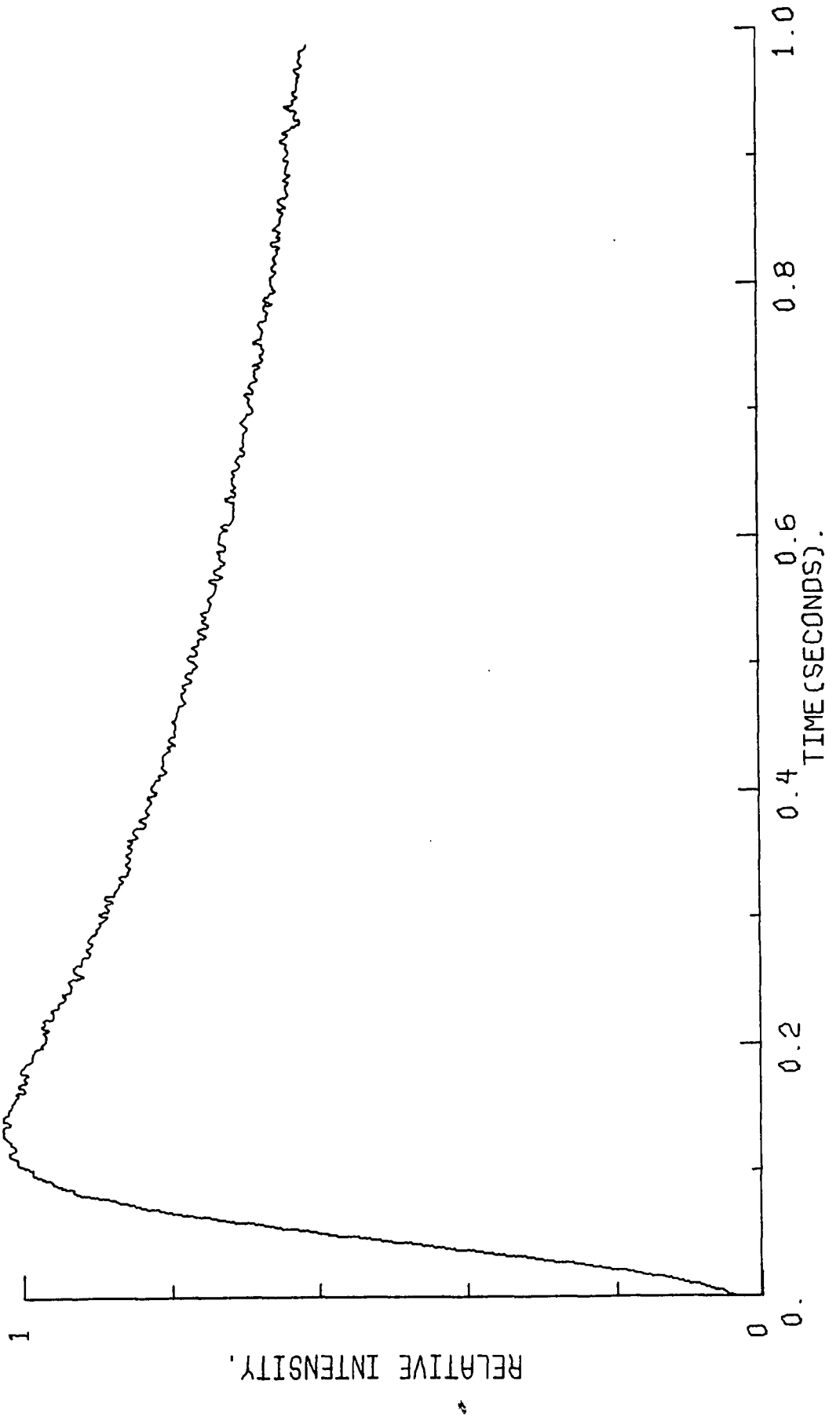


Reproduced with permission of the copyright owner. Further reproduction prohibited without permission.

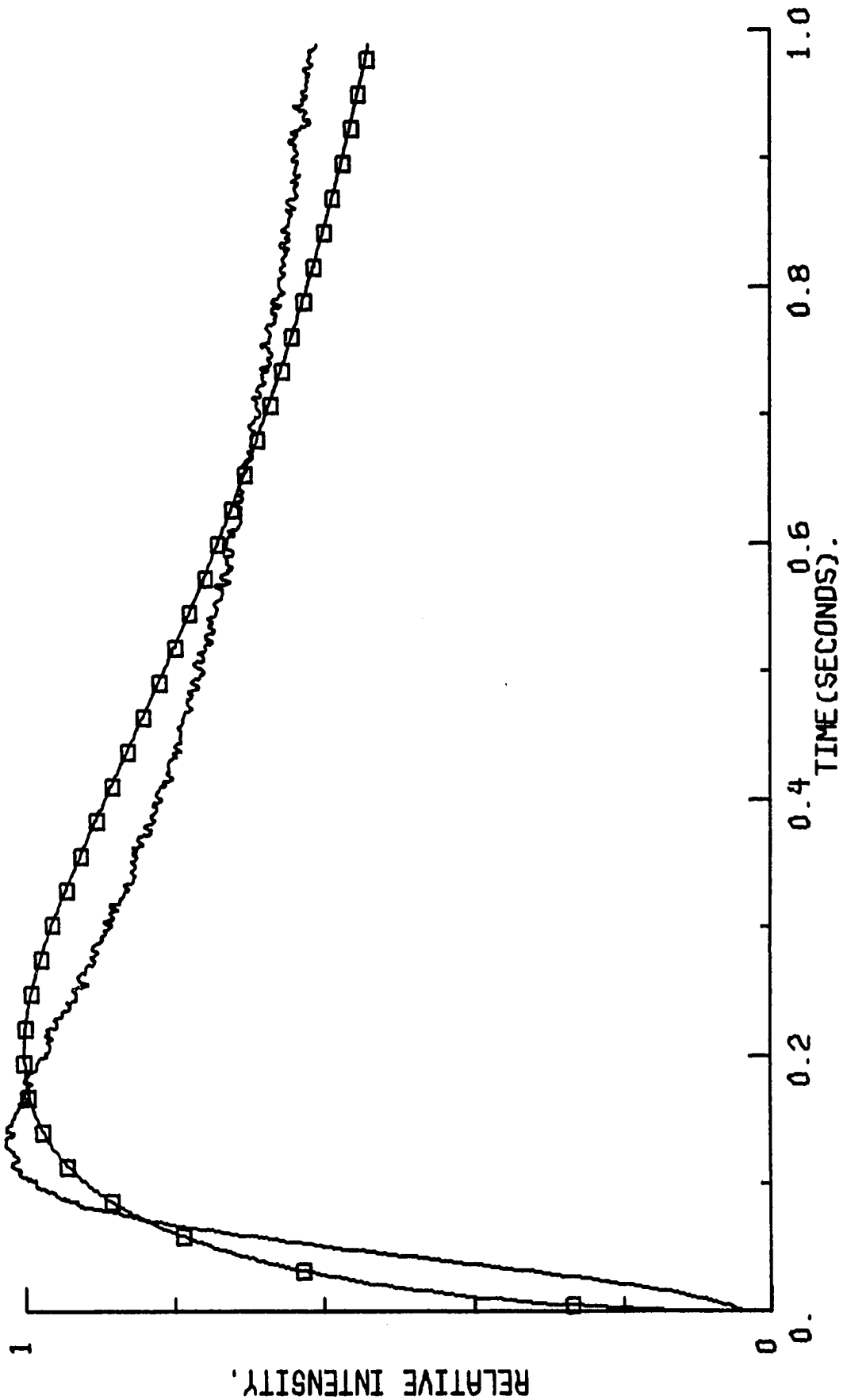


Reproduced with permission of the copyright owner. Further reproduction prohibited without permission.

Figure 19. The Intensity-Time Plots of $1.74 \times 10^{-4}$ M Fluoranthene Collected Using the Total Emission Band for (a) Raw Data, (b) "Fixed" Smoothed Data, and (c) Composite of "Fixed" Smoothed Data and Fitted Data (open squares).

Reproduced with permission of the copyright owner. Further reproduction prohibited without permission.

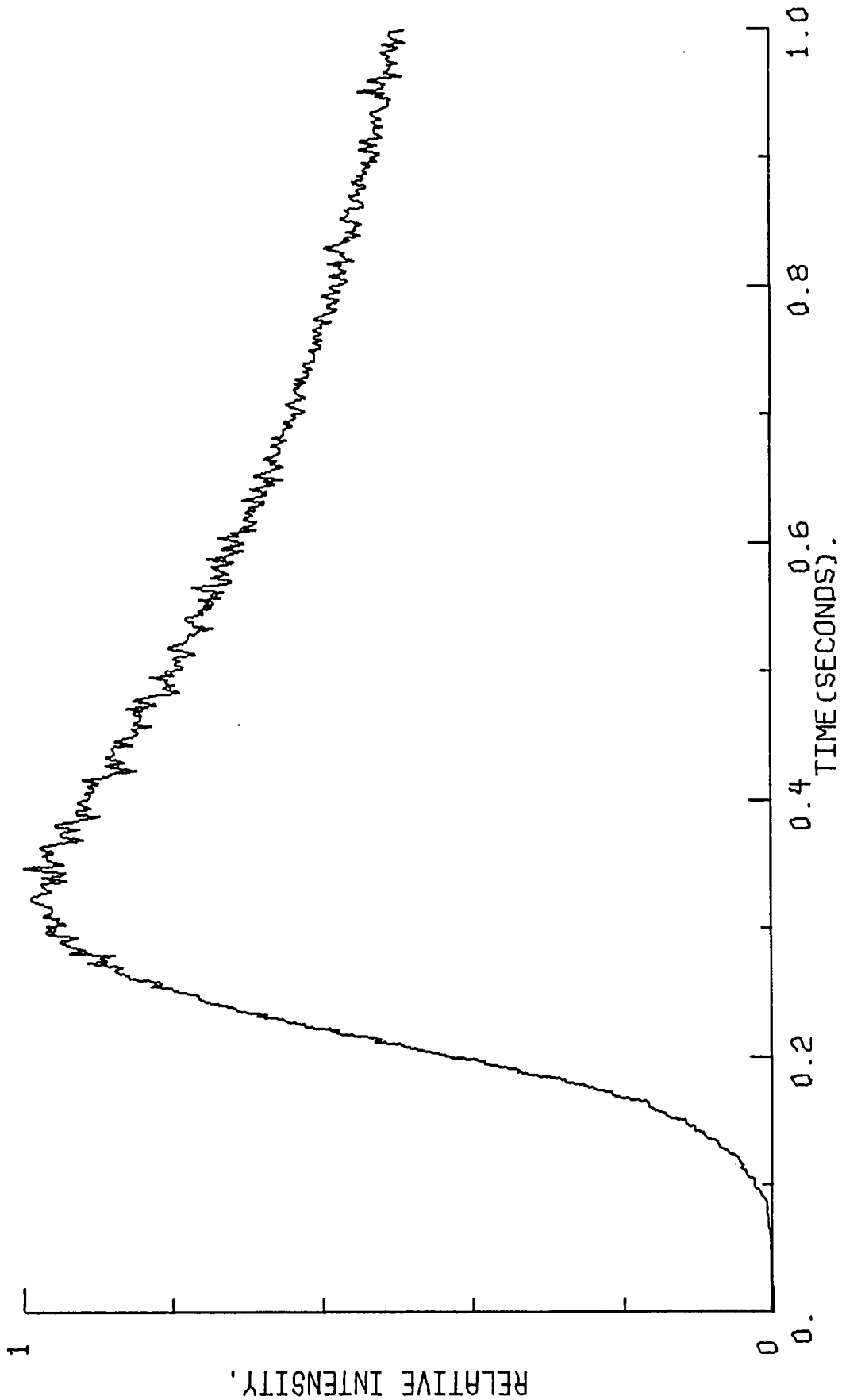


Reproduced with permission of the copyright owner. Further reproduction prohibited without permission.

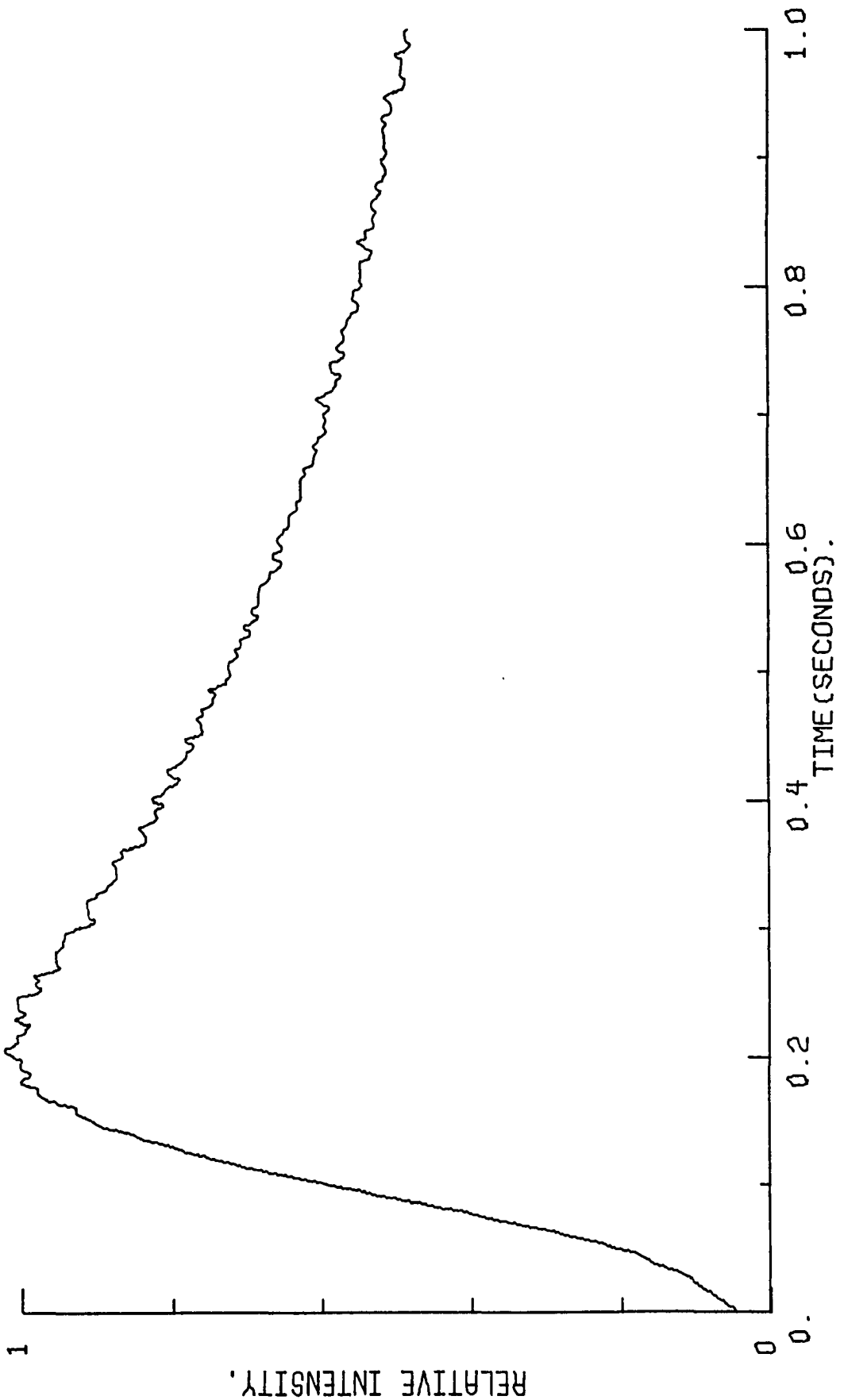


Reproduced with permission of the copyright owner. Further reproduction prohibited without permission.

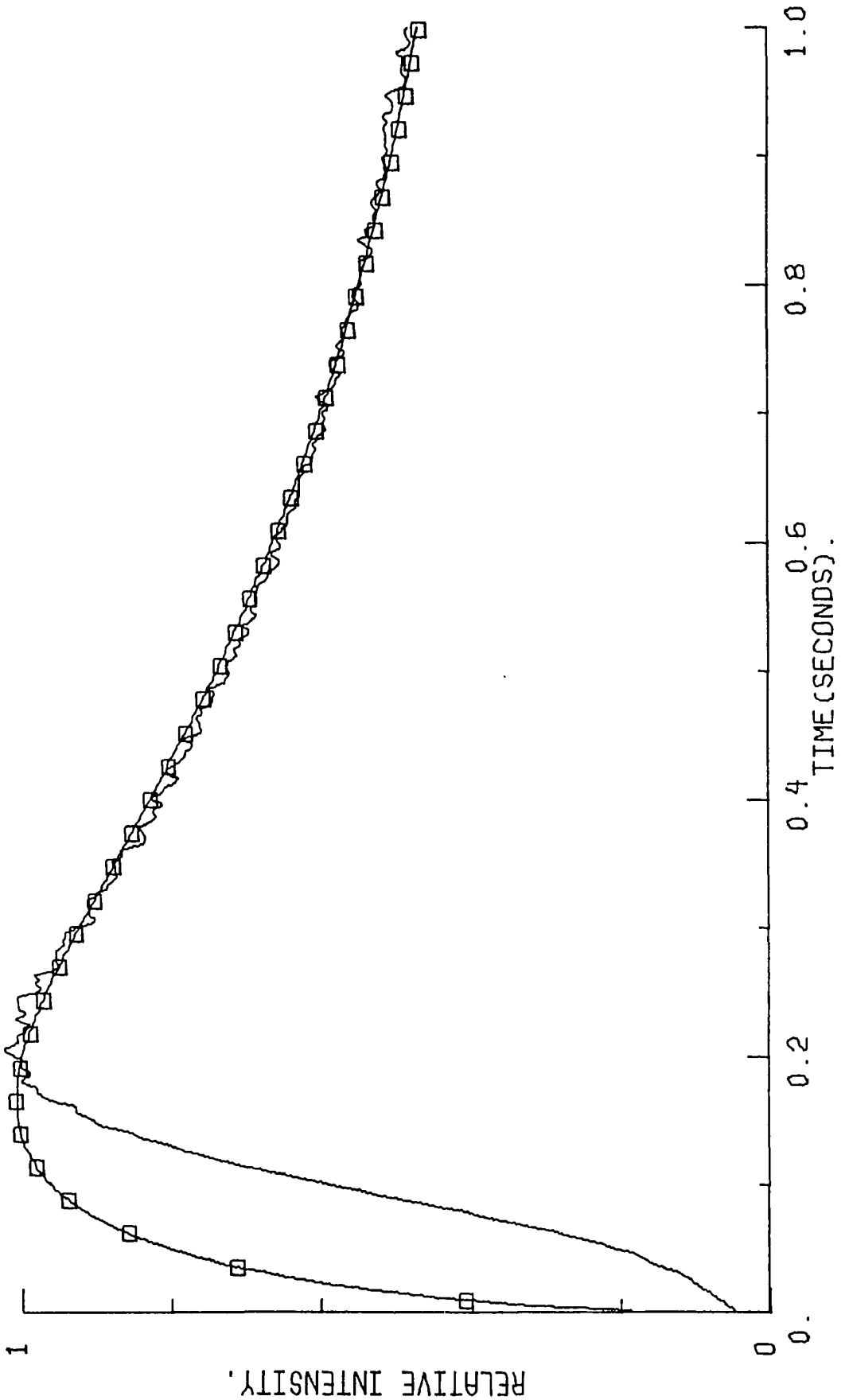


Reproduced with permission of the copyright owner. Further reproduction prohibited without permission.

Figure 20. The Intensity-Time Plots of $4.32 \times 10^{-4}$ M Fluoranthene Collected Using the Total Emission Band for (a) Raw Data, (b) "Fixed" Smoothed Data, and (c) Composite of "Fixed" Smoothed Data and Fitted Data (open squares).

Reproduced with permission of the copyright owner. Further reproduction prohibited without permission.

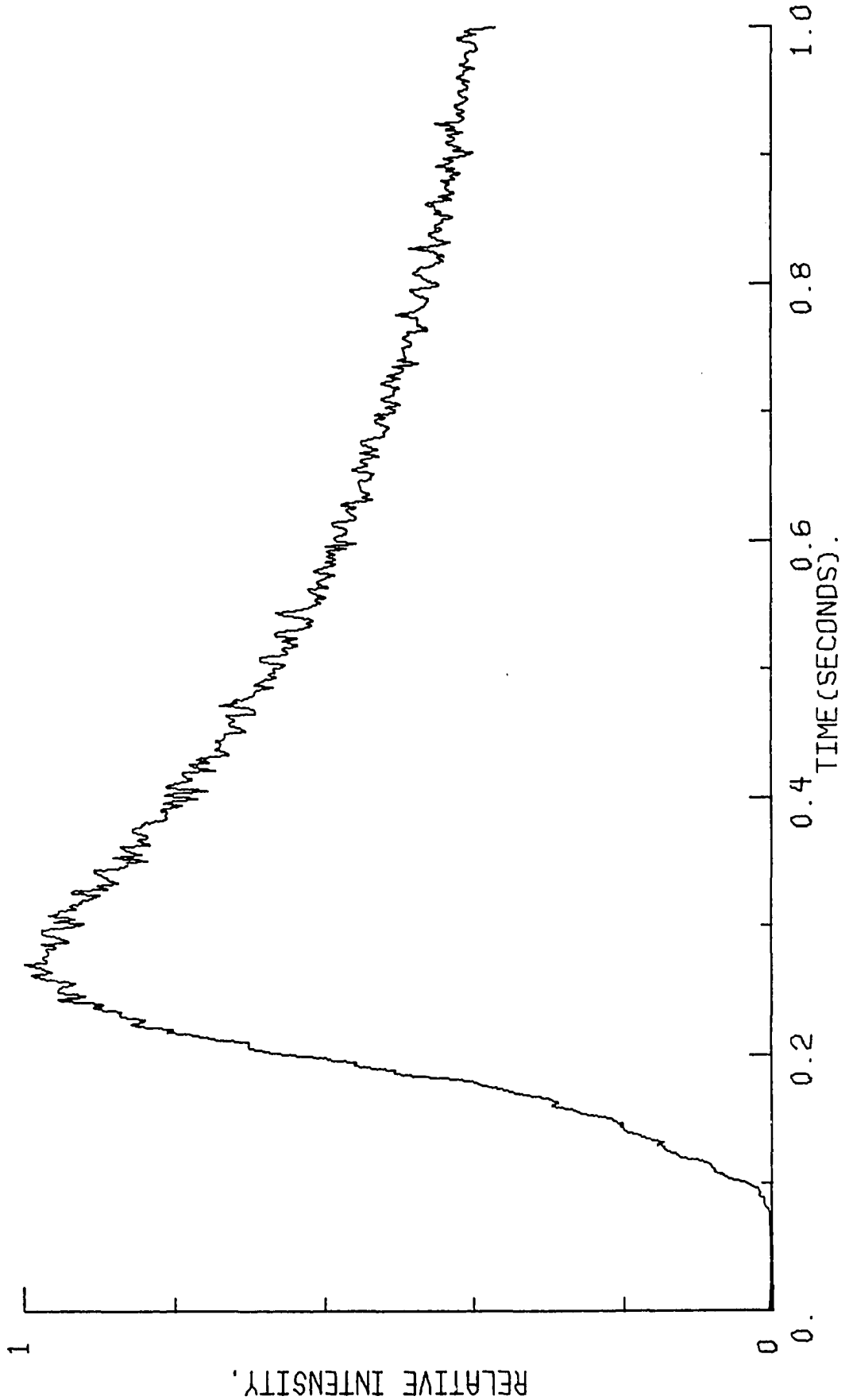


Reproduced with permission of the copyright owner. Further reproduction prohibited without permission.

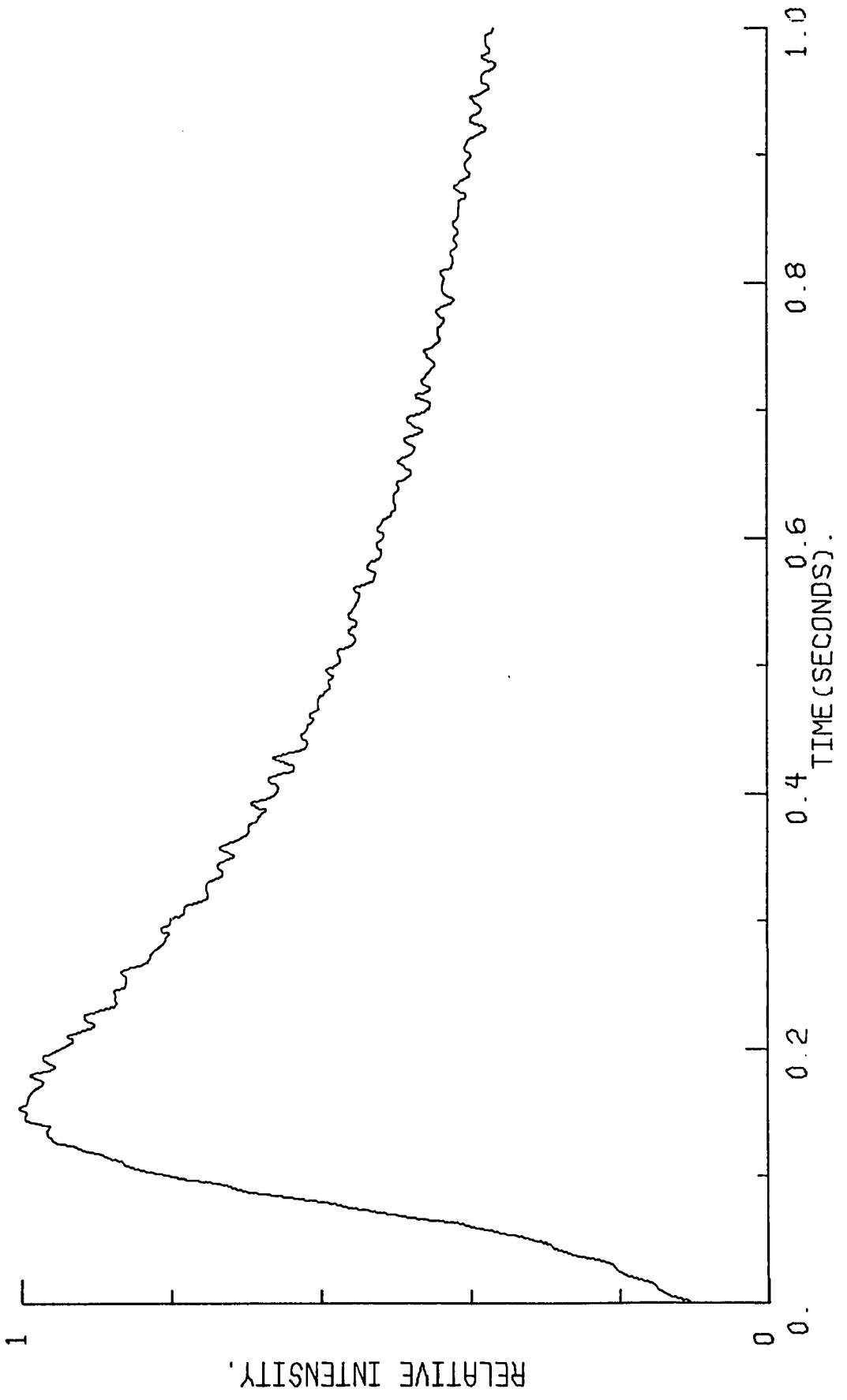


Reproduced with permission of the copyright owner. Further reproduction prohibited without permission.

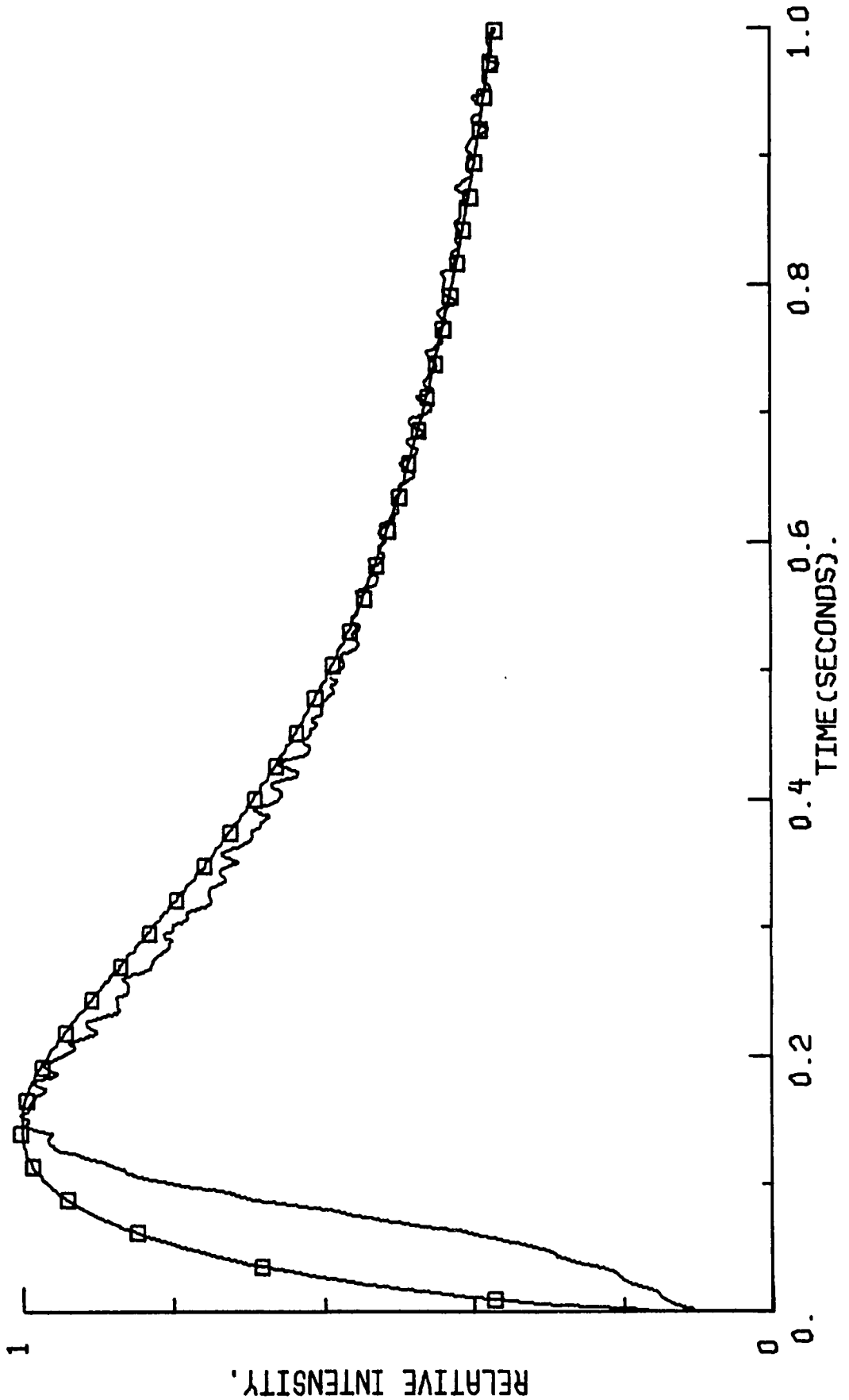


Reproduced with permission of the copyright owner. Further reproduction prohibited without permission.

Figure 21. The Intensity-Time Plots of $1.08 \times 10^{-3}$ M Fluoranthene Collected Using the Total Emission Band for (a) Raw Data, (b) "Fixed" Smoothed Data, and (c) Composite of "Fixed" Smoothed Data and Fitted Data (open squares).

Reproduced with permission of the copyright owner. Further reproduction prohibited without permission.

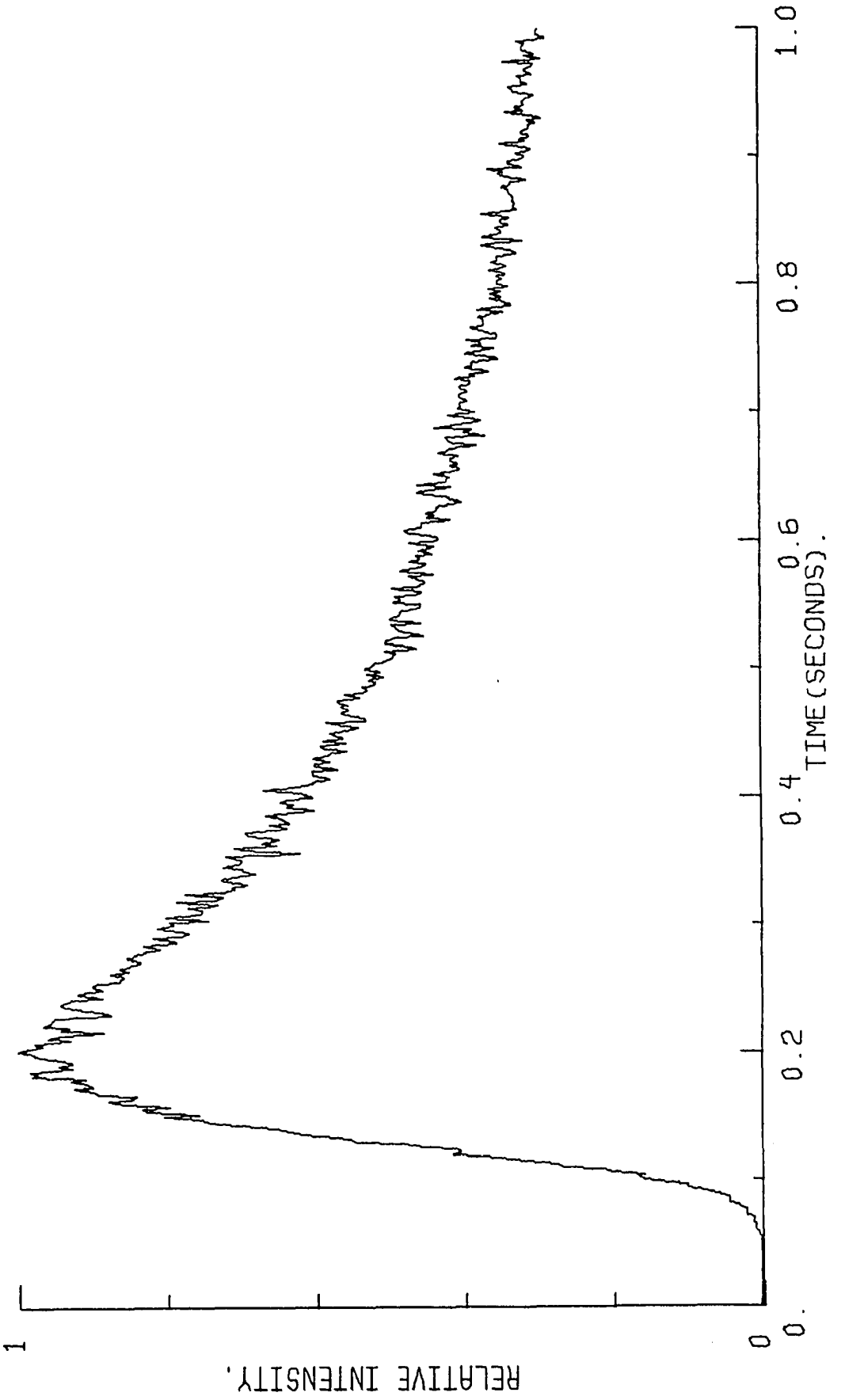


Reproduced with permission of the copyright owner. Further reproduction prohibited without permission.

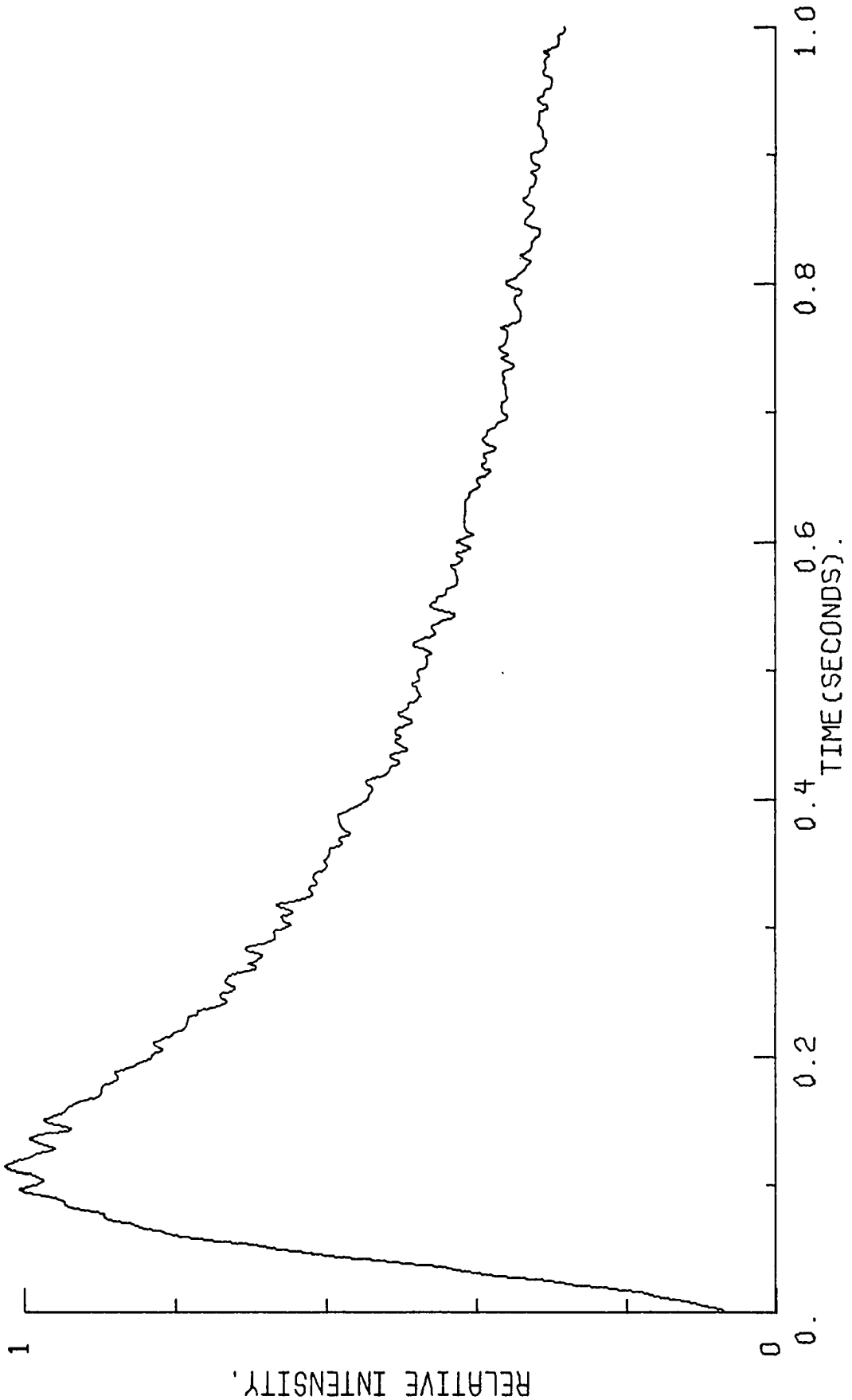


Reproduced with permission of the copyright owner. Further reproduction prohibited without permission.

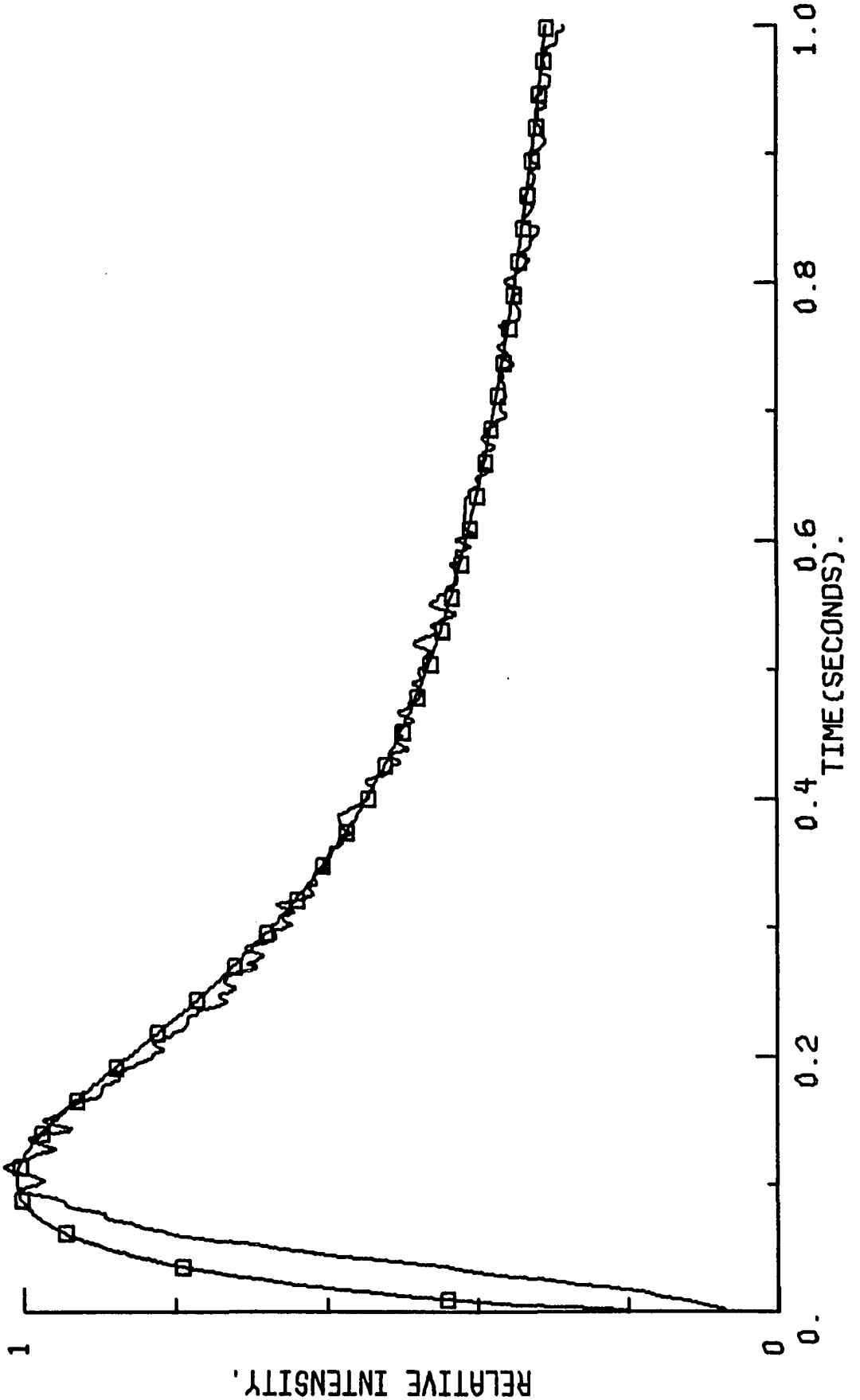


Reproduced with permission of the copyright owner. Further reproduction prohibited without permission.

Figure 22. The Intensity-Time Plots of $2.70 \times 10^{-3}$ M Fluoranthene Collected Using the Total Emission Band for (a) Raw Data, (b) "Fixed" Smoothed Data, and (c) Composite of "Fixed" Smoothed Data and Fitted Data (open squares).

Reproduced with permission of the copyright owner. Further reproduction prohibited without permission.

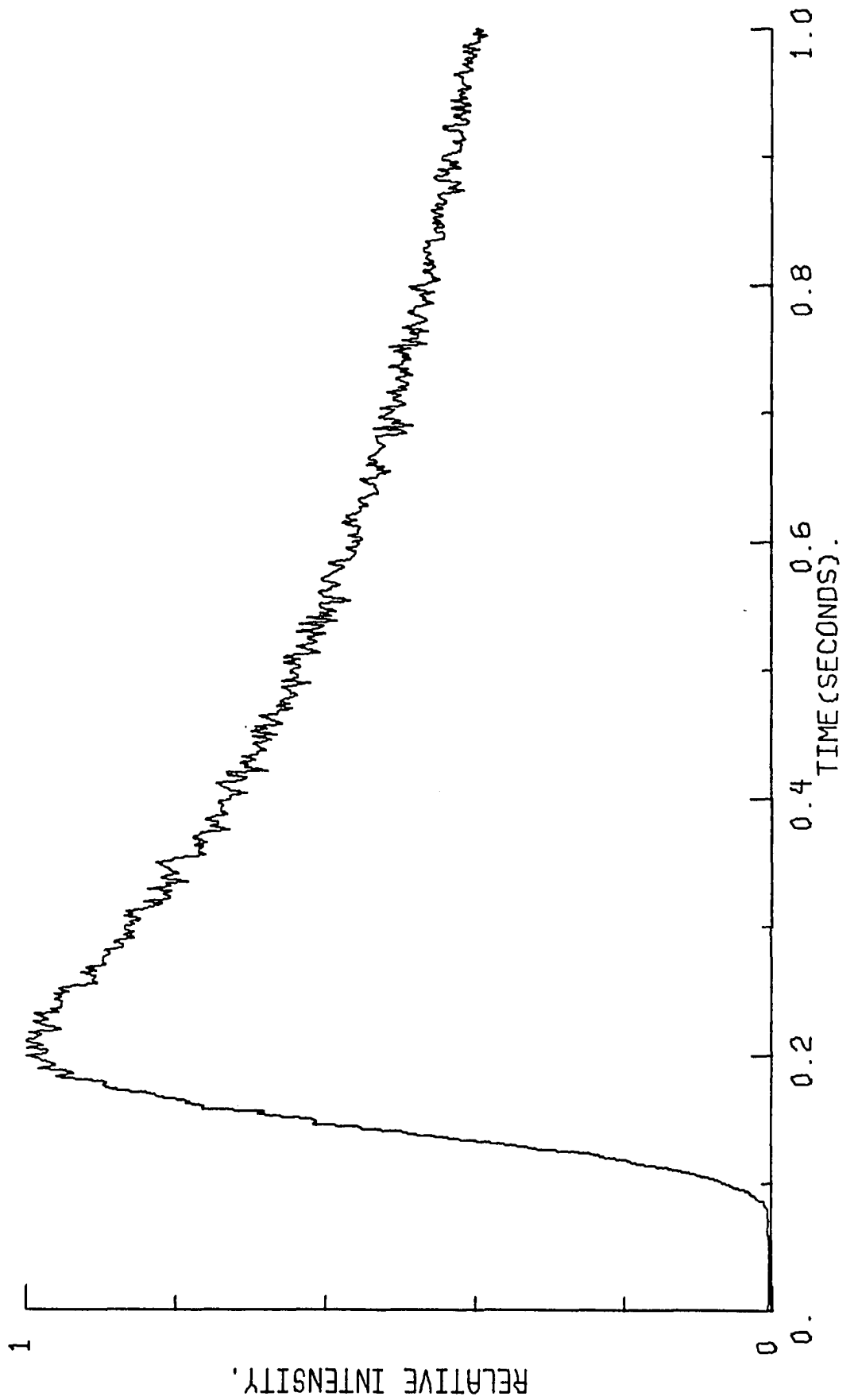


Reproduced with permission of the copyright owner. Further reproduction prohibited without permission.

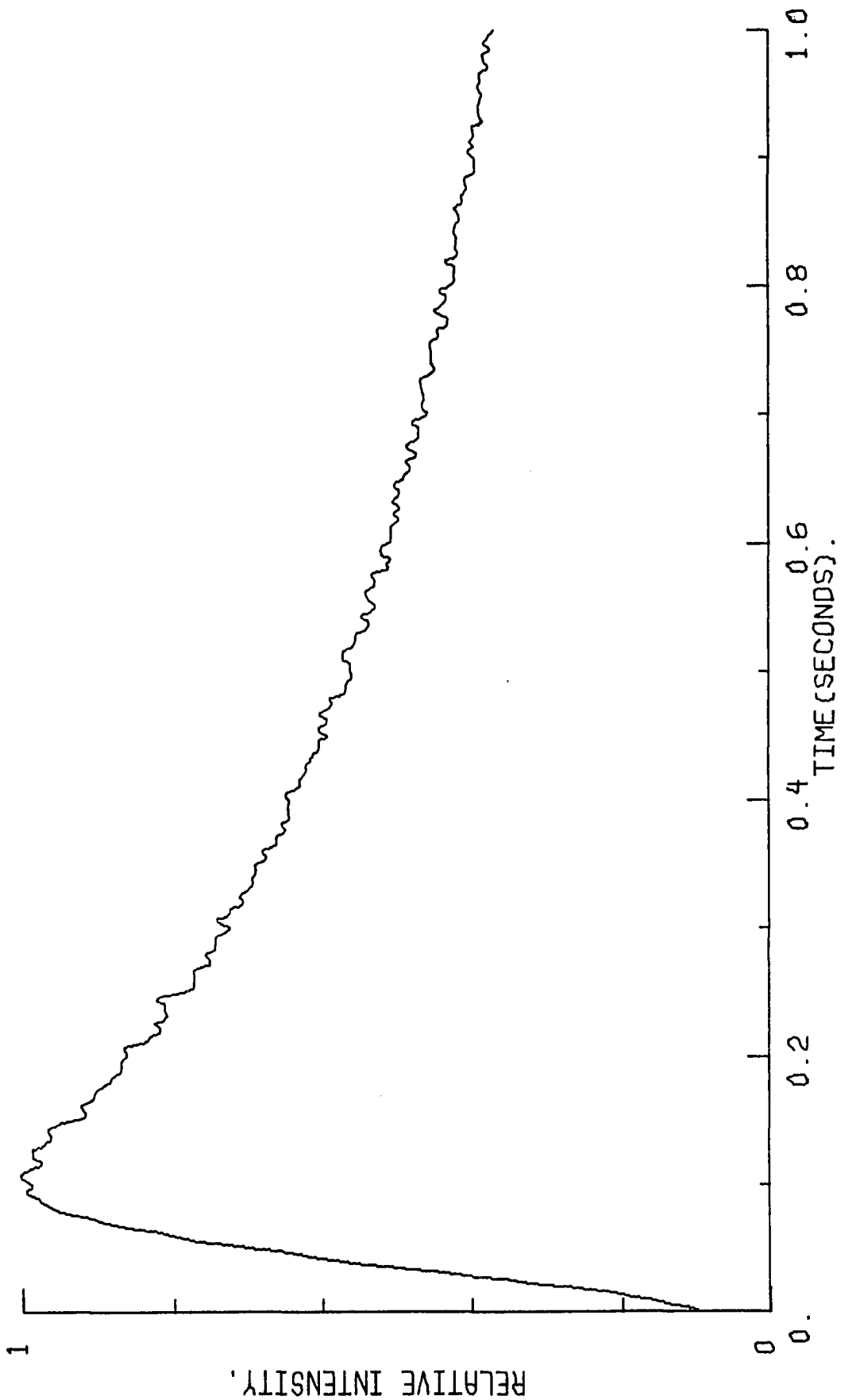


Reproduced with permission of the copyright owner. Further reproduction prohibited without permission.

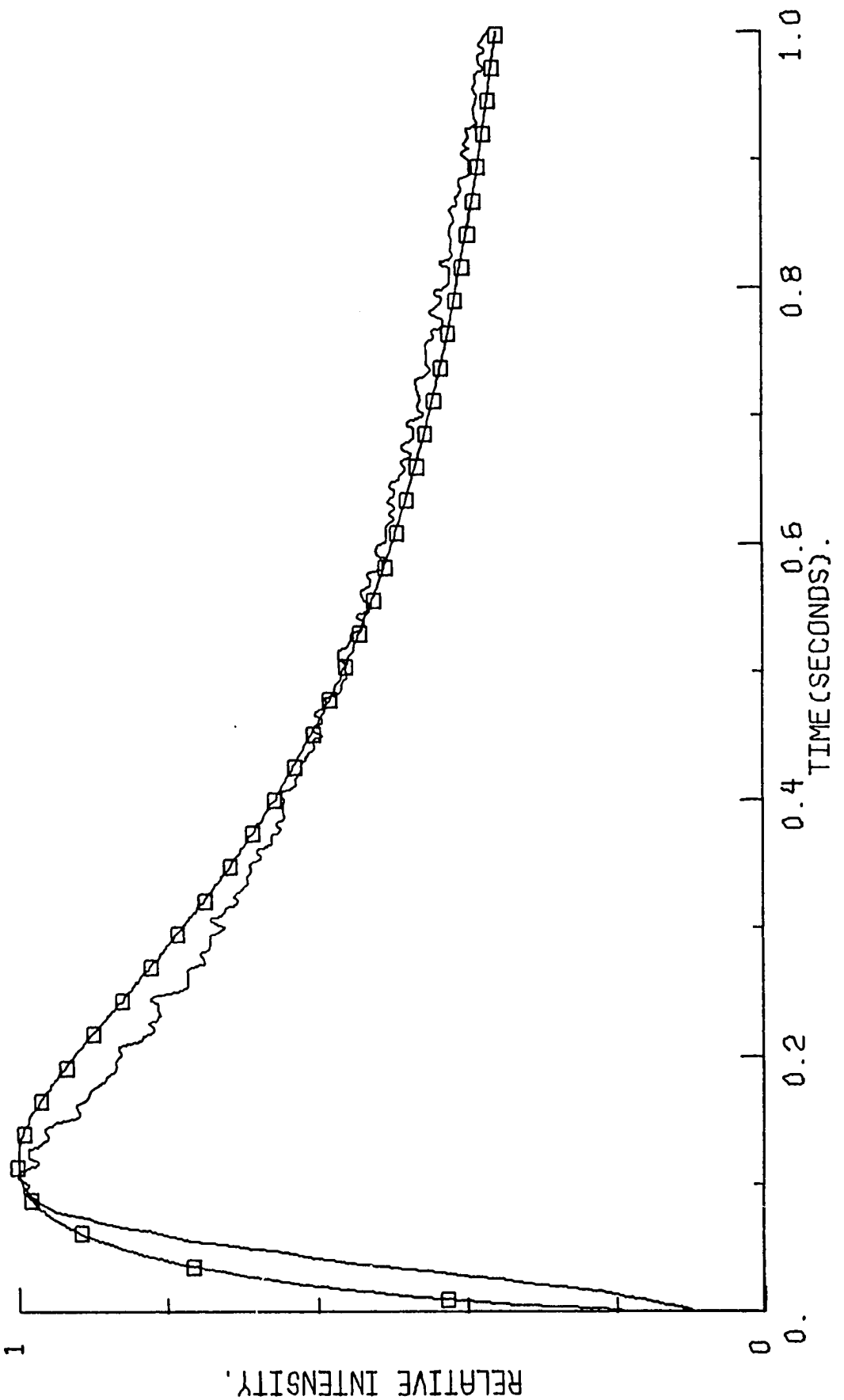


Reproduced with permission of the copyright owner. Further reproduction prohibited without permission.

Figure 23. The Intensity-Time Plots of $1.10 \times 10^{-5}$ M Fluoranthene Collected at the Wavelength of 470 nm for (a) Raw Data, (b) "Fixed" Smoothed Data, and (c) Composite of "Fixed" Smoothed Data and Fitted Data (open squares).

Reproduced with permission of the copyright owner. Further reproduction prohibited without permission.

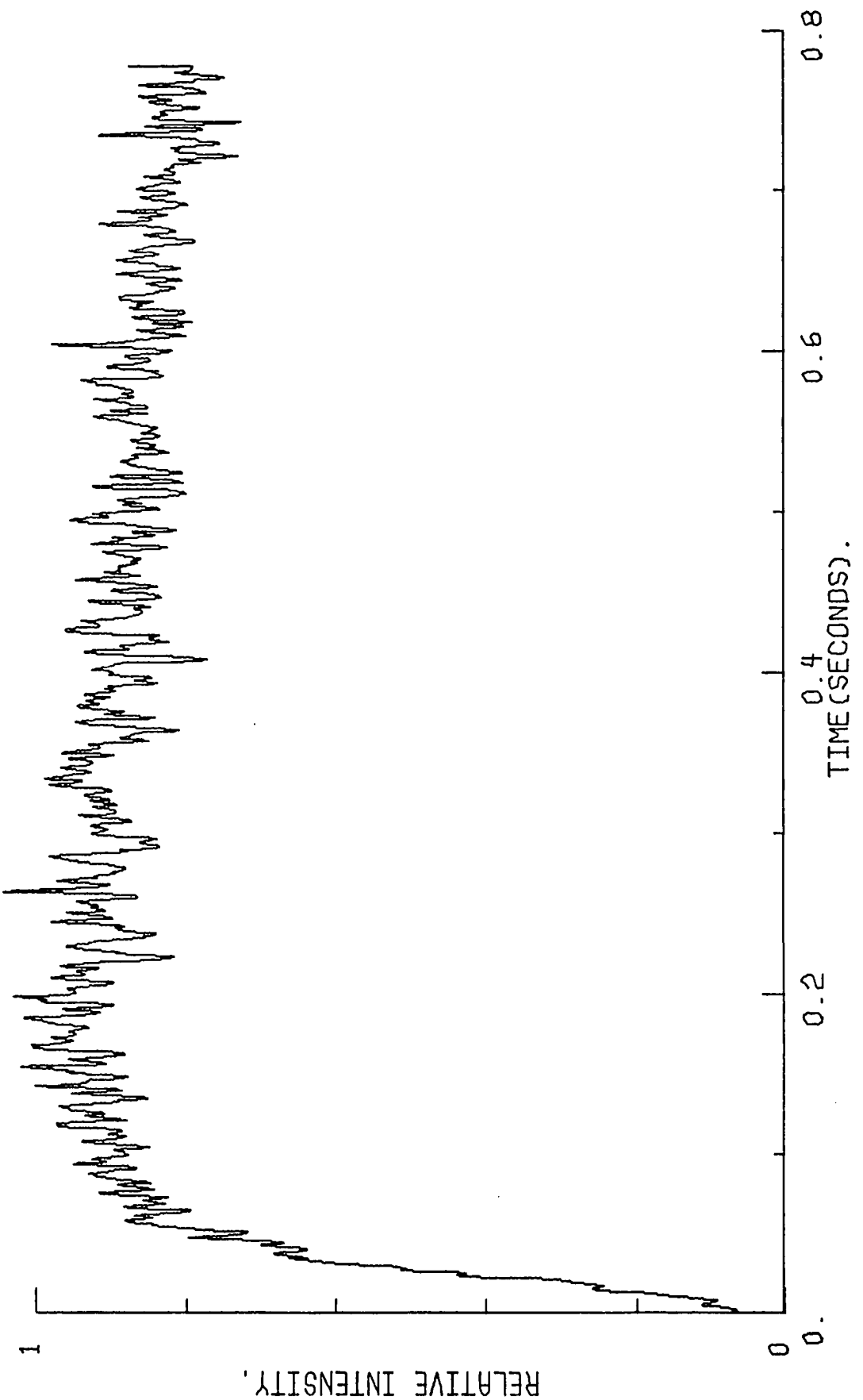


Reproduced with permission of the copyright owner. Further reproduction prohibited without permission.

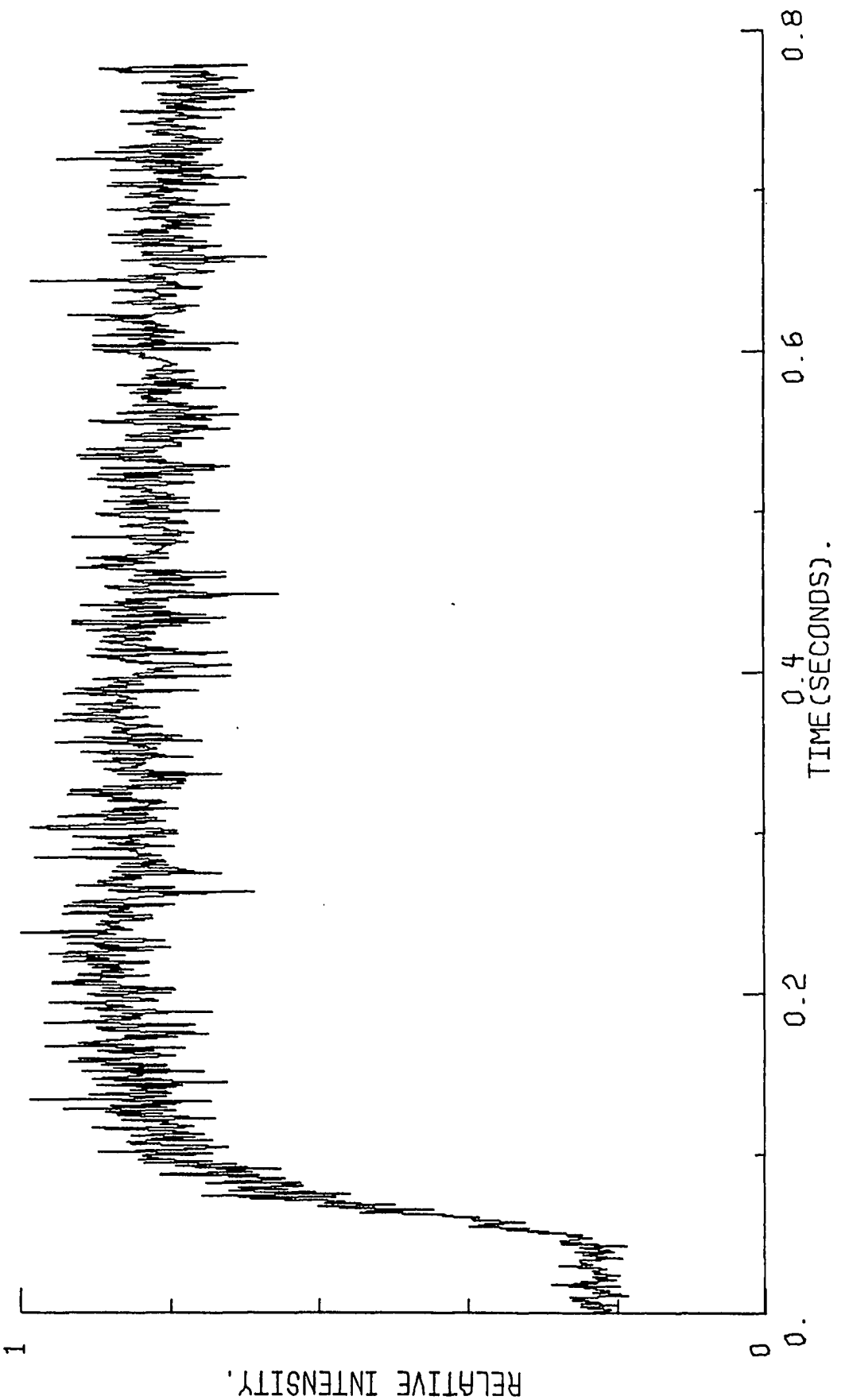


Reproduced with permission of the copyright owner. Further reproduction prohibited without permission.

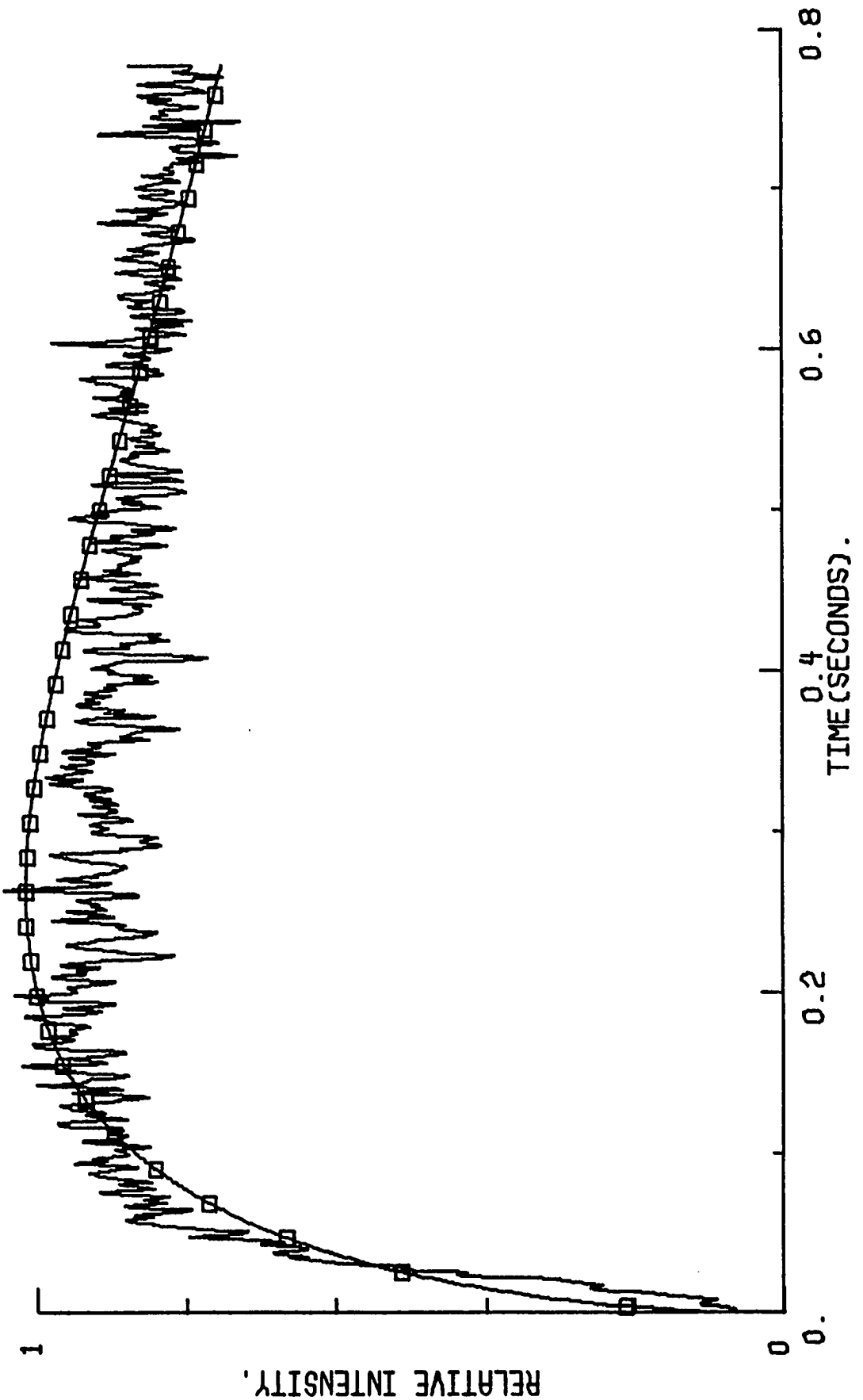


Reproduced with permission of the copyright owner. Further reproduction prohibited without permission.

Figure 24. The Intensity-Time Plots of $1.08 \times 10^{-3}$ M Fluoranthene Collected at the Wavelength of 470 nm for (a) Raw Data, (b) "Fixed" Smoothed Data, and (c) Composite of "Fixed" Smoothed Data and Fitted Data (open squares).

Reproduced with permission of the copyright owner. Further reproduction prohibited without permission.

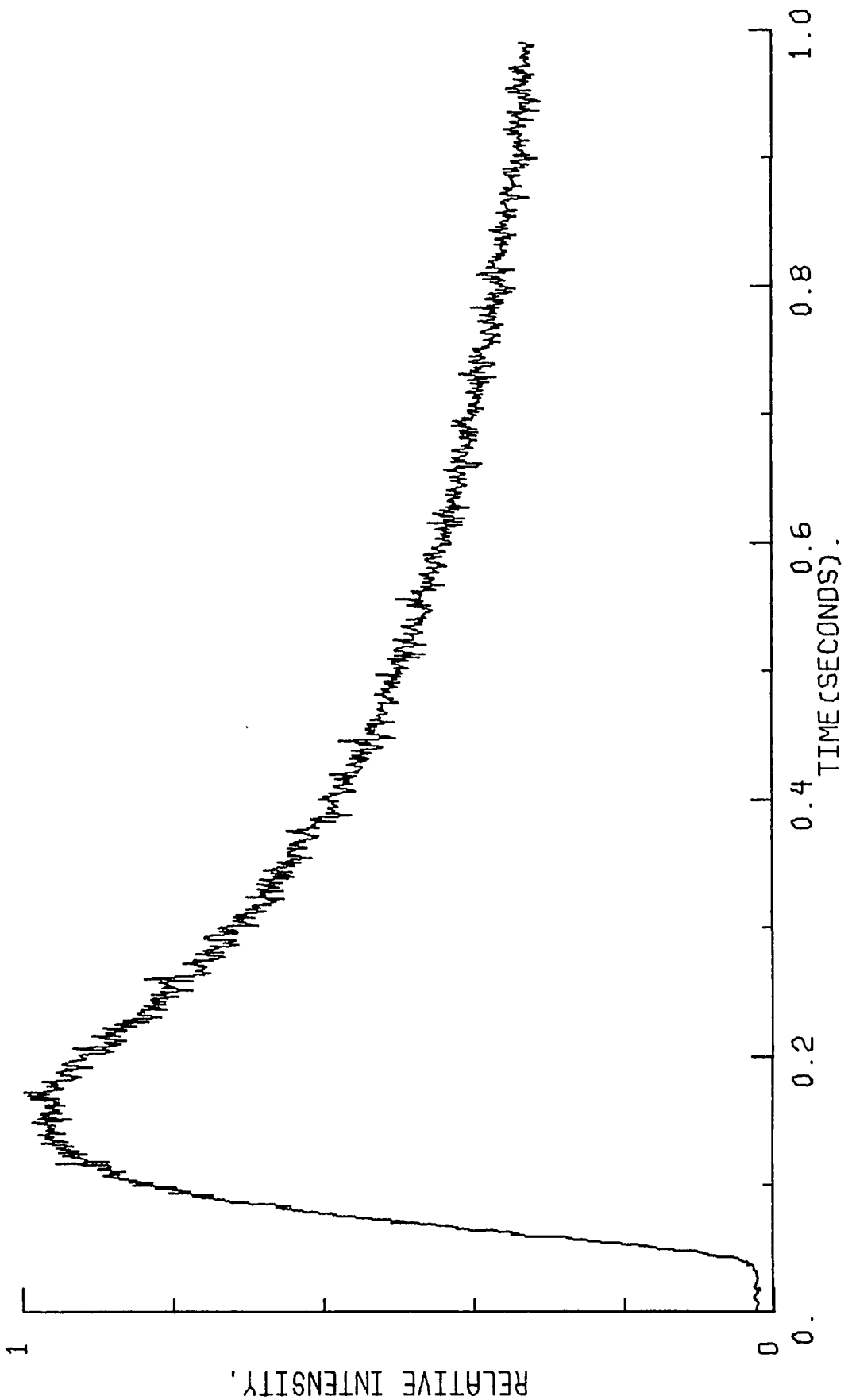


Reproduced with permission of the copyright owner. Further reproduction prohibited without permission.

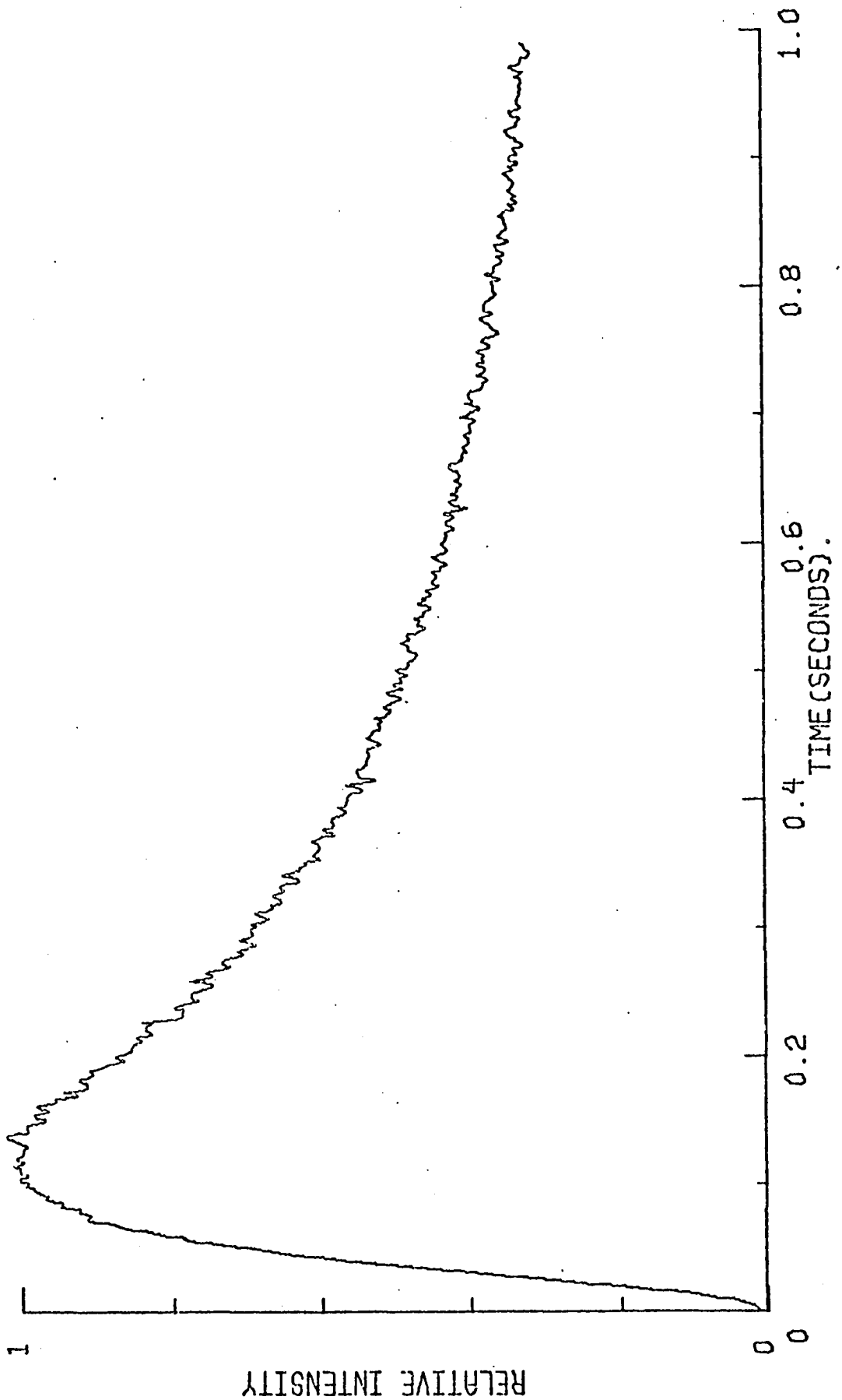


Reproduced with permission of the copyright owner. Further reproduction prohibited without permission.

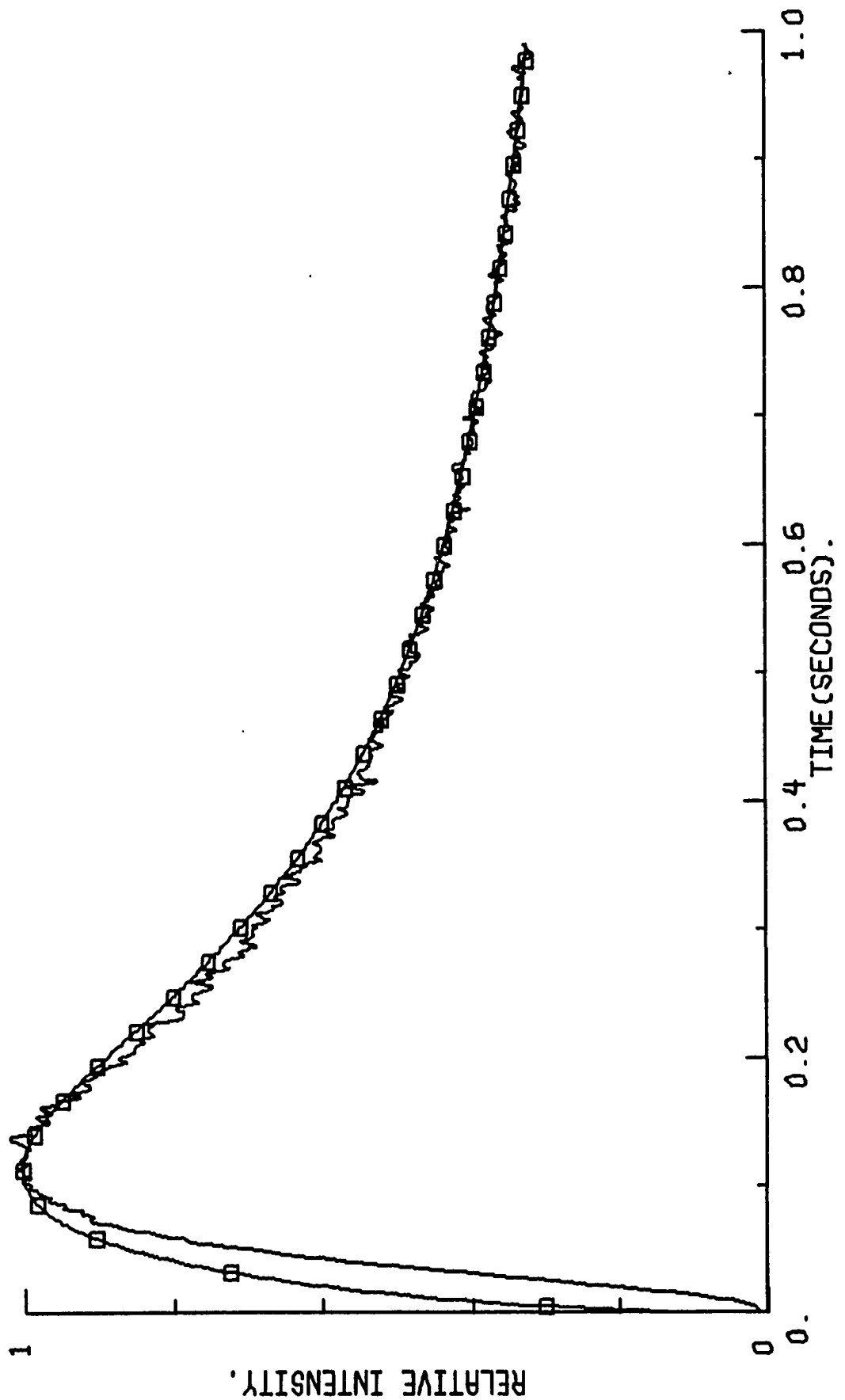


Reproduced with permission of the copyright owner. Further reproduction prohibited without permission.

Figure 25. The Intensity-Time Plots of $2.70 \times 10^{-3}$ M Fluoranthene Collected at the Wavelength of 470 nm for (a) Raw Data, (b) "Fixed" Smoothed Data, and (c) Composite of "Fixed" Smoothed Data and Fitted Data (open squares).

Reproduced with permission of the copyright owner. Further reproduction prohibited without permission.

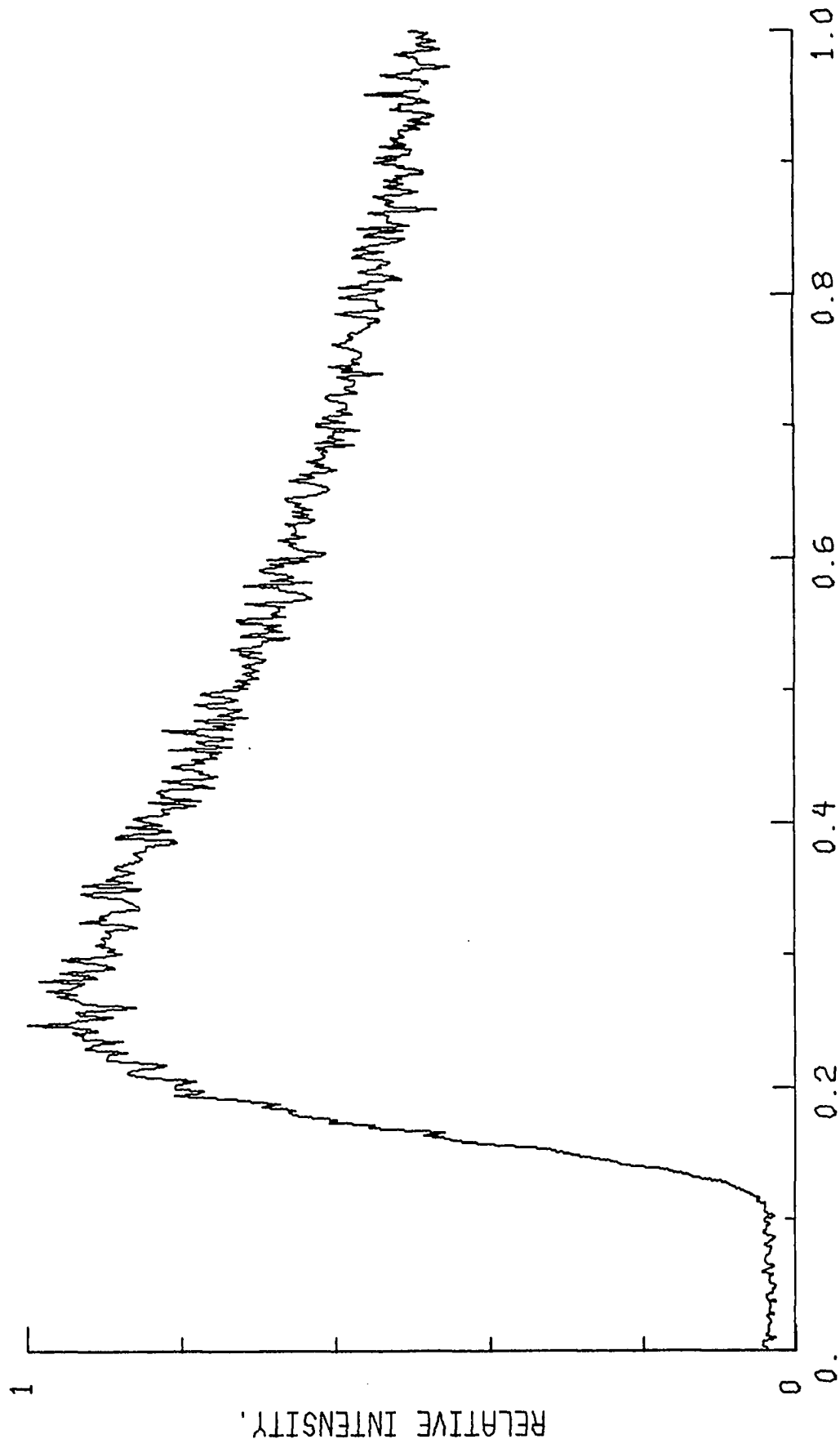


Reproduced with permission of the copyright owner. Further reproduction prohibited without permission.

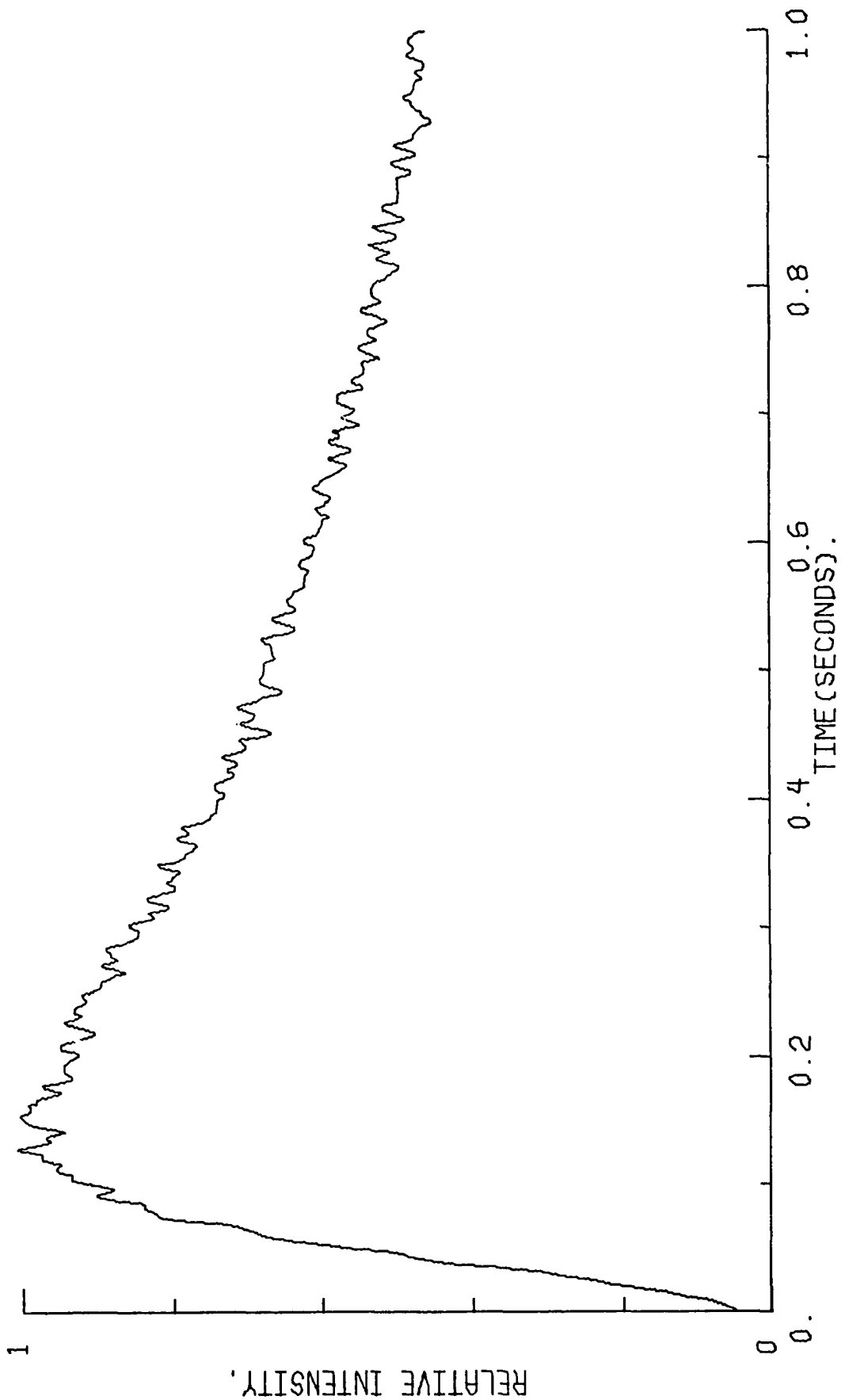


Reproduced with permission of the copyright owner. Further reproduction prohibited without permission.

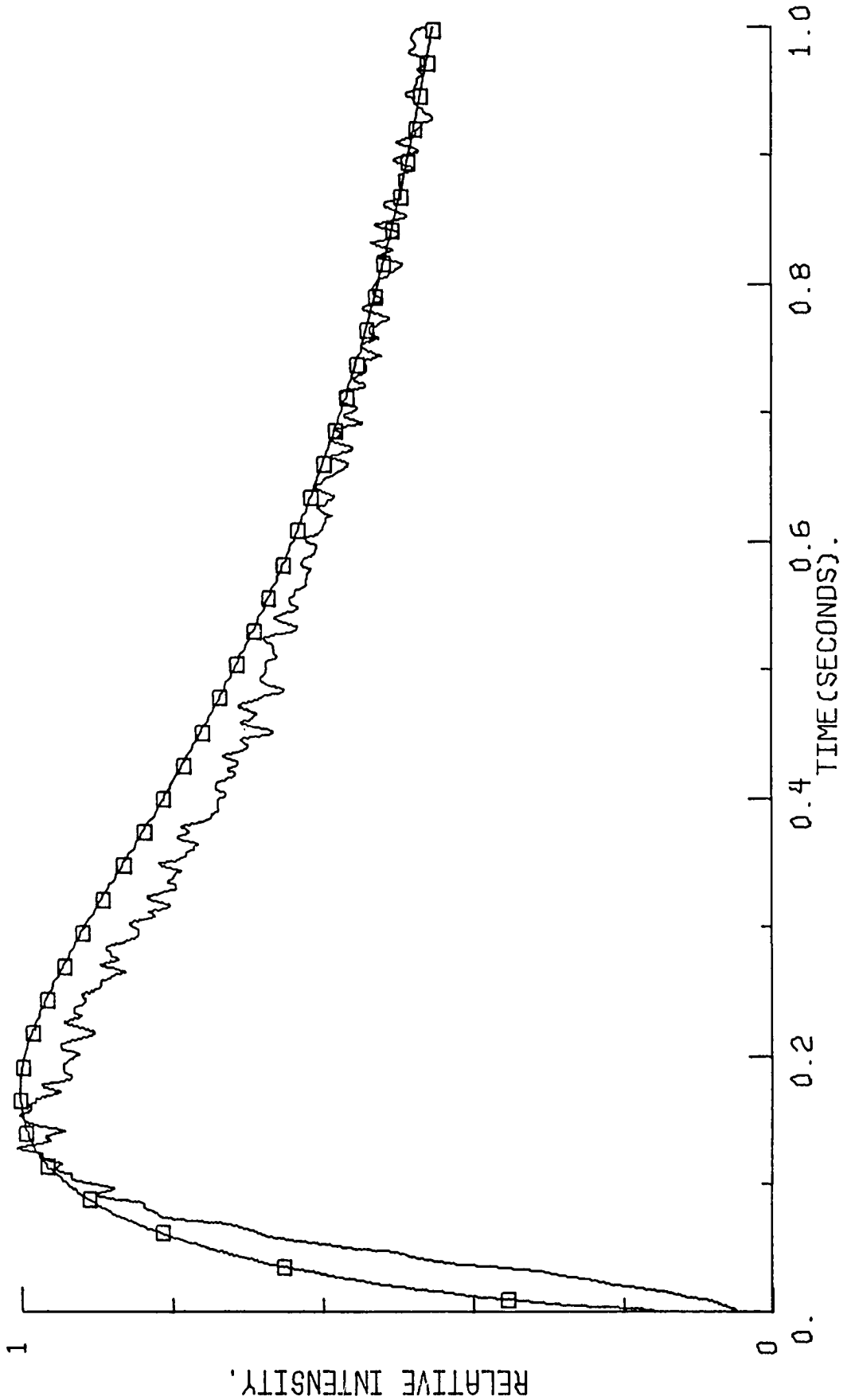


Reproduced with permission of the copyright owner. Further reproduction prohibited without permission.

Figure 26. The Intensity-Time Plots of $7.46 \times 10^{-6}$ M DPA Collected at the Wavelength of 435 nm for (a) Raw Data, (b) "Fixed" Smoothed Data, and (c) Composite of "Fixed" Smoothed Data and Fitted Data (open squares).

Reproduced with permission of the copyright owner. Further reproduction prohibited without permission.

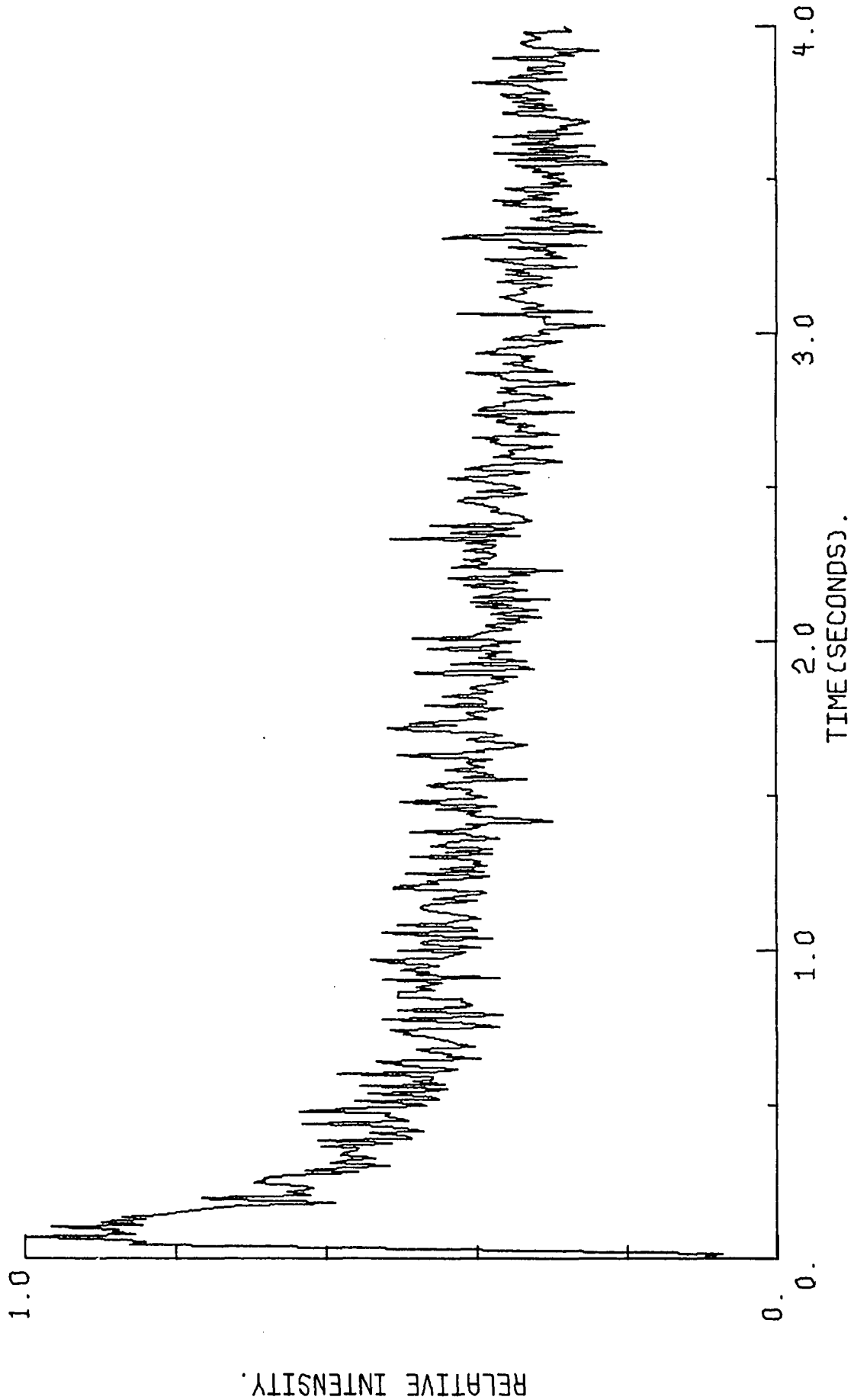


Reproduced with permission of the copyright owner. Further reproduction prohibited without permission.

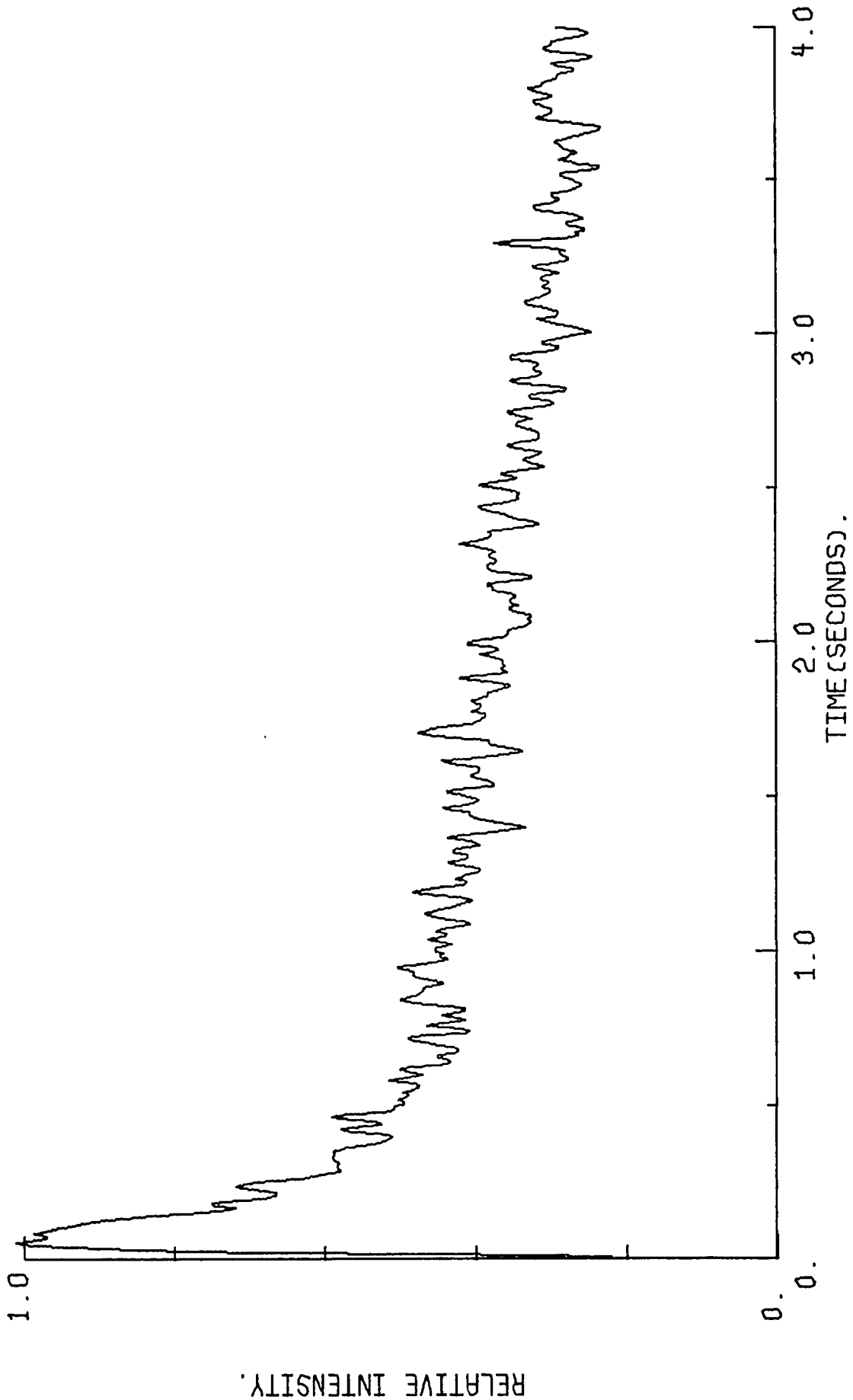


Reproduced with permission of the copyright owner. Further reproduction prohibited without permission.

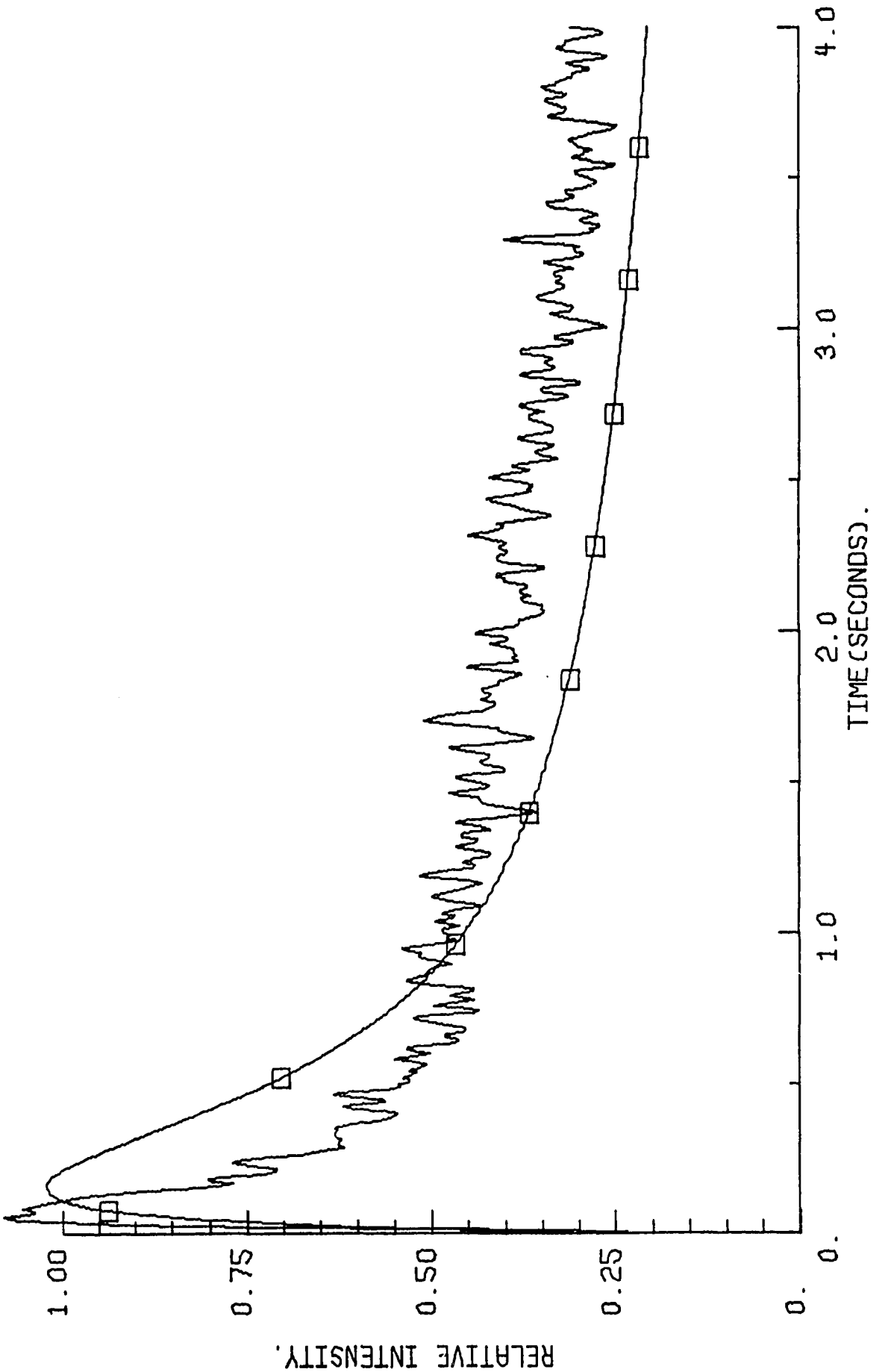


Reproduced with permission of the copyright owner. Further reproduction prohibited without permission.

Figure 27. The Intensity-Time Plots of $3.73 \times 10^{-5}$ M DPA Collected at the Wavelength of 435 nm for (a) Raw Data, (b) "Fixed" Smoothed Data, and (c) Composite of "Fixed" Smoothed Data and Fitted Data (open squares).

Reproduced with permission of the copyright owner. Further reproduction prohibited without permission.

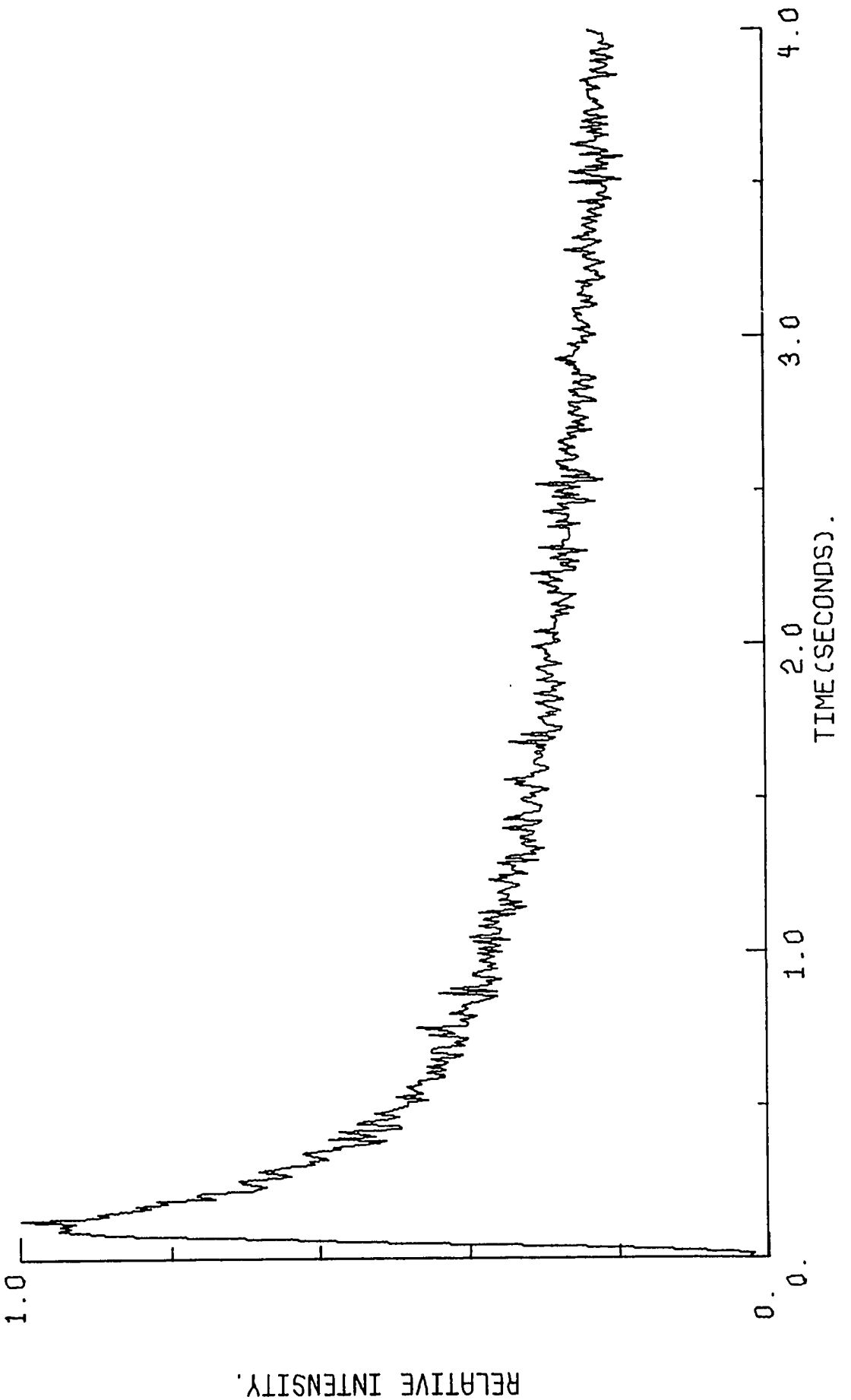


Reproduced with permission of the copyright owner. Further reproduction prohibited without permission.

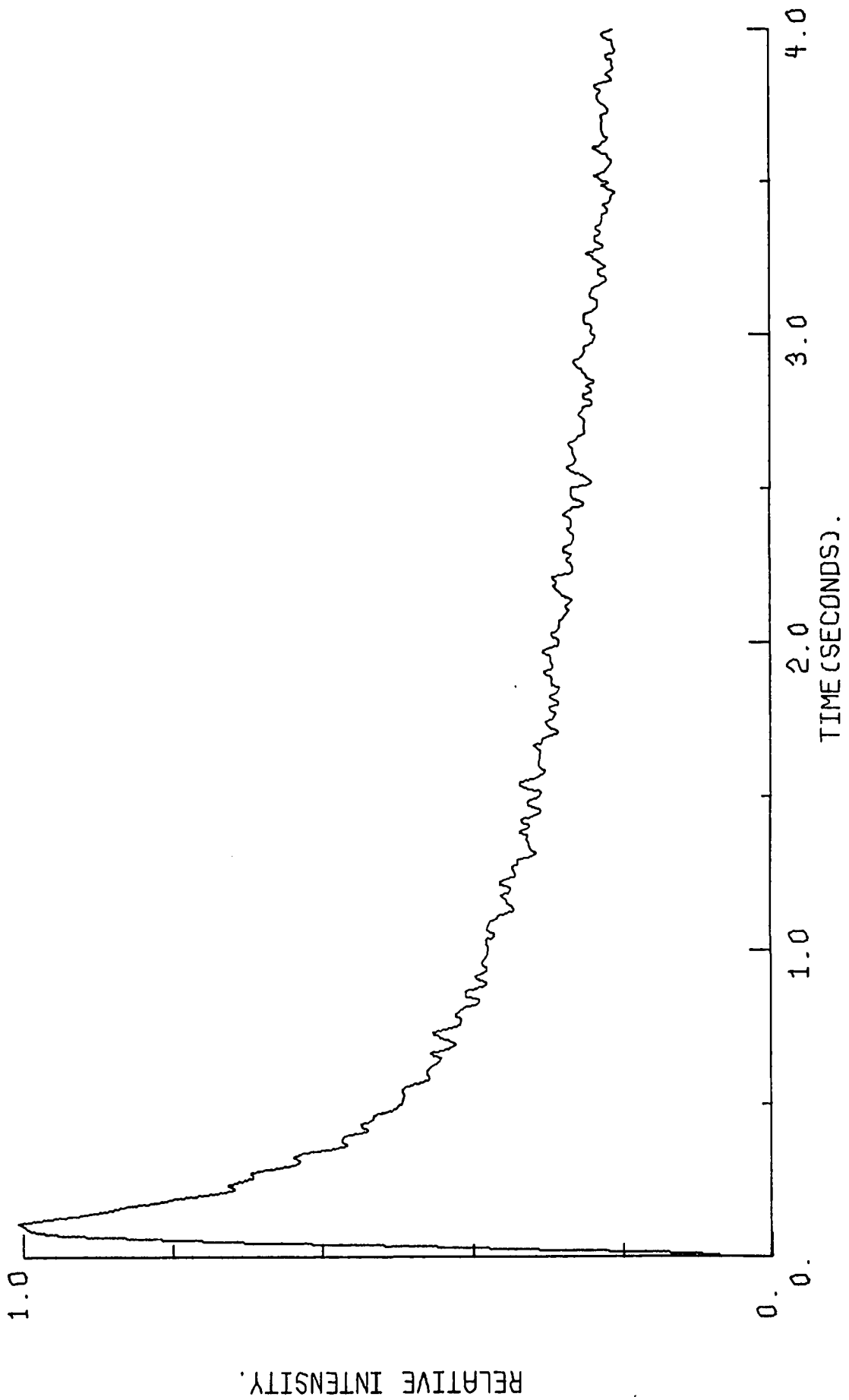


Reproduced with permission of the copyright owner. Further reproduction prohibited without permission.

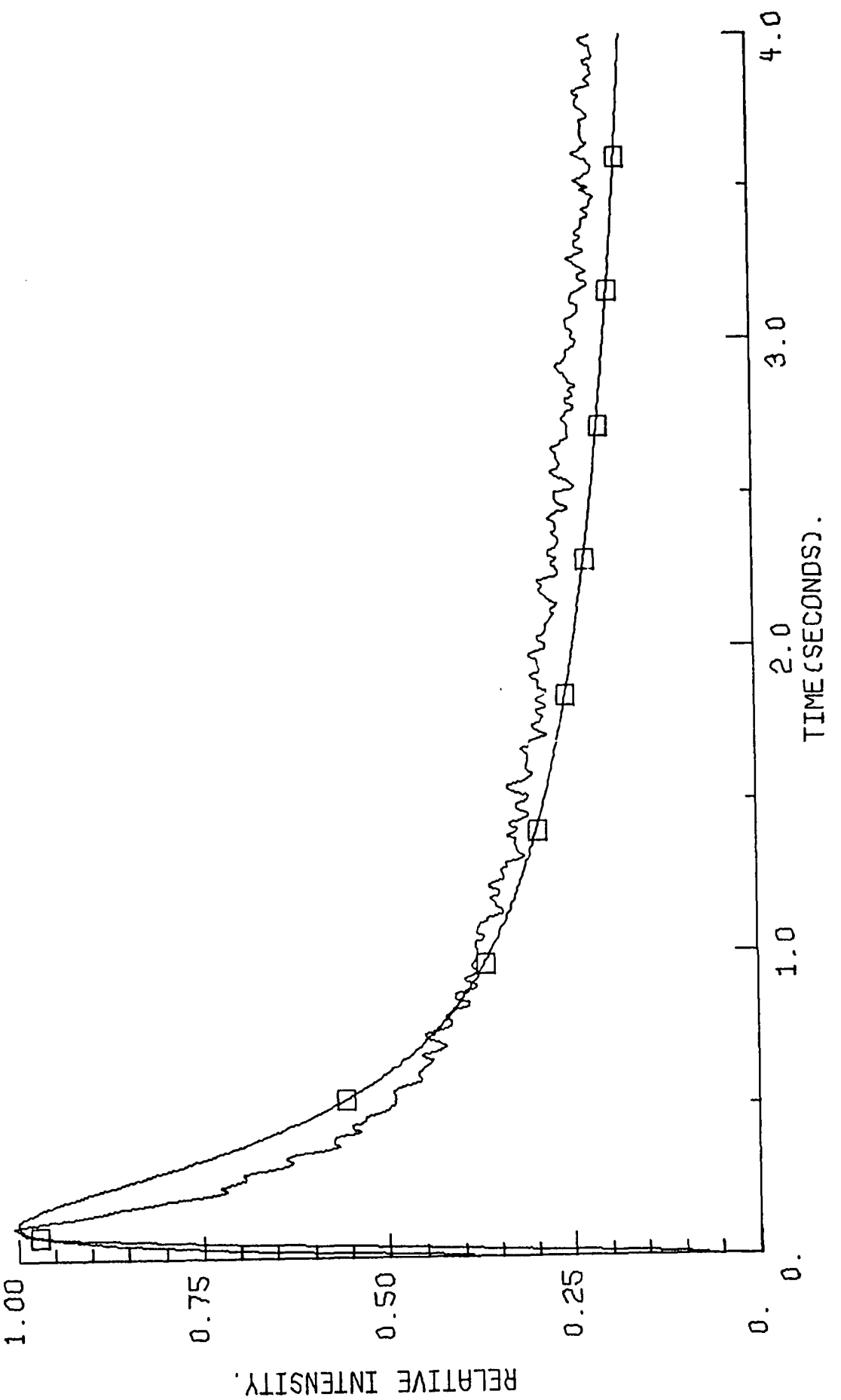


Reproduced with permission of the copyright owner. Further reproduction prohibited without permission.

Figure 28. The Intensity-Time Plots of $1.86 \times 10^{-4}$ M DPA Collected at the Wavelength of 435 nm for (a) Raw Data, (b) "Fixed" Smoothed Data, and (c) Composite of "Fixed" Smoothed Data and Fitted Data (open squares).

Reproduced with permission of the copyright owner. Further reproduction prohibited without permission.

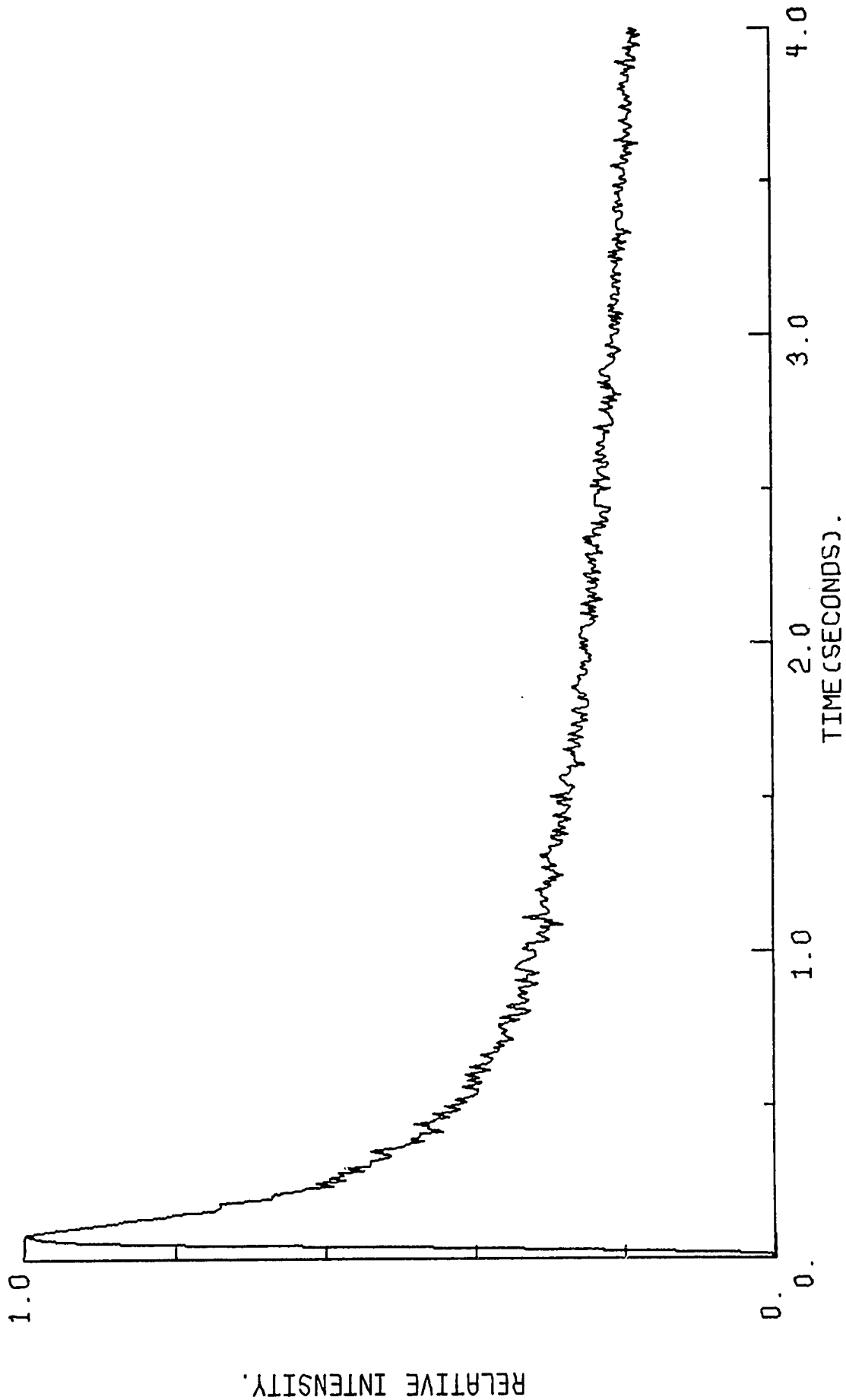


Reproduced with permission of the copyright owner. Further reproduction prohibited without permission.

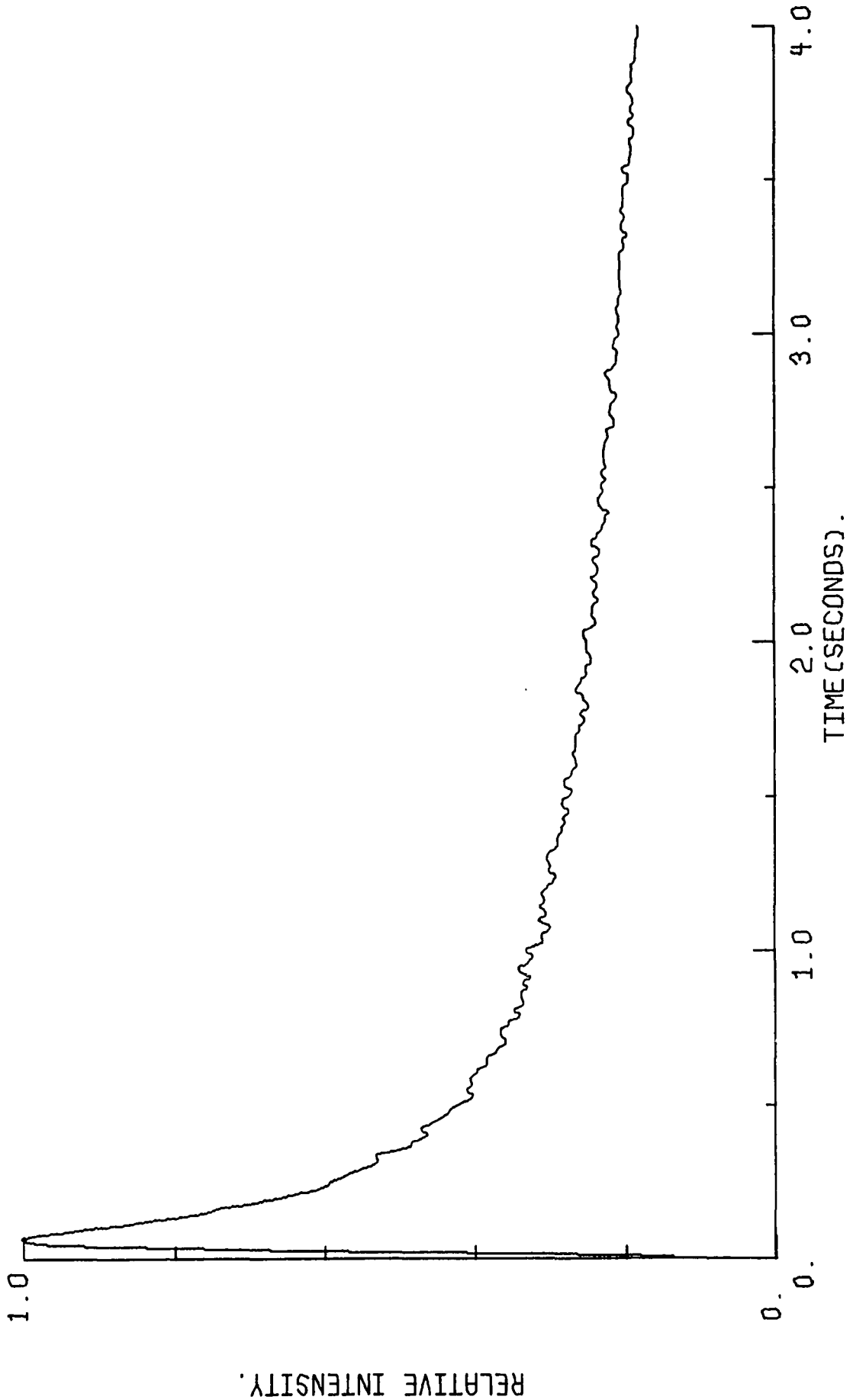


Reproduced with permission of the copyright owner. Further reproduction prohibited without permission.

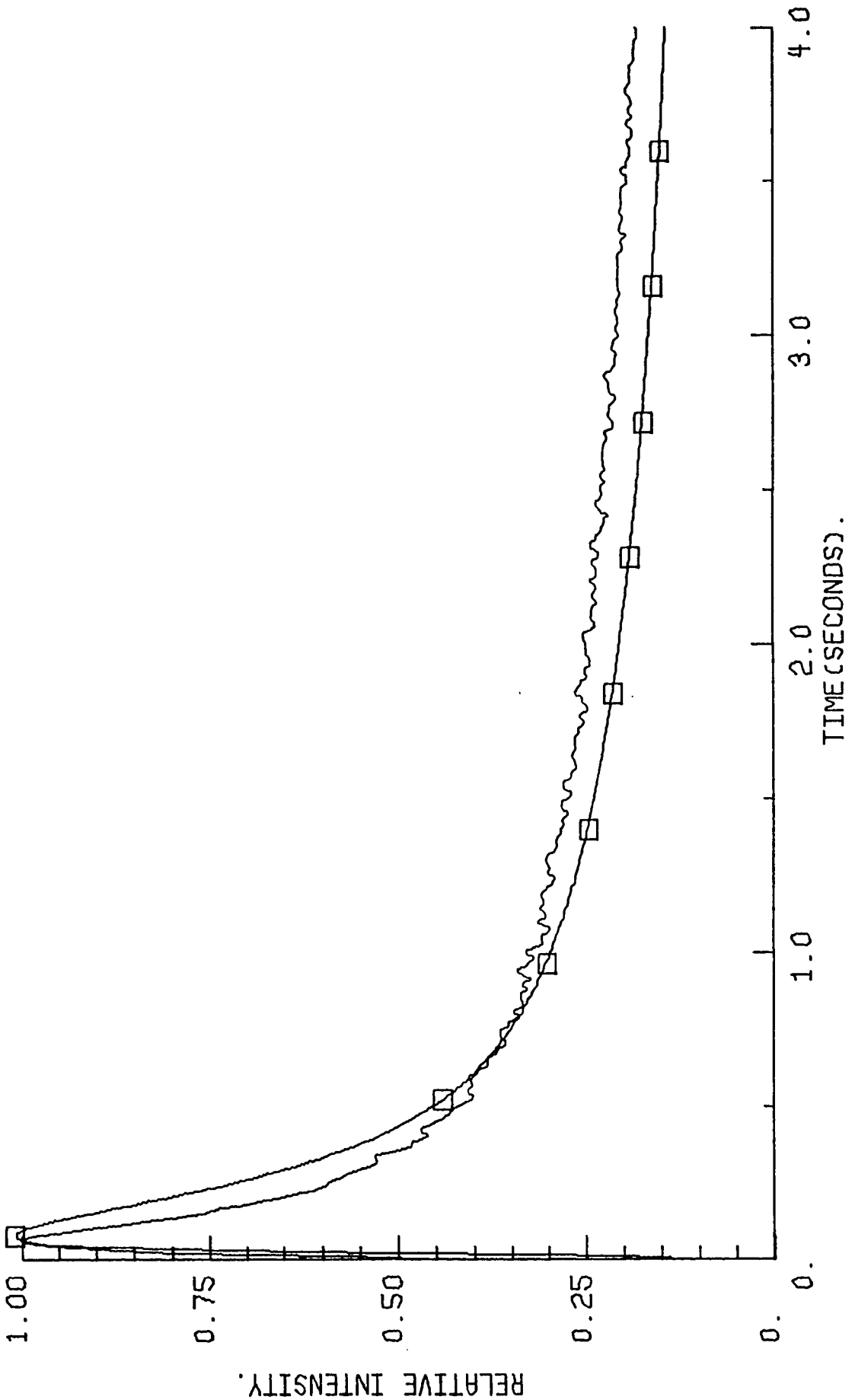


Reproduced with permission of the copyright owner. Further reproduction prohibited without permission.

Figure 29. The Intensity-Time Plots of $9.32 \times 10^{-4}$ M DPA Collected at the Wavelength of 435 nm for (a) Raw Data, (b) "Fixed" Smoothed Data, and (c) Composite of "Fixed" Smoothed Data and Fitted Data (open squares).

Reproduced with permission of the copyright owner. Further reproduction prohibited without permission.

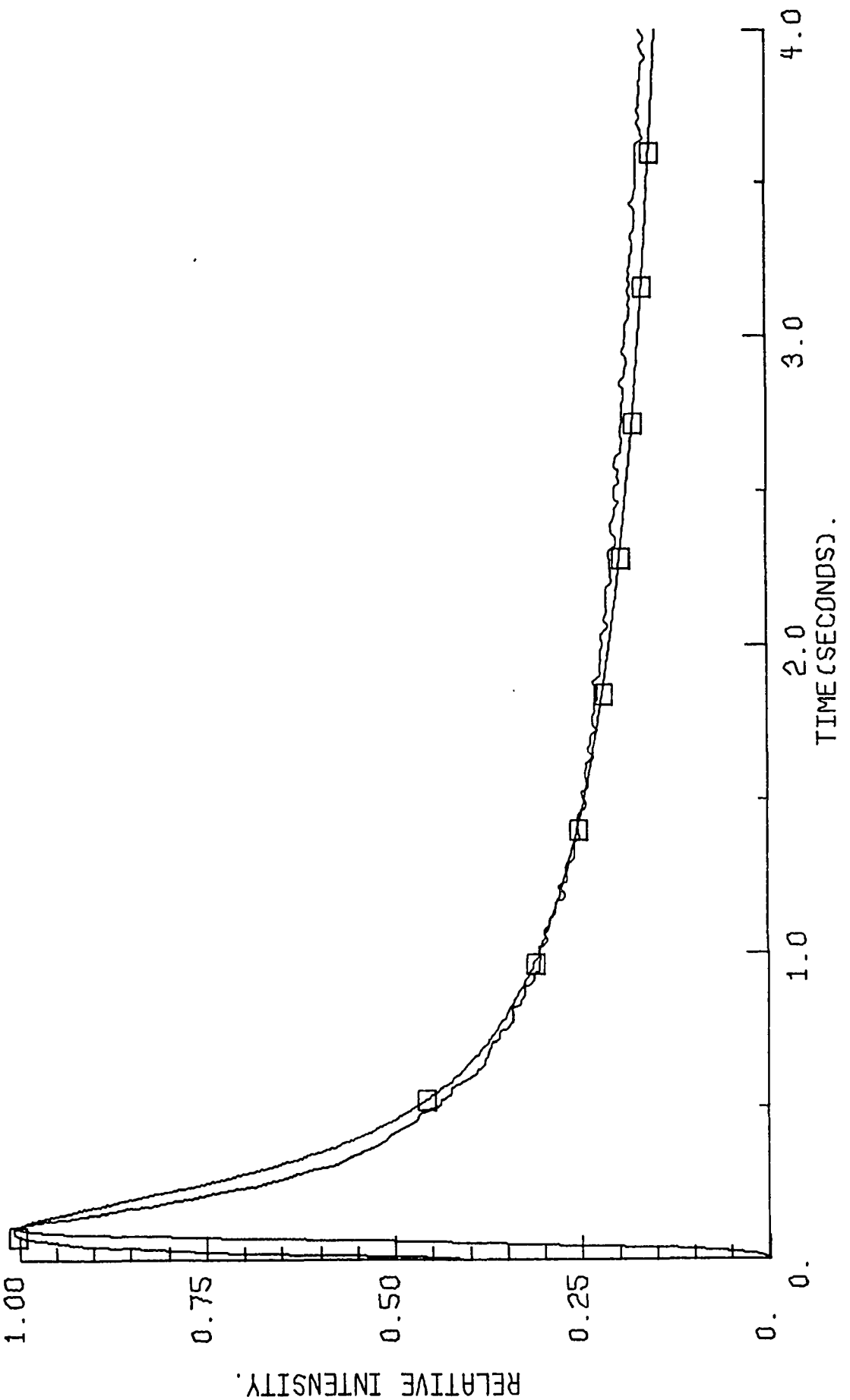


Reproduced with permission of the copyright owner. Further reproduction prohibited without permission.

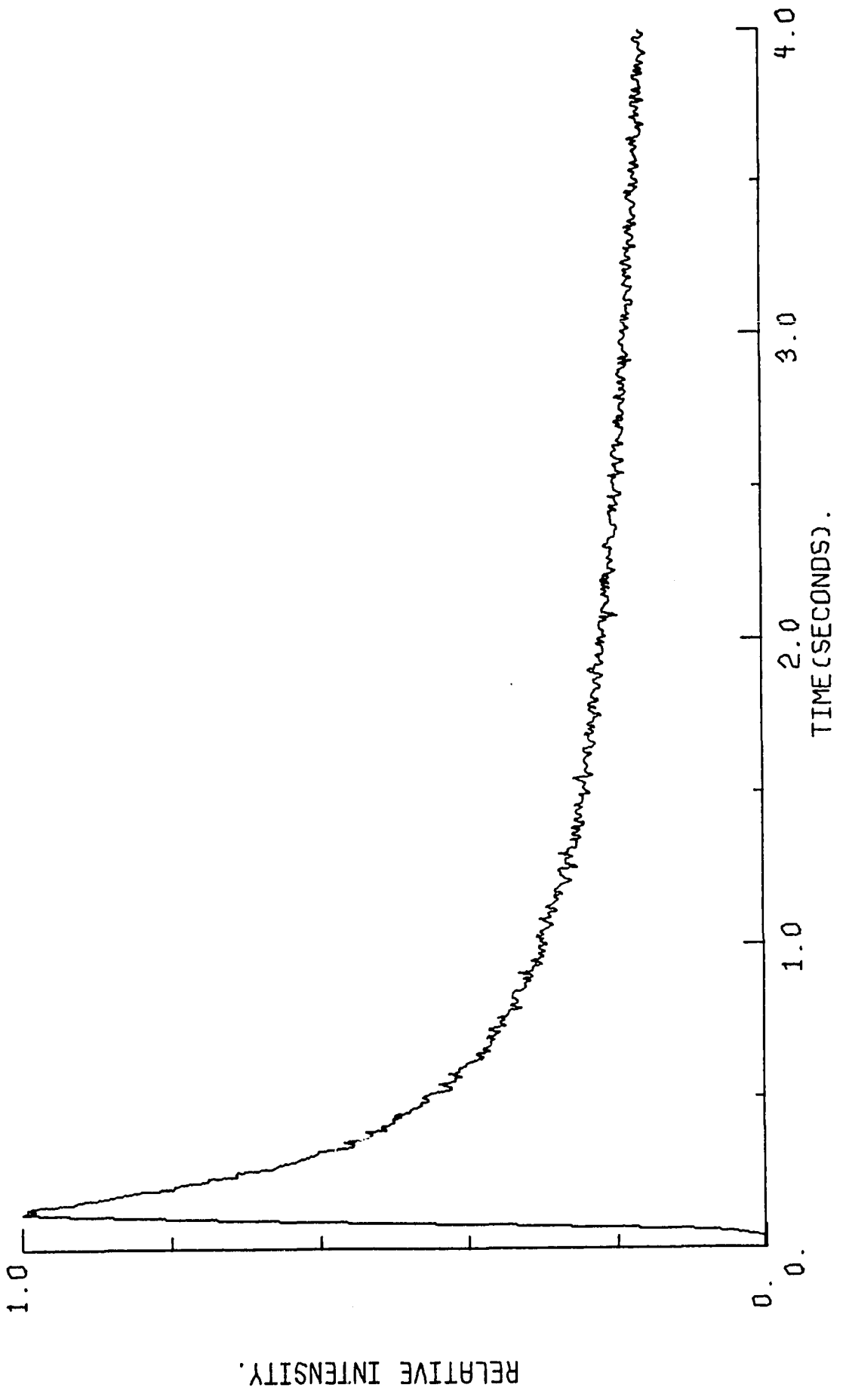


Reproduced with permission of the copyright owner. Further reproduction prohibited without permission.

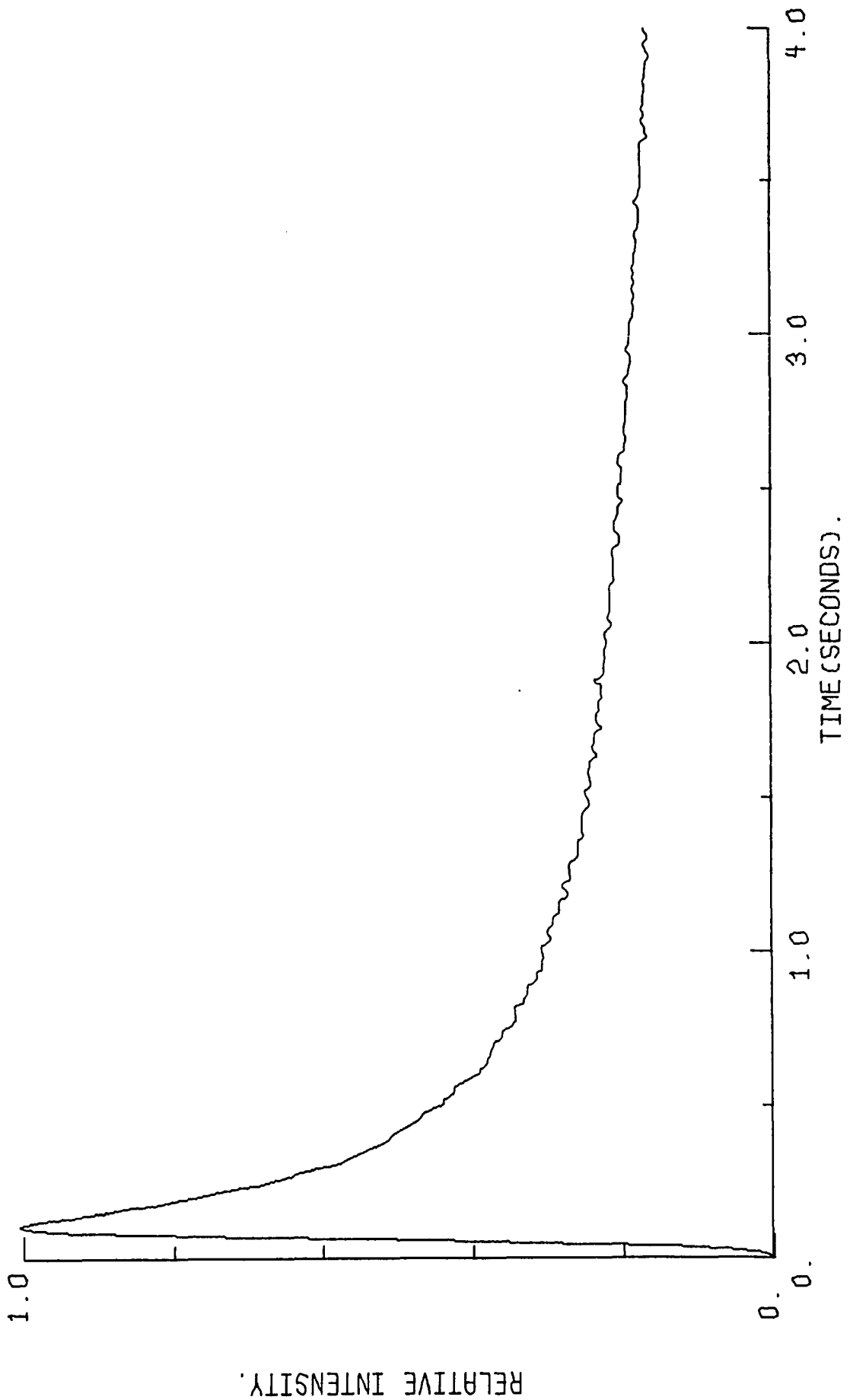


Reproduced with permission of the copyright owner. Further reproduction prohibited without permission.

Figure 30. The Intensity-Time Plots of 4.6- x $10^{-3}$ M DPA Collected at the Wavelength of 435 nm for (a) Raw Data, (b) "Fixed" Smoothed Data, and (c) Composite of "Fixed" Smoothed Data and Fitted Data (open squares).

Reproduced with permission of the copyright owner. Further reproduction prohibited without permission.

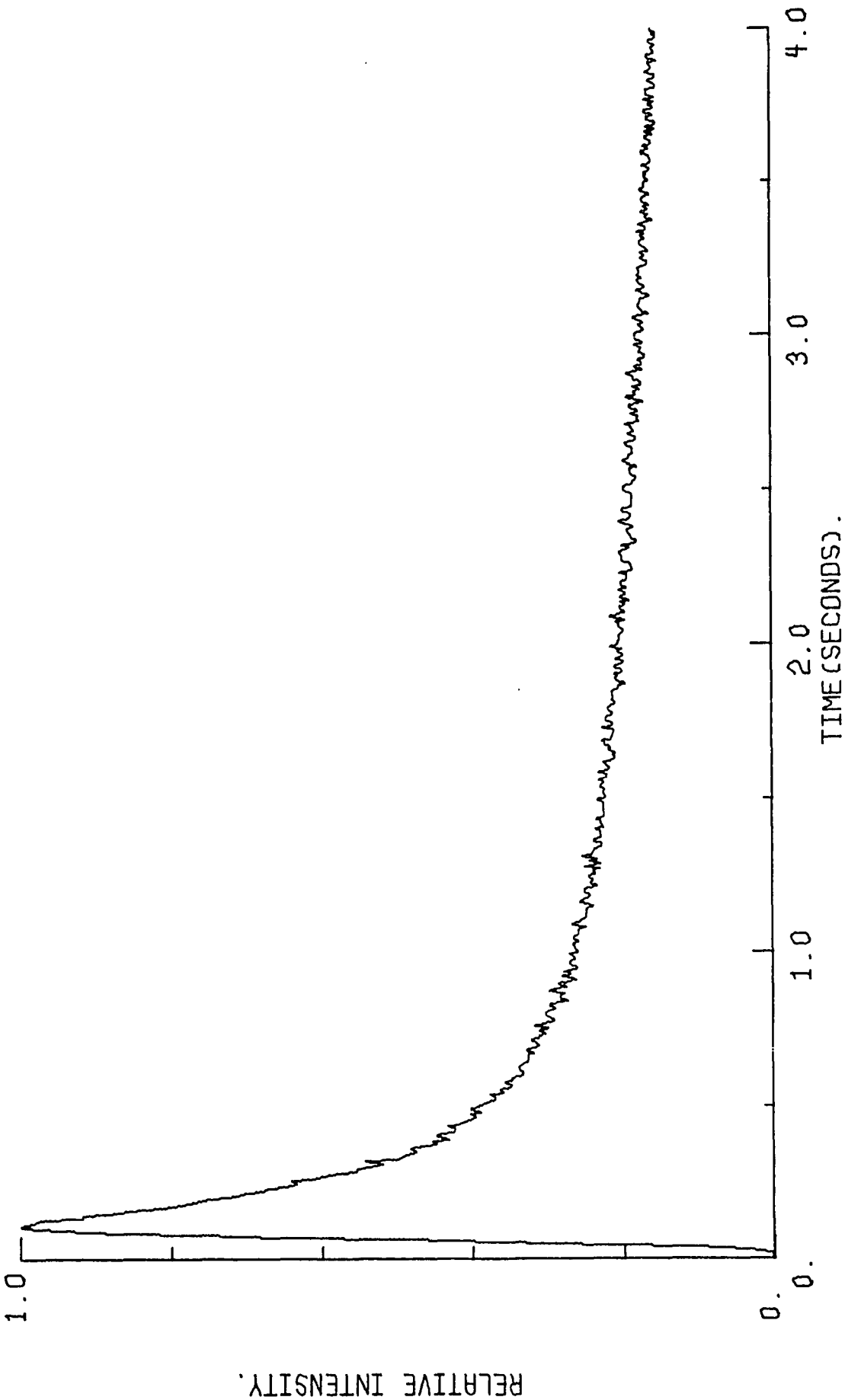


Reproduced with permission of the copyright owner. Further reproduction prohibited without permission.

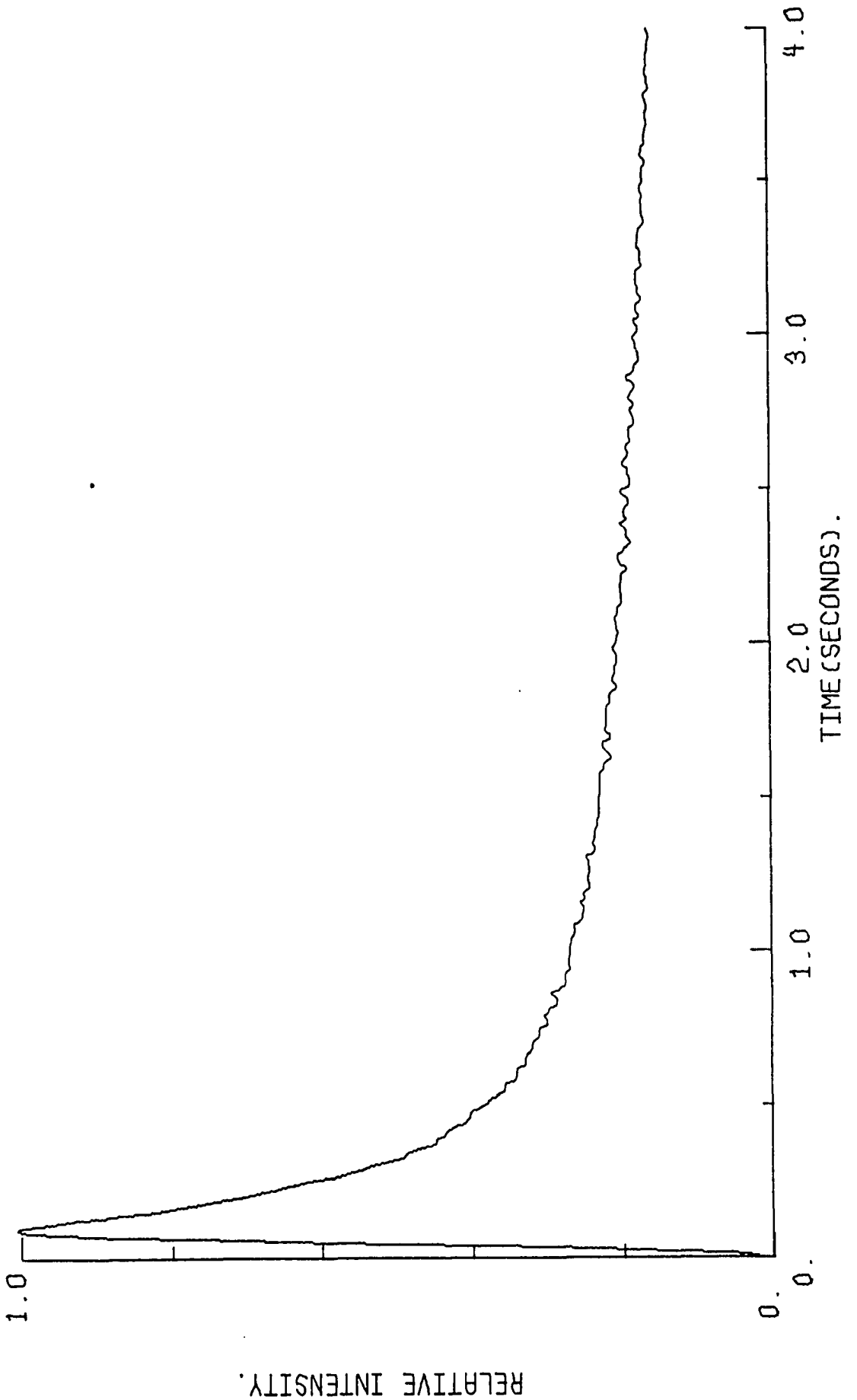


Reproduced with permission of the copyright owner. Further reproduction prohibited without permission.

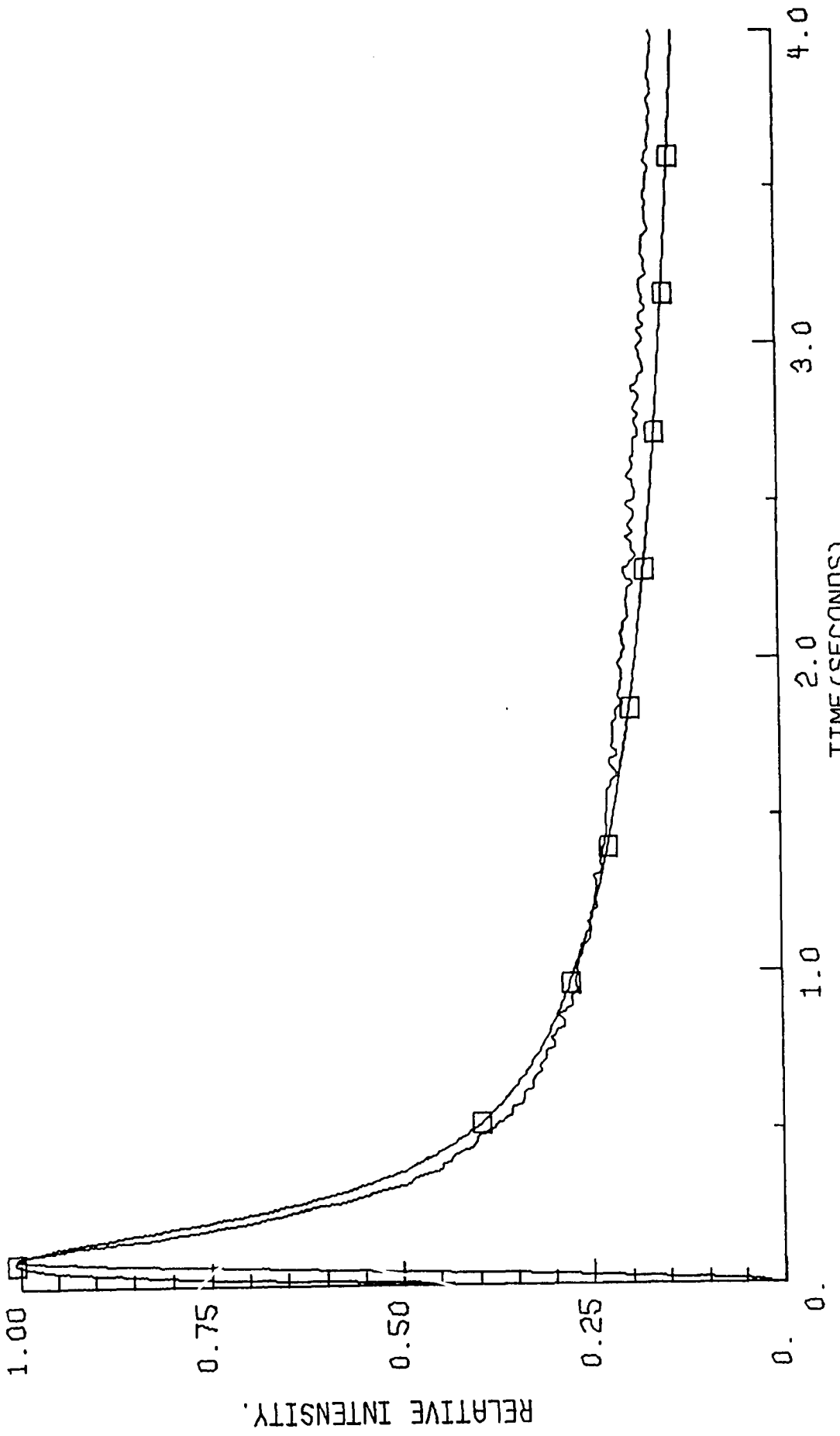


Reproduced with permission of the copyright owner. Further reproduction prohibited without permission.